Université catholique de Louvain
Secteur des sciences de la santé

Institute of Neurosciences

Promoter: Prof. Christian Raftopoulos

Dr. Edward Fomekong received his MD degree in 1988 at the University of Yaoundé Medical School. He worked for several years as a GP and was admitted for an internship in France where he graduated as a Neurosurgeon in 1997. He then joined the Neurosurgery Department of the Saint-Luc University Hospital. While collaborating with Professor Christian Raftopoulos, he developed his expertise in spine surgery, pituitary pathologies, chronic pain, spasticity, and peripheral nerve surgery.

Globalement, 70- 85 % des individus présenteront des douleurs lombaires chroniques à un moment donné de leur existence. La prise en charge doit être multimodale et pluridisciplinaire. En cas d'échec d'un traitement conservateur bien conduit, la chirurgie peut être une alternative. Différents auteurs ont développé et mis à disposition plusieurs technologies pour faciliter l'acte chirurgical tout en augmentant son efficacité. Dans une salle d'opération dédiée à la chirurgie du rachis, nous avons pratiqué la chirurgie guidée par l'imagerie 3D en utilisant des dernières évolutions en matière de navigation rachidienne. Par ailleurs, pour la première fois dans le rachis humain, nous avons appliqué des greffons osseux autologues issus des cellules souches méchenchymateuses provenant de la graisse avec des résultats encourageants sans effets secondaires. D'autres études sont en cours pour confirmer nos travaux.

Overall, 70–85% of individuals will present with chronic low back pain (CLBP). Concepts for its management are multimodal and multidisciplinary. If conservative management fails, surgery becomes an option. Spinal stabilization with fusion is considered a valid option for treating CLBP refractory to conservative management. Efforts have been made to make spinal fusion more efficient as well as more accurate. In a dedicated operating room equipped with intraoperative 3D fluoroscopy and an advanced navigation system, we have demonstrated that these new technologies can help to improve pedicle screw placement during spinal fusion procedures while decreasing the drawbacks associated with imaging utilization. For the first time in humans, we have also safely and efficiently applied osteodifferentiated adipose mesenchymal stem cells to spinal fusion as a graft material. Extended studies are ongoing to confirm our findings.

2018

Edward Fomekong

New Technologies and Bioengineering in lumbar spinal fusion

Impact of intraoperative three-dimensional fluoroscopy and navigation in lumbar spinal fusion

Edward Fomekong

June 2018

Thesis submitted in fulfillment
of the requirements for a
PhD degree in Medical Sciences

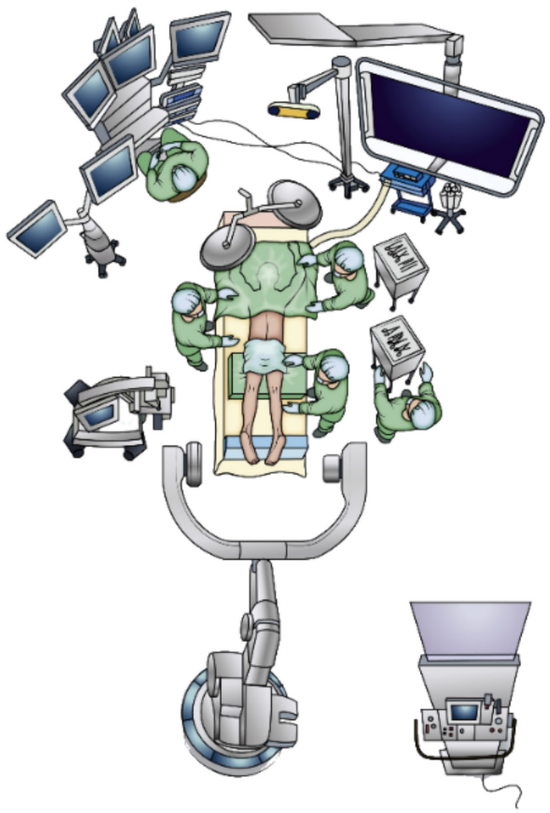

Impact of intraoperative three-dimensional fluoroscopy and navigation in lumbar spine fusion

Application of new Technologies and Bioengineering

PhD THESIS

Edward FOMEONG

JUNE 27, 2018

edward.fomekong@uclouvain.be
+32473651414

SUMMARY

Overall, 70–85% of individuals will present with chronic low back pain (CLBP). Concepts for its management are multimodal and multidisciplinary. If conservative management fails, surgery becomes an option. Spinal stabilization with fusion is considered a valid option for treating CLBP refractory to conservative management. Efforts have been made to make spinal fusion more efficient as well as more accurate. In a dedicated operating room equipped with intraoperative 3D fluoroscopy and an advanced navigation system, we have demonstrated that these new technologies can help to improve pedicle screw placement during spinal fusion procedures while decreasing the drawbacks associated with imaging utilization. For the first time in humans, we have also safely and efficiently applied osteodifferentiated adipose mesenchymal stem cells to spinal fusion as a graft material. Extended studies are ongoing to confirm our findings

RÉSUMÉ

Globalement, 70- 85 % des individus présenteront des douleurs lombaires chroniques à un moment donné de leur existence. La prise en charge doit être multimodale et pluridisciplinaire. En cas d'échec d'un traitement conservateur bien conduit, la chirurgie peut être une alternative. Différents auteurs ont développé et mis à disposition plusieurs technologies pour faciliter l'acte chirurgical tout en augmentant son efficacité. Dans une salle d'opération dédiée à la chirurgie du rachis, nous avons pratiqué la chirurgie guidée par l'imagerie 3D en utilisant des dernières évolutions en matière de navigation rachidienne. Par ailleurs, pour la première fois dans le rachis humain, nous avons appliqué des greffons osseux autologues issus des cellules souches méchenchymateuses provenant de la graisse avec des résultats encourageants sans effets secondaires. D'autres études sont en cours pour confirmer nos travaux.

MEMBERS OF THE JURY

Promotor :	Professor Christian Raftopoulos Université Catholique de Louvain ***christian.raftopoulos@uclouvain.be***
President of the jury :	Professor André Mouraux Université Catholique de Louvain ***andre.mouraux@uclouvain.be***
Members :	Professor Bruno Vande Berg Université Catholique de Louvain ***bruno.vandeberg@uclouvain.be***
	Professor Richard Assaker Université de Lille, France ***richard.assaker@chru-lille.fr***
	Professor Jean D'Haens Universitair Ziekenhuis Brussel ***jean.dhaens@uzbrussel.be***
	Professor Bart Depreitere Universitair Ziekenhuis Leuven ***bart.depreitere@uzleuven.be***

DEDICATIONS

My MD thesis was dedicated to my wife, Rose. I dedicate the present work to my children Franklin, Joël-Christian, Anne-Dominque, and my beloved little granddaughter Cassandre.

It’s not that I’m so smart, it’s just that I stay with problems longer.

Albert Einstein

Satisfaction lies in the effort, not in the attainment, full effort is full victory.Live as if you were to die tomorrow. Learn as if you were to live forever.

Mahatma Gandhi

You may not always have a comfortable life and you will not always be able to solve all the world's problems at once but don't ever underestimate the importance you can have because history has shown us that courage can be contagious, and hope can take on a life of its own.

Michelle Obama

ACKNOWLEDGMENTS

I am delighted to thank the rector of the Université Catholique de Louvain, M. Vincent Blondel, and the CEO of Cliniques Universitaires Saint-Luc, for having given me the opportunity to carry out my research in these prestigious institutions. But most of all, I must extend my deep gratitude to my supervisor, Prof. Christian Raftopoulos. In fact, since I first joined his department on December 6, 1997, I knew our collaboration would be fruitful for me. As time passed, I learned more and more from him and completed my internship at Nancy University Hospital. I progressively appreciated his scientific approach to any situation, and soon started thinking that going one step further and initiating a PhD research project would be worthwhile if I was to continue working in a university hospital. When I spoke with him about the idea, he immediately agreed to support me in my project. I deeply thank him and hope we still have many years to work together for our patients.

I am grateful to Professor André Mouraux, the president of my thesis committee. He has been always available to all my requests and kindly organized all the meetings necessary for the fulfilment of the course of this thesis. I also thank Professor Richard Assaker from the university of Lille France, and Professor Bruno Vande Berg for their interest in the research subject and their recommendations during the whole process of the thesis. Many thanks also to Professor Jean D'Haens from the Vrije Universiteit Brussel and Professor Bart Depreitere from the Katholieke Universiteit Leuven for having accepted to be the external members of the thesis committee.

I should also thank my colleagues for having been very kind and patient with me during the process of preparing my thesis. I am grateful to my assistants for their daily help. A special thanks to the medical students who from time to time never hesitate to help in data collection.

I was indirectly supported by many persons who I cannot name in detail here. This is an opportunity for me to thank them and appreciate their efforts. This is especially true with regards to our secretaries and nursing staff of our hospitalization unit 72, and operating theater.

I am proud to have a family who supports me unconditionally. Without their encouragement, I would not have completed this research thesis.

Last but not least, I am proud to have friends such as Marie-Agnès A.F.D. and Gilbert T.N. who, day after day, encouraged me and did not hesitate to help in reviewing my manuscripts

TABLE OF CONTENTS

LIST OF FIGURES

LIST OF TABLES

LIST OF ACRONYMS AND ABBREVIATIONS

Abbreviations	Definitions
2D	two-dimensional
3D	three-dimensional
AMSC(s)	adipose mesenchymal stem cell(s)
BB	bank bone (bone + demineralized bone
BM-MSCs	bone marrow-derived mesenchymal stem
BMP(s)	bone morphogenic protein(s)
CAN	computer-assisted navigation
CLBP	chronic low back pain
CT	computed tomography
DBM	demineralized bone matrix
FBSS	failed back surgery syndrome
GMP	good manufacturing practice
HyOR	hybrid operating room
ioi	intraoperative imaging
io3DF	intraoperative 3-dimensional fluoroscopy
ioNav	intraoperative navigation
K-wire	Kirschner wire
MI	minimally invasive
MIS	minimally invasive surgery
MISS	minimally invasive spine surgery
MI-TLIF	minimally invasive transforaminal lumbar
MSCs	mesenchymal stem cell(s)
NSAID(s)	nonsteroidal anti-inflammatory drug(s)
ND	non-degenerative
ODI	Oswestry disability index

OR	operating room
OS	open surgery
PPS	percutaneous pedicle screw
RCT(s)	Randomized controlled trial (s)
SD	standard deviation
TLIF	transforaminal lumbar interbody fusion
VAS	visual analog scale

Chapter 1 INTRODUCTION

1.1 CHRONIC LOW BACK PAIN

1.1.1 Definition and epidemiology

The lifetime prevalence of low back pain has been reported as 70–85% in industrialized countries. The annual prevalence of back pain ranges from 15% to 45%, with peak prevalence averaging 30% [1-5]. Peak prevalence occurs between ages 35 and 55, and the adult incidence is 5% per year [6, 7]. Back pain is the fifth most common reason for a patient to visit a physician's office in the United States [8] and worldwide prevalence has been reported to be the highest in Western Europe [9].

Acute low back pain is usually self-limiting (recovery rate 90% within 6 weeks) but 2–7% of people develop chronic pain. Patients with persistent or fluctuating pain that lasts longer than 3 months are defined as having chronic low back pain (CLBP). Recurrent and chronic pain account for 75% to 85% of total workers' absenteeism [6, 10]. The direct medical costs and lost wages due to back pain have reached $253 billion annually in the United States [11]. It has been estimated that $30 to $50 billion is spent annually for the treatment of CLBP in the United States [12].

1.1.2 Management

Currently, the management of chronic pain in general is multimodal and multidisciplinary, with the aim of maximizing pain reduction, quality of life, independence, and mobility. An array of treatments, many with limited scientific evidence of their efficacy, have been promoted for the management of CLBP at great cost to public health agencies because they focus solely on

anatomical structures of the low back region instead of considering the individual patient.

CLBP is now considered a biopsychosocial illness involving physical, behavioral, occupational, and socioeconomic factors. Furthermore, the pain experience and disability of an individual are determined by an array of psychosocial factors, including previous pain experiences, beliefs and fears about CLBP, general and psychosocial health, job satisfaction, economic status, education, ongoing litigation, compensation claims, and social well-being [13].

1.1.2.1 Optimal conservative management

The mainstay of treatment for symptomatic degenerative lumbar spine is conservative management [14]. Evidence-based clinical practice guidelines are in general agreement to advise physical activity and pharmacotherapy combined with multidisciplinary psychosocial and behavioral approaches. Patients should receive education regarding their condition while limiting bed rest. In addition, most guidelines recommend the use of paracetamol, nonsteroidal anti-inflammatory drugs (NSAIDs), light opioids, physical exercises, spinal injections, and spinal manipulation [15, 16]

1.1.2.1.1 Physical and psychological management

Several authors have stressed the evidence of the efficacy of physical, psychological, and rehabilitation treatments [17-19]. These interventions are offered as part of the multimodal and interdisciplinary programs that include psychoeducation, cognitive restructuring, acceptance, and commitment therapies. Nevertheless, physical therapy likely reduces low back pain by less than 30% and improves function by less than 20% [20]

1.1.2.1.2 Pharmacological management

The goal of pharmacological treatment is to reduce pain and associated complaints and improve functional status and quality of life. Many interventional therapies are in fact forms of targeted pharmacological therapy.

1.1.2.1.3 Surgical management

Only a minority of patients with CLBP are clearly indicated for spinal surgery. Indications for surgery should be considered only in patients with refractory CLBP who have failed to respond to a prolonged period of optimal appropriate conservative management. Nevertheless, the overuse of surgical approaches in patients suffering from CLBP is increasing in several countries. Generally, four main options are offered.

1.1.2.1.3.1 Surgical decompression

The first surgical option for the management of CLBP is decompression, which aims to partially or totally remove the lumbar anatomical structures that are thought to be the cause of neural impingement. Decompression includes microdiscectomy and spinal canal recalibration where stenosis is diagnosed [21, 22]. Evidence strongly supports the equivalence (and possible superiority) of minimally invasive spine surgery (MISS) techniques to traditional open procedures, but the need for high-quality evidence and randomized controlled trials (RCTs) in this field remains [23].

1.1.2.1.3.2 Surgical fusion and stabilization

Spinal fusion has the objective of joining adjacent vertebrae anteriorly, posteriorly, or circumferentially with the help of bone grafts (autograft or allograft) or surgical hardware. Fusion is thought to alleviate symptoms that may be related to excessive movement in an unstable vertebral

motion segment due to advanced degenerative changes. It should be used with caution. A study by Froholdt et al. found no difference in the 9-year outcomes of 124 patients with CLBP randomly assigned to lumbar fusion surgery or interventions such as cognitive behavioral therapy with exercise. Both groups reported less pain and better function at 9 years versus baseline and at a 1-year follow-up, but more patients who received surgery used pain medication and were out of work compared with the group that did not undergo surgery [24]. Nevertheless, in a recent review of RCTs as well as prospective and retrospective nonrandomized studies comparing fusion and nonsurgical procedures (mainly physical therapy) assessing different fusion approaches such as instrumented and non-instrumented posterolateral fusion and posterior or anterior lumbar interbody fusion[25], the authors recommended spinal fusion surgery as a viable treatment option for reducing pain and improving function in patients with CLBP that is refractory to nonsurgical care when a diagnosis of disc degeneration can be made.

RCTs comparing conservative management and surgical treatment of CLBP have been published over the past decades[26-29]. Surgery has been demonstrated by a recent meta-analysis[30] and a systematic review[31] of RCT to be associated with small but statistically significant improvements in Oswestry Disability Index (ODI) scores over the follow-up periods compared to non-surgical care.

Multiple techniques and approaches are currently used for spinal stabilization, among which the most common are transforaminal lumbar interbody fusion (TLIF), posterior lumbar interbody fusion, extreme lateral interbody fusion, and, after careful evaluation, anterior lumbar interbody fusion. Since Harrington and Tullos [32] first placed a pedicle screw through a

vertebral isthmus, spinal fusion using pedicle screw stabilization has become accepted worldwide as a surgical option to address CLBP that is refractory to optimal conservative management. Pedicle screws can be inserted using open or MISS. Malposition of the pedicle screw remains a significant concern. A variety of devices have been introduced to reduce pedicle violation during screw insertion. Image-guided methods include computed tomography (CT)-based two-dimensional (2D) fluoroscopy and three-dimensional (3D) fluoro-guided navigation. Usually, CT navigation requires preoperative scanning and transfer to the navigation platform and registration to assist pedicle screw insertion. A 2D fluoroscopy provides intraoperative 2D images and offers real-time visualization of the pedicle anatomy without a registration procedure. 3D-fluoroscopy-based navigation combines the advantages of both 2D fluoro and CT navigation without complex registration procedures. It provides real-time CT-like 3D images intraoperatively. In a recent meta-analysis comparing image-guided techniques to increase pedicle screw accuracy, Du et al. [33] concluded that there are significant differences among the three navigation systems and study suggest that the 3D FluoroNav system may be superior in reducing pedicle violation. Their conclusion agrees with the meta-analysis performed by Tian et al. [34]. They also compared navigation systems to conventional free-hand methods and found that the best pedicle screw accuracy rate came from 3D fluoroscopy navigation.

MIS has evolved increasingly within the last decade in the field of spine surgery. Proponents of MIS versus open surgery support that it leads to reduced blood loss, shorter recovery, and less postoperative pain, while minimizing soft-tissue dissection and maintaining the structural integrity of the paraspinal muscles. Issues relating to the required learning curve,

operating time, and radiation exposure to patients and operating staff associated with MIS have been widely studied in the literature.

Different approaches have been developed to increase pedicle screw accuracy and minimize the potential harm of a misplaced pedicle screw to vascular, neural, and other structures[35-42]. Several studies have shown that image-guided surgery significantly improves pedicle screw insertion compared to conventional non-assisted approaches [35, 38, 43-46]. With the development of image-assisted procedures, radiation exposure of patients and operating staff is a great concern. Image-based spine navigation is expected to increase pedicle screw accuracy while decreasing the amount of radiation, but conflicting evidence is reported in the literature [47-62]. In a meta-analysis comparing minimally invasive (MI)-TLIF and open surgery, Tian et al. concluded that MI-TLIF resulted in less blood loss and shorter hospital stay but was associated with greater intraoperative X-ray exposure[63]. We have been using MI-TLIF with intraoperative 3-dimensional fluoroscopy (io3DF) since 2009 and our surgical technique is the basis of the method in the present thesis.

To achieve solid fusion, a bone graft is often used. Several types of bone substitutes and bone grafts have been used to perform spinal fusion. Bone morphogenic protein (BMP) has successfully been used in spinal fusion. The commercially available form is the recombinant human (rh) BMP-2 approved by the US Food Drug and Administration for use in anterior lumbar interbody fusion within a titanium tapered cage[64, 65]. All other uses are considered off label. Catastrophic complications have been reported upon utilization of the rhBMP-2 including malignancies[66, 67], heterotopic ossification[68], early fusion graft lucency, subsidence, endplate resorption,

cage migration[69], dysphasia, and dysphonia[70]. Another limitation of the use of BMP is its highcost compare to other allografts.

An ideal bone graft will have osteoconductive, osteoinductive, and osteogenic properties [71]. Autologous iliac crest bone graft has these properties, and has long been considered the optimal source of bone graft material for spinal fusion, providing reliable results in various procedures [72]. Unfortunately, iliac crest bone harvesting is associated with several disadvantages [73, 74] and a relatively high risk of pseudarthrosis in up to 10-15% of all patients [75]. The incidence of complications ranges from 9.4% to 49%, with that of major complications ranging from 0.7% to 25% [76-81]. Autologous iliac crest grafts can provide fusion rates ranging from 87% to 100%, but because of donor site morbidity, research has focused on finding a novel alternative. Tissue engineering may offer the ultimate solution for replacing iliac bone grafts.

Over the last decade, research on adipose mesenchymal stem cells (AMSCs) has increased considerably [82-89]. Osteodifferentiated AMSCs have been used in humans, but prior to the present research, not in spinal fusion.

1.1.2.1.3.3 Disc arthroplasty

The third surgical option to treat CLBP is disc arthroplasty with increased popularity as an alternative to fusion. Nevertheless, there is no evidence to suggest that the use of disc arthroplasty results in better short- or long-term functional outcomes than fusion in properly selected patients [90, 91].

1.1.2.1.3.4 Spinal neuromodulation

Finally, a subset of patients suffering from CLBP may present with so-called failed back surgery syndrome (FBSS). FBSS describes a situation

in which the outcome of the spine surgery does not meet the pre-surgical expectations of the patient and surgeon. It may be caused by inaccurate patient selection, technical failure, or surgical complications and sequelae, and encompasses pain driven by both nociceptive and neuropathic mechanisms, with axial low back pain and radicular lower limb distribution [92, 93]. Spinal cord stimulation is advocated as an advanced pain management therapy for patients with FBSS even though there is no clear evidence that it is an effective treatment for CLBP without a radicular component.

1.2 THESIS HYPOTHESIS

As evidenced by the above review, CLBP is a major health problem and one of the most common causes of disability worldwide. Treatment options are abundantly described in the literature, but the prevalence and burden remain critically high. Surgical fusion is one of the major strategies for CLBP therapy and has been evolving in the last decades with increasingly sophisticated technologies. Like other clinicians, we have moved from open surgery to MIS surgery. In this thesis, we assume that new technologies are likely to improve pedicle screw insertion while providing less radiation exposure to patients and operating room (OR) staff. For fusion, we have abandoned autologous bone graft harvested at the anterior or posterior iliac crest because of the associated complications. Our current graft material is demineralized bone matrix (DBM) which is a type I collagen matrix cleared for mineral bone and containing bone inductors. It is produced from human allographs. Knowing that the best graft is autologous, and to avoid a second surgical site and potential associated complications, we sought a novel source of autologous bone graft material.

In the present thesis, we formulate the following hypotheses:

The quality of spinal fusion depends on the quality of the grafting, surgical procedure and spinal stabilization with pedicle screws. Therefore, new technologies are likely to have a positive effect on improving spinal stabilization and, consequently, spinal fusion.

The development of new technologies would be correlated with safety for patients and caregivers, especially with regards to ionizing radiation exposure from the fluoroscopic devices.

New graft materials are required to overcome the limitations of existing grafts. The use of osteodifferentiated AMSCs will be at least comparable to iliac crest autografting without its drawbacks.

1.3 OBJECTIVES

To verify our hypotheses, the objectives were as follows:

To assess the influence of utilizing the combination of intraoperative navigation (ioNav) and io3DF for pedicle screw placement.

To compare a series of patients who underwent surgery with io3DF without the help of ioNav with another series who were operated on using both technologies in combination and determine the influence in terms of pedicle screw accuracy and radiation exposure of patients and OR staff.

To investigate the application of osteodifferentiated AMSCs in spinal fusion procedures.

The secondary objectives were the investigation of early changes occurring after spinal arthrodesis and stabilization, and evaluation of the major risks associated with lumbar spine surgery under conditions of minimal access.

Chapter 2 METHODOLOGY

2.1 STUDY DESIGN AND POPULATION

This study included patients who underwent lumbar spinal fusion at the Cliniques Universitaires Saint-Luc hospital between October 2009 and December 2016. During that period, 241 patients underwent lumbar spine surgery. In this department, spine surgery is mainly performed by two senior surgeons. To avoid patient selection bias, we excluded all patients operated on by any other surgeons, which was a total of 58. Among the remaining patients, 15 were excluded for other reasons, resulting in 168 patients for analysis.

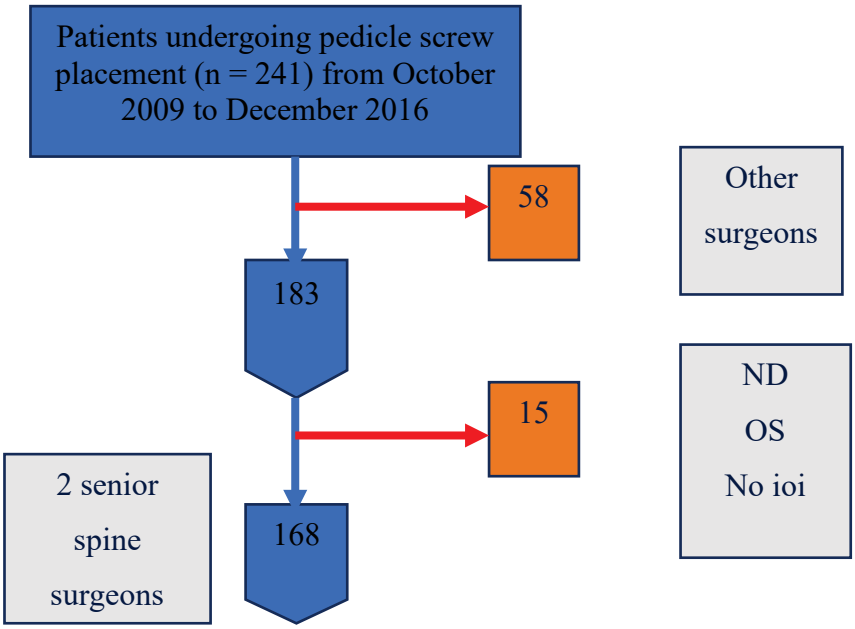

Figure 2-1: Patient' selection flow chart

ND, non-degenerative cases; OS, open surgery; ioi, intraoperative imaging.

Table 2-1: Clinical characteristics of our population

Variables	Group 1	Group 2	*P* Value
Number	102	66	
Sex			
Female	65 (63.7)	37 (56.1)	>0.05
Male	37 (36.3)	29 (43.9)	>0.05
Age, years, mean	57.9 (SD 14.2)	58.4 (SD 13.9)	>0.05
Min	20	23	
Max	83	85	
BMI, kg/m^2, mean	26.9 (SD 4.0)	26.8 (SD 3.9)	>0.05
Min	18.9	20.3	
Max	40.9	36.7	
Pain			
Lumbar	66 (64.7)	40 (60.6)	>0.05
Radicular	27 (26.5)	21 (31.8)	>0.05
Mix	9 (8.8)	5 (7.6)	>0.05
VAS	7.5 (SD 1.6)*	7.3 (SD 1.5)†	>0.05
Min	2	3	
Max	10	10	
Motor deficits	16 (15.7)	8 (12.1)	>0.05
Operative indications			
Spondylolisthesis	50 (49)	30 (45.5)	>0.05
Disc arthrosis	35 (34.3)	26 (39.4)	>0.05
Other	17 (16.7)	10 (15.1)	>0.05
Previous lumbar surgery	31 (30.4)	24 (36.4)	>0.05
Disc hernia	11 (10.8)	13 (19.7)	>0.05
Lumbar stenosis	13 (12.8)	4 (6.1)	>0.05
Other	7 (6.9)	7 (10.6)	>0.05
Screws per patient			
2	1 (1)	1 (1.5)	>0.05
4	87 (85.3)	59 (89.4)	>0.05
5	1 (1)	0 (0)	>0.05
6	11 (10.8)	5 (7.6)	>0.05
8	1 (1)	1 (1.5)	>0.05
9	1 (1)	0 (0)	>0.05
Screws per level	438 (100)	276 (100)	
L1	2 (0.5)	0 (0)	>0.05
L2	3 (0.7)	4 (1.4)	>0.05
L3	31 (7.1)	10 (3.6)	>0.05
L4	132 (30.1)	68 (24.6)	>0.05
L5	190 (43.4)	128 (46.4)	>0.05
S1	80 (18.3)	66 (23.9)	>0.05

Data in parentheses are percentages except where noted to be SD.
Min, minimum; Max, maximum; BMI, body mass index; VAS, visual analog scale.
*Data missing for 2 patients.
†Data missing for 1 patient.

Data in parenthesis are percentage except where noted to be SD
Min, minimum; Max, maximum; BMI, body mass index; VAS, visual analog scale.
*, Data missing for 2 patients
**, Data missing for 1 patient

Among the 168 patients finally included, 102 were operated on using io3DF alone and 66 using a combination of io3DF and the ioNav system. The research included three main phases: two prospective and one retrospective:

The first prospective phase investigated the accuracy of percutaneous pedicle screw placement in a subgroup of patients operated on using both io3DF and spine navigation.

The second prospective phase investigated the application of an autologous osteodifferentiated AMSC graft in spinal interbody fusion. In the index study, the radiological fusion was assessed.

The third phase of our research, we compared a subgroup of patients operated on using io3DF alone and patients operated on with the assistance of io3DF in combination with ioNav. Percutaneous pedicle screw accuracy, intraoperative radiation, surgical duration, and complications were assessed.

A rare specific complication of MISS is also reported.

2.2 INTRAOPERATIVE IMAGING

From 2009 to 2013, we used the Artis Zeego® 3D fluoroscopy robotic system (Siemens, Erlangen, Germany) without any navigation. Data on surgical and radiological outcomes at our institution during this period have been published [94]. In September 2013, we acquired the new-generation Artis Zeego, the Zeego Q. Since then, all of our procedures involving pedicle screw placement have been performed using that device.

We started using ioNav in November 2013 when we acquired a Curve® navigation system with infrared tracking camera (Brainlab, Munich, Germany).

All pedicle screws were implanted using the VIPER 2 from Depuy Synthes®. In all cases, a transforaminal approach for discectomy and percutaneous pedicle screw was used, according to the following workflow:

The transforaminal approach to the disc was performed on the side of radicular symptoms, if any. If there were none, then it was performed from the surgeon's preferred side. The procedure was performed under 2D fluoroscopic verification. io3DF was acquired after the discectomy and images were automatically downloaded to the navigation system.

Using dedicated software on the navigation station, screws were registered and implanted under navigation control.

The next step consisted of intraoperative verification using the Zeego system. The senior surgeon assessed the accuracy of the pedicle screw placement using the classification system of Wang et al. [95] commonly used to assess percutaneous pedicle screw (PPS) accuracy [96]. Penetration of the internal, external, superior, or inferior cortical walls of the pedicles was measured in millimeters. Briefly, violations were defined as grade 0, no pedicle breach; grade 1, violation ≤2 mm; grade 2, violation of 2–4 mm; and grade 3, violation ≥4 mm. As it was previously demonstrated that there is no clinical or structural difference between screws with a cortical violation <2 mm and those without perforation [97], we decided not to change the position of screws with a grade 1 violation.

2.3 RADIATION RISK AND ASSESSMENT

It is well demonstrated with level 2 evidence radiation exposure is greater with MIS surgery compared with open procedures[98-101]. In a

prospective series, Fransen[99] gathered radiation dose and exposure time from various procedures, including percutaneous lumbar spine fusion, and found that fluoroscopic time for open pedicle screw placement was 44 seconds per procedure and 8 seconds per screw. Percutaneous pedicle screw placement was 145 seconds per procedure and 27 seconds per screw. The average radiation exposure per screw was 3.2 times higher when performed percutaneously as compared with the open procedures.

Spine surgeons should have basic knowledge regarding the quantification of ionizing radiation. Being aware of radiation exposure risk, especially while performing MIS surgeries, they can potentially minimize these risks by optimizing utilization of the fluoroscopic devices by increasing the distance between the surgeon and the radiation ionizing device and using barriers and advanced image guidance navigation-assisted technologies[102].

Radiation doses from fluoroscopic use are measured in two ways, the direct dose and the effective dose. The direct dose is the dose delivered to the skin or organ from the ionizing radiation device measured in milliGrays. Radiation injuries to the skin from fluoroscopy are always located on the X-ray tube side of the body. The effective dose is the dose related to the relative risk of cancer measured in Sieverts. The sievert, named after the Swedish medical physicist Rolf Maximilian Sievert, measures the amount of energy emitted by the radiation per a given amount of tissue mass.

The traditional unit of radiation dosage applied to humans is the rem (Roentgen equivalent man) defines as the dosage in rads that will cause the same amount of biological injury as one rad of X-rays or gamma rays. Sievert replaces rem to allow for comparisons across different imaging modalities

and distributions across the body. The ionizing physical radiation dose absorbed is measured in grays (Gy), the international unit named after the British physicist Louis Harold Gray. One sievert equals 100 rem and one rem equals 0.01 gray. Therefore, one sievert equals one gray.

For basic understanding of direct dose and effective dose, a single posterior anterior chest radiograph delivers a direct skin dose of 140 mGy to the posterior chest. The effective dose, multiplied by the weighted factor, is 0.03 mSv. A chest CT dose is 7 mSv [103, 104]. A lumbar radiograph is 1.5 mSv and a lumbar CT is 15 mSv [105]. The maximum dose of radiation exposure is regulated nationally and internationally and must be understood by the spine surgeon, who may be exposed daily to radiation.

Radiation-related variables were collected from the Zeego software. The device reports all doses delivered to a patient during the procedure. For our initial series, surgeons systematically wore a dosimeter, which was subsequently abandoned upon the acquisition of the ioNav. When using the Curve spine navigation system, the dosimeter of the surgeon did not show any radiation, as controlled and confirmed by the radio-physiologic department. Notably, the OR staff left the operating theater during 3D image acquisition.

2.4 COMPLICATION ASSESSMENT

We assessed any side effect of the surgery immediately and during the hospital stay. All patients were seen for outpatient consultations at 3 months (earlier if required, though this was rare).

2.5 STATISTICAL ANALYSIS

For quantitative variables, the mean values, standard deviations (SD), and maximum and minimum values were analyzed using a t-test. For qualitative variables, the Fisher's test was used. *P* values less than 0.05 were considered to indicate statistical significance

2.6 SUMMARY OF THE SURGICAL TECHNIQUE

Key steps in the minimally invasive TLIF procedure (MI-TLIF) as performed during the research period

The TLIF approach is a 360° procedure that preserves the laminar arch. Because TLIF is most often unilateral, it also preserves the contralateral articular facet, which helps to avoid potential complications associated with bilateral access. Although this procedure aims to reduce surgical complications, it is certainly not without risks. It is surgically demanding and requires intricate anatomical and surgical knowledge. **Error! Reference source not found.** through **Error! Reference source not found.** (below) describe the surgical room and the different phases of the procedures from installation to screw placement.

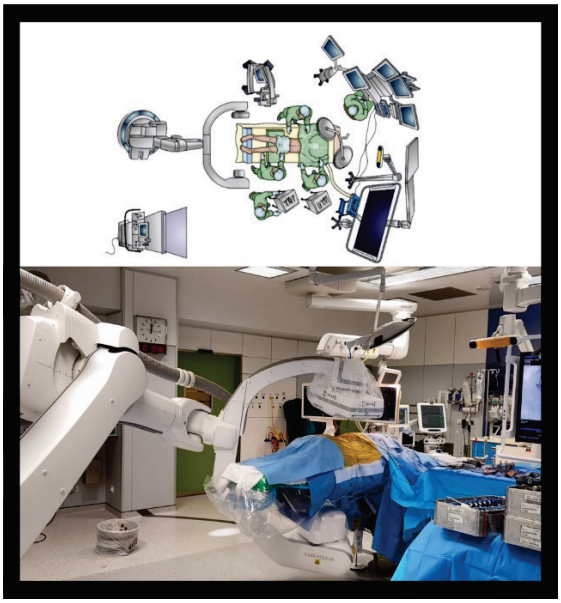

Figure 2-2: OR setup

The patient lies feet first and prone in reference to the 3D fluoroscope. The senior surgeon stands on the side of the TLIF. The navigation system is positioned cranially near the anesthetist.

Figure 2-3: Incision

The incision is made at the level of the facet joint to be resected/fused, 4 to 5 cm from the midline to allow the surgeon to work obliquely into the spinal canal from outside the pars interarticularis and to easily place pedicle screws. The distance from the midline is related to the size of the patient.

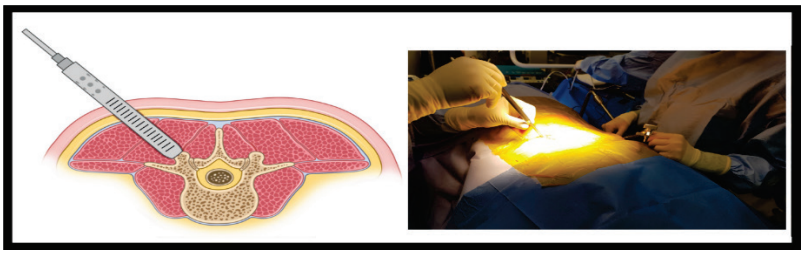

Figure 2-4: Insertion of muscle dilators

Sequential dilation is performed by passing successively larger dilators over the one previously inserted. It is recommended that the depth is measured from the second or third dilator as they will be flush to the bone and produce the most accurate measurement. The depth should be determined at the point where the skin contacts the dilator, and the appropriate retractor size should be selected based on the measured depth

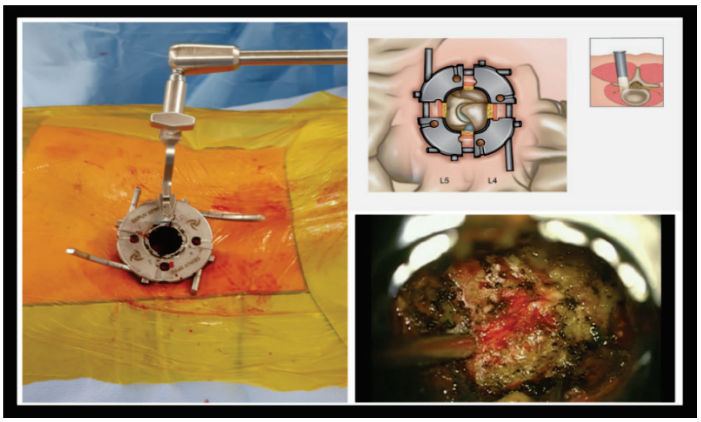

Figure 2-5: Visualization of the articular process.

Microscopic visualization gives excellent magnification and illumination, which allows for identification of the inferior articulating facet.

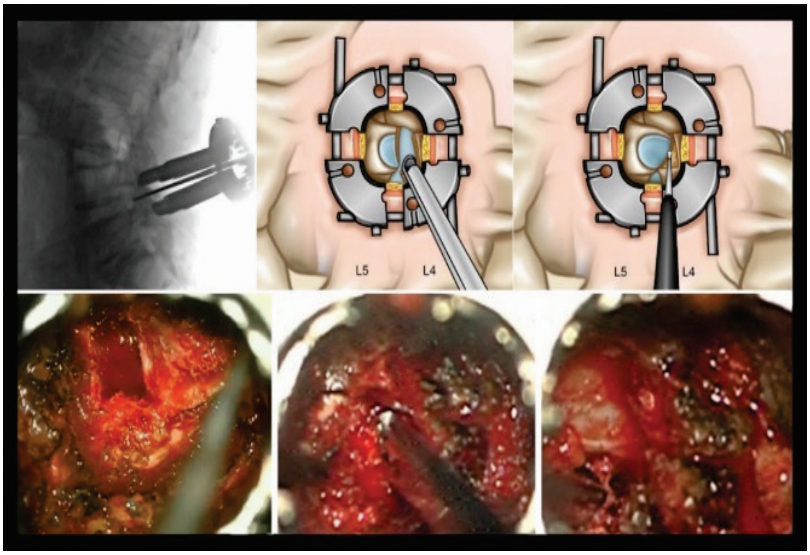

Figure 2-6: Opening of the articular processes.

The superior facet is resected from its tip down to the superior border of the pedicle, and the inferior facet is also resected to expose the ligamentum flavum overlying the disc. The ligamentum flavum is resected using Kerisson forceps.

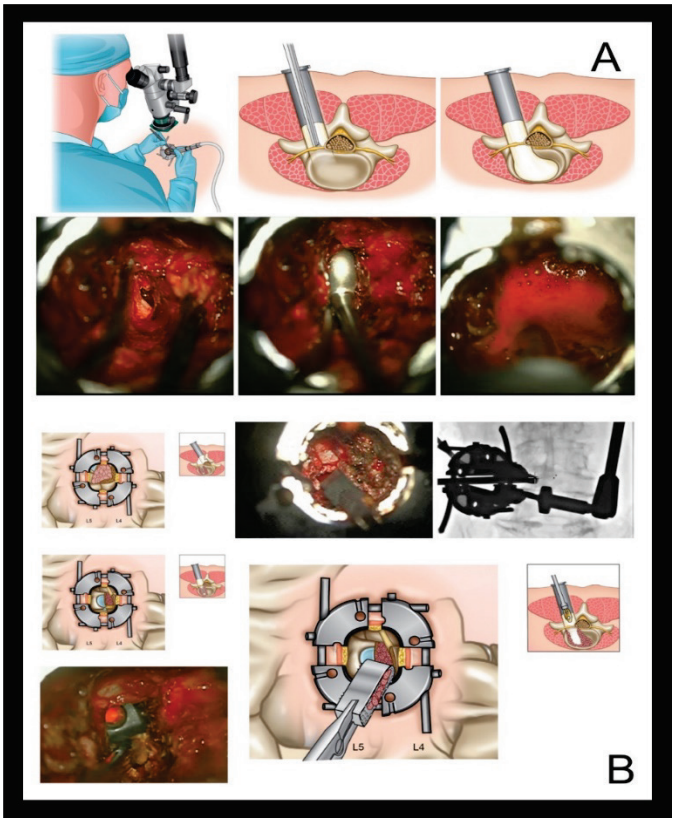

Figure 2-7: Discectomy, grafting, and cage insertion

A: Following removal of the ligamentum flavum under the microscope, the disc can be seen at the floor of the spinal canal. The exiting nerve root passes under the remaining pars interarticularis at the superior margin of the field. A thorough discectomy is then performed. Cartilage from the vertebral endplates is removed to expose the bony endplates. The disc space can be visualized and rinsed with iodine solution.

B: Morselized demineralized bone matrix is placed into the anterior portion of the discectomy space. The discectomy space was filled with a structural implant containing additional bone graft material.

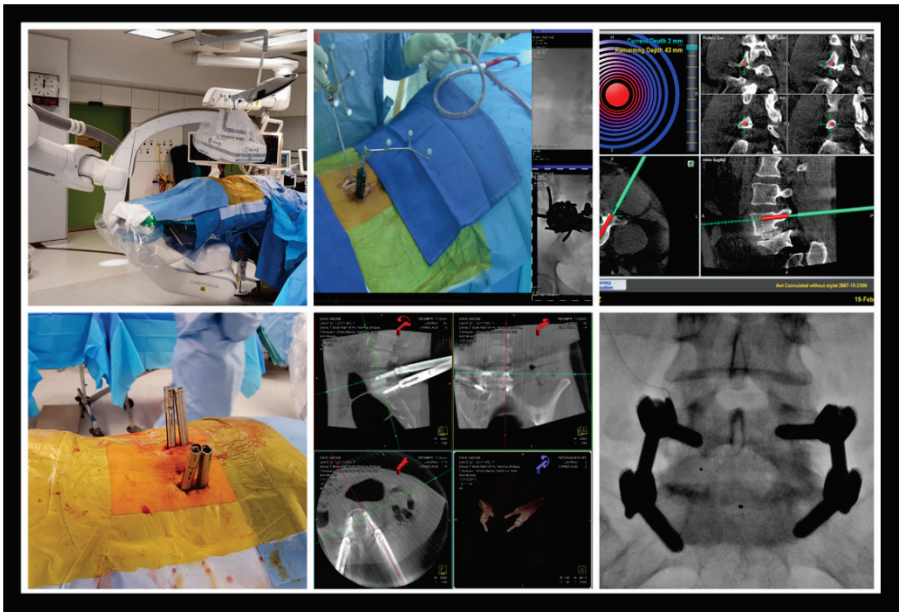

Figure 2-8: Osteosynthesis under io3DF and ioNav

The io3DF is performed and automatically transferred to the navigation system. The pedicle screws are registered and placed using spine navigation. A final io3DF is performed and the accuracy of pedicle screw placement is checked before insertion of rods and closure of the wound.

Chapter 3 PEER-REVIEWED PUBLICATIONS ARISING FROM THIS RESEARCH

3.1. Spine Navigation Based on Three-Dimensional Robotic Fluoroscopy for Accurate Percutaneous Pedicle Screw Placement: A Prospective Study of 66 Consecutive Cases. **Fomekong E**, Safi SE, Raftopoulos C. *World Neurosurg.* 2017 Dec;108:76-83. doi: 10.1016/j.wneu.2017.08.149. Epub 2017 Sep 1. PMID: 28870824

3.2. Comparative Cohort Study of Percutaneous Pedicle Screw Implantation without Versus with Navigation in Patients Undergoing Surgery for Degenerative Lumbar Disc Disease. **Fomekong E**, Pierrard J, Raftopoulos C. *World Neurosurg.* 2017 Dec 20. pii: S1878-8750(17)32196-4. doi: 10.1016/j.wneu.2017.12.080. PMID: 29274453

3.3. Application of a three-dimensional graft of autologous osteodifferentiated adipose stem cells in patients undergoing minimally invasive transforaminal lumbar interbody fusion: clinical proof of concept. **Fomekong E,** Dufrane D, Berg BV, André W, Aouassar N, Veriter S, Raftopoulos C. *Acta Neurochir (Wien)*. 2017 Mar;159(3):527-536. doi: 10.1007/s00701-016-3051-6. Epub 2016 Dec 30. PMID: 28039550.

3.1 SPINE NAVIGATION BASED ON THREE-DIMENSIONAL ROBOTIC FLUOROSCOPY FOR ACCURATE PERCUTANEOUS PEDICLE SCREW PLACEMENT: A PROSPECTIVE STUDY OF 66 CONSECUTIVE CASES

Fomekong E, Safi SE, Raftopoulos C

3.1.1 Summary of the study

The objectives of this study were to showcase our unique spine-dedicated OR utilizing io3DF in combination with spine navigation. Several items were assessed, including pedicle screw accuracy, radiation exposure to patients and OR staff, learning curve, and complications associated with the setup. We hypothesized that this OR setup would help reduce radiation exposure to patients and enable surgeons to achieve a better accuracy rate for pedicle screw placement than previously reported.

We prospectively included 66 patients diagnosed with CLBP refractory to optimal conservative management. They all underwent surgery using Siemens Zeego 3D fluoroscope in combination with the Brainlab navigation system. Patients' mean age was 59 years, and 58% were female.

The final pedicle screw accuracy was 99.6%, no measurable radiation exposure to surgeons and OR staff could be detected, and there were no procedure-related complications.

We concluded that our results compared favorably with the literature.

3.1.2 Published Paper

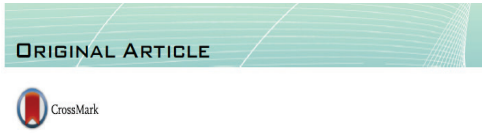

Spine Navigation Based on 3-Dimensional Robotic Fluoroscopy for Accurate Percutaneous Pedicle Screw Placement: A Prospective Study of 66 Consecutive Cases

Edward Fomekong, Salah Edine Safi, Christian Raftopoulos

Abstract

Background: Minimally invasive spine surgery is associated with obstructed visibility of anatomical landmarks and increased radiation exposure, leading to higher incidence of pedicle screw mispositioning. To address these drawbacks, intraoperative three-dimensional fluoroscopy (io3DF) and navigation are being increasingly used. We aimed to present our dedicated multifunctional hybrid operating room (HyOR) setup and evaluate the accuracy and safety of io3DF image-guided spinal navigation in transforaminal lumbar interbody fusion with percutaneous pedicle screw (PPS) placement.

Methods: The HyOR includes a fixed 3D multi-axis robotic fluoroscopy arm that moves automatically to the preprogrammed position when needed. An initial io3DF assessment is performed to collect intraoperative images, which are automatically transferred into the navigation system. These data are used to calibrate the PPSs and insert them under computer-assisted navigation. A second io3DF is performed for verifying PPS position.

Results: Between January 2014 and December 2016, 66 consecutive patients (age, 58.6±14.1 years) were treated for refractory lumbar degenerative pain. Seventy-three spinal levels were treated, and 276 screws were placed, with 4.2±0.76 screws per patient. There was no measurable radiation to the HyOR staff, while the mean radiation dose per patient was 378.3 μGym2. The overall accuracy rate of PPS placement was 99.6%. There were no significant procedure-related complications.

Conclusions: Spine navigation based on io3DF images enabled us to avoid radiation exposure to the OR team while delivering minimal but sufficient radiation doses to our patients. This approach achieved an accuracy rate of 99.6% for PPS placement in the safe zone, without significant complications.

Introduction

Percutaneous pedicle screw placement is widely used as a minimally invasive spine surgery technique (MISS). However, MISS precludes direct visualization of key anatomical landmarks, which may lead to malpositioning of pedicle screws [106]. Most spine surgeons are more familiar with the open approach to the spine; nevertheless, even for the open technique, the rate of misplaced screws remains high, ranging from 10% to 31% in large series of patients [37, 51, 107, 108]. To increase pedicle screw precision and overcome the disadvantages associated with the lack of visibility of anatomical landmarks during MISS, computer-assisted technologies have been developed over the past two decades, becoming increasingly adopted in clinical practice [39, 109-111]. Innocenzi et al. recently demonstrated that navigation ensures greater accuracy in open as well as percutaneous procedures [112]. Compared to

conventional fluoroscopy, computed tomography (CT)-based fluoroscopy entails less radiation exposure to both the surgical staff and the patient [113, 114]. At our institution, we have developed an operating room (OR) setup dedicated to optimizing the integration of imaging investigations during MISS procedures in spinal surgery. The new OR setup includes the second-generation Zeego 3D fluoroscope (Artis Zeego; Siemens, Erlangen, Germany) and the latest BrainLAB Curve navigation system (BrainLAB, Munich, Germany). We hypothesized that this OR setup would help reduce radiation exposure to patients and enable surgeons to achieve a better accuracy rate for pedicle screw placement than previously reported.

Therefore, the aims of the present study were to showcase the setup of this unique hybrid OR and to report our experience with such tools in terms of pedicle screw accuracy, radiation exposure, and complications in a prospective series of patients. To the best of our knowledge, no study has reported the outcomes of OR setups involving a combination of the Zeego II and BrainLAB Curve navigation system for spinal pedicle screw insertion.

Materials and Methods

Between January 2014 and December 2016, we prospectively enrolled 66 patients who underwent transforaminal lumbar interbody fusion (TLIF). The present study received approval from our local ethical committee under the number 2016/I2AOU/365. All patients provided informed consent for undergoing the procedures.

Setup of our multifunctional hybrid OR

We previously reported our experience with percutaneous pedicle screw (PPS) placement using a robotic three-dimensional (3D) fluoroscope, namely the-first generation Artis Zeego system (Artis Zeego I; Siemens Healthcare, Erlangen, Germany) [94]. On the basis of our experience with intraoperative three-dimensional fluoroscopy (io3DF) and several years of using the BrainLAB navigation system, we have set up an OR, equipped with second generation of Zeego (Artis Zeego II) and BrainLab curve navigation system (Fig. 1). The setup that aims to facilitate spinal procedures when instrumentation is required (Fig. 2). Our new OR is multifunctional. Specifically, while it is mainly used for performing spinal procedures, the OR can also be used for various other procedures including oncology-related procedures (surgeries for brain tumors), functional surgery (deep brain stimulation), and epilepsy surgery (placement of intraparenchymal electroencephalography electrodes). The 66 patients included in our study underwent TLIF access for placement of a cage filled with autogenous bone graft mixed with demineralized bone matrix. The hybrid OR includes a fixed 3D multi-axis robotic fluoroscopy arm that moves automatically to the preprogrammed position when needed. An initial io3DF assessment is performed to collect intraoperative images, which are automatically transferred into the navigation system. These data are used to calibrate the PPSs and insert them under computer-assisted navigation. A second io3DF is performed for verifying PPS position.

Recording and transferring io3DF images using the second-generation Artis Zeego system

The first-generation Zeego system was initially developed and optimized for cardiac surgery (interventional transfemoral aortic angiography, valve implantation, or percutaneous coronary intervention transarterial chemotherapy). It was used in our institution by cardiac surgeons in these indications. We recently acquired the new floor-mounted robotic multi-axis 3D Zeego II system (Fig. 1A), which implements a new approach for generating images (Q technology). Specifically, the Zeego II includes a new flat-emitter X-ray tube that generates powerful pulses with small focal spots, providing improved resolution in obese patients or for steep angulations. Additionally, it comes with advanced software applications to support precise guidance during interventions. In addition to increasing image quality and reducing radiation dose, the new Zeego comes with an interface that is easier to use and is equipped with an embedded proprietary software (syngo DynaCT; Siemens Healthcare) for acquiring CT-like images. Specifically, the Zeego II can be used as a standard C-arm for acquiring two-dimensional (2D) fluoroscopy images and, when needed, as an io3DF arm to obtain 3D volumetric CT-like images by automated rotation around the surgical table. To obtain 3D images during spine procedures, our system is configured to acquire 397 projection images during a 6-s spin cycle. During 3D image acquisition, all staff members (including the anesthesiologist) leave the OR to avoid radiation exposure. The acquired images are automatically transferred either to the dedicated workstation (Syngo X workplace; Siemens Healthcare) or to the BrainLAB navigation system via the hospital network. On each station, the images are automatically reconstructed to volumetric

multi-planar images or as volumetric rendering images ready to be used intraoperatively.

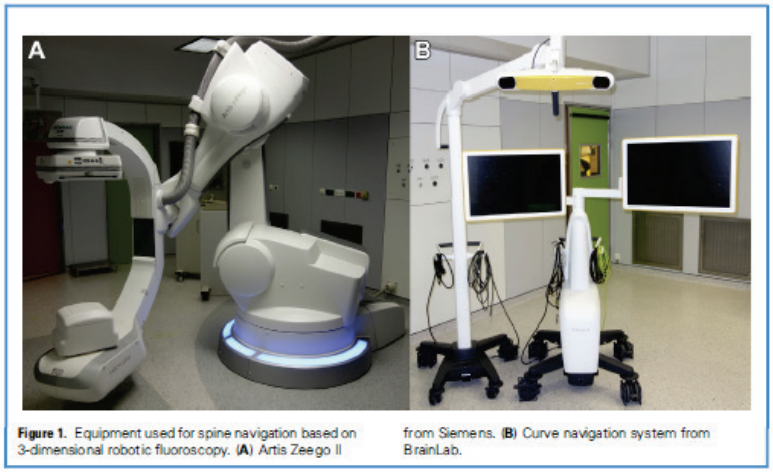

Figure 1. Equipment used for spine navigation based on 3-dimensional robotic fluoroscopy. **(A)** Artis Zeego II from Siemens. **(B)** Curve navigation system from BrainLab.

Figure 3-1: Hardware used for the research

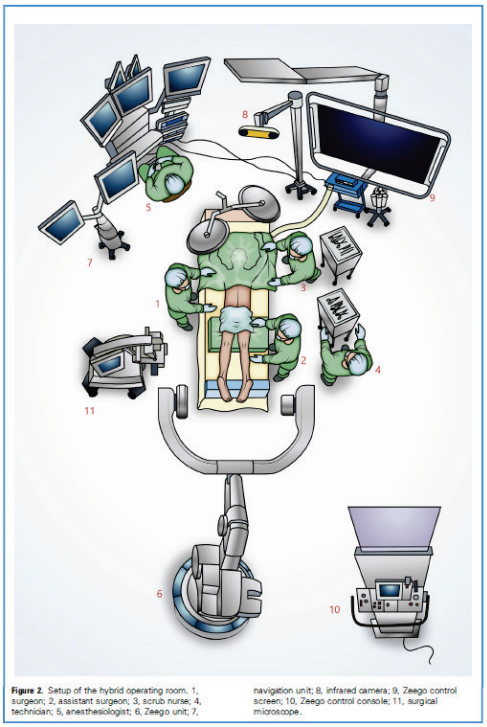

Figure 2. Setup of the hybrid operating room. 1, surgeon; 2, assistant surgeon; 3, scrub nurse; 4, technician; 5, anesthesiologist; 6, Zeego unit; 7, navigation unit; 8, infrared camera; 9, Zeego control screen; 10, Zeego control console; 11, surgical microscope.

Spine navigation using the BrainLAB system

The OR setup also includes an infrared tracking camera navigation system, namely BrainLAB Curve (Fig. 1B). BrainLAB has its own 3D navigation software (Spine & Trauma 3D), which uses a patient reference in the form of a small array of spherical markers that reflect infrared beams emitted by the camera (patient reference array). The patient reference array is usually attached to a spinous process of one of the affected vertebrae. The automatic image registration module uses a pre-calibrated isocenter definition (stored in the built-in BrainLAB Curve software) marked by flat infrared markers located on the detector side of the Zeego C-Arm. All infrared markers need to be visible to the stereoscopic infrared camera of the BrainLAB Curve navigation system. Right before the Zeego system acquires images to be sent to the navigation system, BrainLAB detects the location of the C-arm with respect to that of the patient reference array. The automatic image registration module then receives the cone-beam CT data from the Zeego system. Because of the spatially pre-calibrated isocenter, the navigation software can superimpose the cone-beam CT image onto the patient reference array. The Zeego system C-arm is then retracted to its preregistered standby position so that spine navigation may proceed begin without any manual intervention such as surface matching or point referencing.

PPS placement using the Viper 2 system

PPS placement was performed with the Viper 2 System (DePuy Synthes Spine, Raynham, MA) using a combination of spinal navigation and io3DF image guidance. The Viper system comes with awls, probes,

screwdrivers, and taps pre-calibrated for use after a few validation steps performed by the BrainLAB software. For the system to navigate an instrument, its axis and diameter must first be calibrated, then verified. To be calibrated and used, the instrument must have a marker array with the reflective marker spheres attached on the corresponding pins and visible to the infrared camera of BrainLAB. The verification step is a fully automated process for pre-calibrated instruments, whereas standard instrumentation needs to be calibrated intraoperatively using an instrument calibration matrix (ICM4) from BrainLAB and verified manually. All screws used in this setup are cannulated to be passed over the Kirschner wires (K-wires).

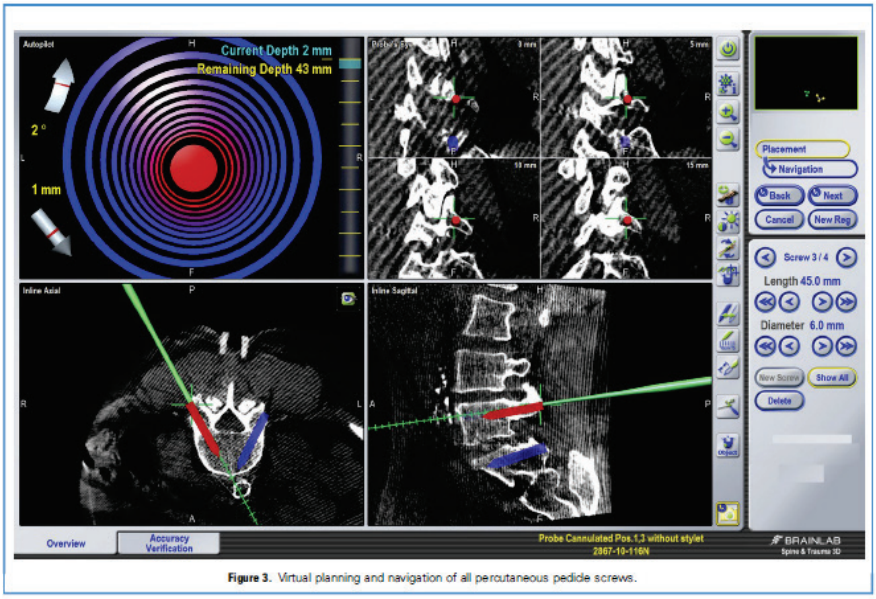

Figure 3. Virtual planning and navigation of all percutaneous pedicle screws.

Figure 3-2 : Registration and navigation of pedicle screws

Assessment of PPS placement accuracy

To assess the accuracy of PPS placement, we employed a grading system based on 2-mm increments in pedicle violation. This system is the

most widely used and accepted method to evaluate screw misplacement based on CT scans. Because the images obtained with the Zeego II are CT-like, and because PPS placement is performed without direct visualization of the screw position, we assessed PPS placement in terms of the grade of pedicle violation, as described by Wang et al [95]: grade 0, no pedicle breach; grade 1, violation ≤2 mm; grade 2, violation of 2–4 mm; and grade 3, violation ≥4 mm. Penetration of the internal, external, superior, or inferior cortical walls of the pedicles was measured in millimeters. A senior neurosurgeon evaluated the accuracy of the PPS position on the Zeego workstation immediately after the final io3DF was performed. Before the present manuscript was written, an independent physician not involved in the surgery reviewed all cases to double check the pedicle violation grades. All discrepancies between the original evaluation of the surgeon and the evaluation provided by the independent physician were discussed until consensus was achieved.

Our workflow and surgical technique

The indications for TLIF and PPS placement were chronic low back and/or leg pain resulting from degenerative disc disease or isthmic spondylolisthesis refractory to conservative medical management. We recently described our surgical technique in previous papers [94, 115]. In brief, the steps are as follows. (1) After inducing general anesthesia with endotracheal intubation, patients were placed in the prone position on a Maquet OR table feet first (i.e., with the feet beside the base of the Zeego II system; Fig. 2). (2) Two-dimensional fluoroscopy was performed to delineate the region of interest, and the nearest spinous process was identified to insert the navigation reference array. (3) Through a 2-cm midline incision, the spinous process was dissected. The reference array was firmly attached to the

spinous process and then oriented cranially towards the infrared camera. (4) Subsequently, the BrainLAB navigation software was used to set up the 3D image acquisition protocol, and the appropriate 3D pre-set program was selected on the Zeego II console. (5) Using the console, the Zeego was sent to the region of interest to perform the automatic 3D test procedure. A final check of the navigation screen confirmed that the software appropriately registered the position of the C arm. A short, 6-second apnea was induced during 3D image acquisition as the C-arm rotated around the patient, and the images were automatically transferred to the navigation system. (6) We then verified the concordance between the 3D images and the patient reference array, followed by planning, storage, and fine-tuning of all screw characteristics (length and diameter) according to the size of each pedicle (Fig. 3). (7) A 2-cm skin incision was made 4–5 cm from the midline at the level of each targeted pedicle, and a metallic guide-wire was then inserted through a pedicle finder. (8) A double-check step could then be performed using 2D fluoroscopy after inserting all the Kirschner guide-wires, to avoid inserting multiple guide-wires into the same pedicle in patients with severe degenerative deformities. (9) The placement of corresponding screws was performed after manually drilling the pedicle entrance if the screw was not self-drilling. (10) After placing all the screws, a final io3DF evaluation was performed to grade the screw placement within the pedicle, which was assessed using the Zeego workstation. (11) The rods system was measured and inserted, and instrumentation was completed. (12) Hemostasis was verified, and two-layer closure of the aponeurosis and skin was performed

using dermal glue at the surface. When TLIF arthrodesis was necessary, an additional 2D fluoroscopy step was usually performed before the aforementioned steps to ensure a safe TLIF approach and adequate intervertebral cage insertion. In our experience, navigation is usually not necessary for creating TLIF access and cage placement. Radiation exposure to the surgeon was limited in the aforementioned 2D fluoroscopy step (step 2), which required proximity of the surgeon and patient. Hence, the risk of radiation exposure of the surgical team was limited by acquiring 3D images remotely from the patient, with the manipulator standing behind a security screen far from the Zeego II X-ray source. The surgeon wore a dosimeter that was subsequently analyzed by the radio-physiology department. To avoid unnecessary radiation exposure, all members of the surgical team left the OR during the 6 seconds of 3D image acquisition.

Table 1. Patient Characteristics

Characteristic	Number	%
Patients	66	100
Female	38	57.6
Male	28	42.4
Age (years) ± SD	58.6 ± 14.1	
BMI	36.7 ± 3.9	
VAS (mean)	7.2	
ODI (mean)	43.2	
Levels and frequency of involvement in surgery		
L2-L3	2	2.7
L3-L4	4	5.5
L4-L5	35	47.9
L5-S1	32	43.8
Total number of levels operated in all patients	73	100
Distribution of screws		
L2	4	1.5
L3	8	2.9
L4	68	24.8
L5	130	47.4
S1	64	23.4
Total number of screws	274	100
Average screw per patient	4.2	
Radiation (dose in µGym2)		
Average number of 3D scans per patient	2.3	
Average dose to surgeon and OR team	0	
Average radiation delivered by 2D fluoroscopy	49.2	
Average radiation delivered by 3D Fluoroscopy	329.2	
Average total radiation dose to patient	378.3	
Average total radiation dose to patient per 3D fluoroscopy	143.1	

SD, standard deviation; BMI, body mass index; VAS, visual analogue scale; ODI, Oswestry disability index; 3D, 3-dimensional; OR, operating room; 2D, 2-dimensional.

Results

Sixty-six patients were operated on using the newly developed workflow. Table 1 shows the baseline characteristics of our case series. There were 38 women (57.6%) and 28 men (42.4%). The mean age and body mass index were 58.6±14.1 years and 26.7±3.9 kg/m^2, respectively. Preoperatively, the pain score was 7.2±1.8 on the visual analog scale, and the Oswestry disability index was 43.2±14.2. Seventy-three vertebral levels were operated on in total. Two hundred seventy-six pedicle screws were implanted.

Radiation exposure

Cumulative radiation exposure to the surgeons remained below measurable levels (<0 millisievert). After the first surgeries performed in the new OR, the senior surgeon's dosimeter was analyzed by our hospital's radio-physiology department, who found undetectable levels of radiation. The cumulative mean radiation exposure per patient was 378.3 μGym^2, and the average radiation exposure per patient during 3D image acquisition was 329.2 μGym². The mean number of 3D scans was 2.3±0.7 per patient (Table 1). In fact, as explained previously, each patient needed at least two 3D scans, one for image registration and another one for final evaluation of pedicle screw position before closure. At the beginning of the series, additional io3DF was often done after Kirschner guide-wires were placed in the pedicles, before implantation of the screws. This step is currently rarely performed.

Pedicle screw accuracy

In total, 263 pedicle screws had no violation (grade 0), 10 screws had a grade 1 violation, and 1 screw had a grade 2 violation. No grade 3 violations

Table 2. Screw Position Evaluation Inside the Pedicle by Vertebral Level

	Vertebral Level						
Grade	L2	L3	L4	L5	S1	Total	%
0	3	7	66	125	64	265	96.0
1	1	3	2	4		10	3.6
2				1		1	0.4
3						0	0.0
Total	4	10	68	130	64	276	100

were observed in this series. As it has been demonstrated that there is no clinical or structural difference between screws with a cortical violation <2 mm and screws without perforation [97], we decided not to change the position of the screws with grade 1 violation. The final check of all 276 screws demonstrated an accuracy rate of 96% associated with our strategy of using a combination of 3D fluoroscopy and spinal navigation. Of the 10 screws with grade 1 violations, seven had external violation. A single screw with grade 2 violation caused internal breach in the left L5 pedicle; however, the patient did not have any complaint postoperatively. No revision surgery was needed because of screw misplacement.

Complications

Postoperative complications included three dural tears that occurred during a TLIF procedure. All tears were sutured immediately, and no further incidents were noted. Two other patients had complications, namely persistent L5 hypoesthesia in one patient and urinary retention in the other. However, both manifestations resolved under gabapentin medication by the 3-month follow-up visit (outpatient consultation). A postoperative workup involving magnetic resonance imaging and CT scans did not reveal the cause of the adverse events. However, it is likely that these symptoms improved as a result of gabapentin treatment.

Discussion

The present study demonstrated that the use of computer-assisted navigation to implant PPSs based on intraoperatively acquired 3D fluoroscopic images can provide an accuracy rate of up to 96% and dramatically reduce the radiation exposure to surgeons and patients. Specifically, total radiation exposure times for patients were reduced by performing the main surgical procedure using a virtual 3D interface on the navigation system. The radiation exposure of the surgeon was undetectable. Since the long-term effects of chronic exposure to X-rays remain unclear [116-118], this technical development is of vital importance. Use of CT-based guidance for percutaneous procedures has been successfully demonstrated in spinal biopsy [119], percutaneous discectomy [120], kyphoplasty [121], aspiration of spinal cysts [122], and during the implantation of pedicle screws [113, 123-126]. Navarro-Ramirez et al. [127] recently published a technique using a similar, but not identical, OR design, and they reported a pedicle screw accuracy of 99% (grades 1 and 2). In fact, in their series, 6.4% of screws had grade 1 violation. If we summate the screws with violation of grade 0 or 1, the pedicle screw accuracy in the present series becomes 99.6%. In agreement with our observations, Villard et al.[128] showed that 3D fluoroscopy-based spinal navigation for lumbar fusion significantly reduced the radiation exposure to surgeons by up to 9.96-fold compared with that associated by freehand techniques.

In a systematic review of the literature published between 1980 and 1993, Yu and Khan [102] found that radiation exposure was higher during MISS procedures than during open procedures. However, use of a computer-assisted navigation system with 3D virtual pedicle screw planning

circumvented the disadvantage of having spinal anatomic landmarks obscured, and hence, prolonged X-ray exposure during surgery was no longer required to improve accuracy. In a study of four cadavers, Smith et al. [129] compared surgeon radiation exposure during C-arm fluoroscopy and computer-assisted image guidance for implantation of pedicle screws, and showed no measurable radiation exposures using navigation, and no differences in the accuracy of screw placement was observed between the techniques.

The present observations suggest that, in experienced hands, omission of the final io3DF step will further reduce radiation doses, and the present calculations demonstrate that one io3DF step delivers 143.1 μGym² to the patient. No dosimeter was applied to the surgeon's face to measure eye exposure, which represents a limitation of the study. However, because the measurements from the dosimeter worn by the surgeon in few cases at the beginning of the series showed undetectable exposures, we presume that eye exposures were likely negligible. Furthermore, the entire surgical staff left the OR to avoid radiation exposure, as the 3D fluoroscope could be activated remotely. By following that protocol, wearing lead-shielded vests during surgery was no longer necessary, as demonstrated by other authors [130, 131].

In the present procedure, performing spinal navigation based on the Zeego II 3D fluoroscopy system reduced the number of intraoperative fluoroscopic acquisitions required. Although 3D scans require greater patient radiation exposures than do 2D acquisition, only two io3DF were required for the entire procedure, thus reducing total radiation exposure. In contrast, assessment of screw positions was performed using additional 3D fluoroscopy at the end of the surgery in patients in whom navigation was not

performed, and most fluoroscopic images were taken in the lateral view, which requires higher doses for good image quality [132]. Therefore, the present navigation technique reduces the radiation exposure to patients during PPS implantation.

Finally, we examined the learning curve evolution over time in our consecutive series of 66 patients. The total operative time for the first 33 patients was 280±84 minutes, compared to 227±56 minutes for the next 33 patients ($p < 0.001$).

Conclusions

The use of computer-assisted navigation based on intraoperative robotic 3D fluoroscopic images increased the accuracy of PPS implantation and decreased total radiation doses to undetectable levels for staff in the OR, which represents one of the key improvements over the OR setup we described in the past.[13] Additionally, our special OR setup offers a very easy-to-handle workflow of PPS placement. The accuracy of PPS placement upon surgery completion was 99.6% (pedicle violation grade 0 or 1), and no permanent complications were noted in this series.

Acknowledgments

We would like to thank Miss Agne Andriuskeviciute for data collection

Conflicts of Interest statement

The authors declare that the article content was composed in the absence of any commercial or financial relationships that could be construed as a potential conflict of interest. Received 3 July 2017; accepted 23 August 2017 Citation: World Neurosurg. (2017) 108:76-83. http://dx.doi.org/10.1016/j.wneu.2017.08.149 Journal homepage: www.WORLDNEUROSURGERY.org Available online: www.sciencedirect.com 1878-8750/$ - see front matter ª

3.1.4 Highlights from this study

MISS is associated with increased radiation exposure.

Utilization of 3D fluoroscopy with navigation prevented radiation exposure to the OR team.

This approach also delivered minimal radiation doses to patients.

Finally, this approach achieved excellent pedicle screw placement accuracy.

3.2 PERCUTANEOUS PEDICLE SCREW IMPLANTATION WITHOUT VERSUS WITH NAVIGATION IN PATIENTS UNDERGOING SURGERY FOR DEGENERATIVE LUMBAR DISC DISEASE

Fomekong E, Pierrard J, Raftopoulos C

3.2.1 The rationale of the study

We began using the Siemens Zeego Q io3DF system in 2009. Our setup was an OR shared with cardiovascular surgeons. We were convinced of the usefulness of the device, but our access to it was limited. Therefore, we acquired the new-generation Artis Zeego Q® in 2013, along with the newly introduced Brainlab Curve® navigation system. We initially published the results of a series of patients operated on using the first-generation Artis Zeego[94]. To update our findings, we initiated a study to compare a series of patients operated on using io3DF alone with a prospective series of those operated on using a combination of io3DF and ioNav. We hypothesized that navigation-assisted PPS implantation provides a higher accuracy than conventional io3DF-guided PPS implantation.

3.2.2 Summary of the study

The major limitation of computer-based 3D fluoroscopy is an increased radiation exposure to patients and OR staff. Combining io3DF with spine navigation seems likely to overcome this shortcoming while increasing the pedicle screw accuracy rate. We compared data from a cohort of patients undergoing lumbar PPS placement using io3DF alone or in combination with spine navigation.

The study included 168 patients who underwent PPS implantation between 2009 and 2016. The primary endpoint was pedicle screw accuracy. The secondary endpoints were radiation exposure of patients and OR staff, duration of surgery, and postoperative complications.

We divided our population into two groups. Group 1 consisted of 102 patients in whom 438 screws were placed without navigation guidance. Group 2 was made up of 66 patients in whom 276 screws were placed with spinal navigation. The mean patient age in both groups was 59 years. The final pedicle accuracy rate was 98% in group 1 and 99.6% in group 2. The average radiation dose per patient was significantly greater in group 1 (571.9 $mGym^2$) than in group 2 (365.6 $mGym^2$) ($P = 0.000088$). The surgery duration and complication rates were not significantly different between the 2 groups ($P > 0.05$).

The study demonstrated that io3DF with spine navigation minimized the radiation exposure of patients and OR staff and provided an excellent PPS accuracy rate compared with io3DF alone, with no permanent complications. This setup is recommended particularly for patients with complex degenerative spine conditions.

3.2.4 The published paper


ORIGINAL ARTICLE

CrossMark

Comparative Cohort Study of Percutaneous Pedicle Screw Implantation without Versus with Navigation in Patients Undergoing Surgery for Degenerative Lumbar Disc Disease

Edward Fomekong, Julien Pierrard, Christian Raftopoulos

ABSTRACT

Background: The major limitation of computer-based 3D fluoroscopy is the increased radiation exposure of patients and the operating room (OR) staff. Adjunction of spine navigation to intraoperative 3D fluoroscopy (io3DF) can likely overcome this shortcoming while increasing the pedicle screw accuracy rate. Thus, we compared data from a cohort of patients undergoing lumbar percutaneous pedicle screw (PPS) placement utilizing io3DF alone or in combination with spine navigation.

Methods: This cohort study consisted of 168 patients who underwent PPS implantation between 2009 and 2016. The primary endpoint was to compare pedicle screw accuracy between the two groups. The secondary endpoints were to compare the radiation exposure of patients and OR staff, duration of surgery, and postoperative complications.

Results: A total of 438 screws were placed without navigation guidance (group 1) and 276 with spine navigation (group 2). The mean patient age in both groups was 58.6 ± 14.1 years. The final pedicle accuracy rate was 97.9% in group 1 and 99.6% in group 2. The average radiation dose per patient was significantly larger in group 1 (571.9 $mGym^2$) than in group 2

(365.6 mGym^2) (P = .000088). Surgery duration and complication rate were not significantly different between the two groups (P > .05).

Conclusion: The io3D fluoroscopy with spine navigation minimizes the radiation exposure of patients and the OR team and provided an excellent PPS accuracy rate with no permanent complications compared to io3DF alone. The setup is recommended, especially for patients with a complex degenerative spine.

INTRODUCTION

Percutaneous pedicle screw (PPS) fixation is a widely used effective method for performing fusion in the lumbar spine; however, the placement of screws can be technically demanding in terms of ensuring their adequate insertion in the pedicle. The percutaneous approach impedes efficient visualization of important anatomical structures and may cause multiple complications due to screw malposition in the pedicle [133-135]. In order to overcome this anatomical barrier, the use of a computer-based 3D navigation approach has increased significantly for spinal instrumentation [35, 39, 42, 109-111, 124, 136-139]. Cadaveric and clinical studies from multiple groups have shown that the accuracy of screw placement is improved by using an intraoperative navigation system [36, 43, 140-146]. Other recent reports based on computer-assisted fluoroscopy have demonstrated a relative reduction in radiation exposure compared to conventional fluoroscopy [113, 114]. We have developed a specialized operating room (OR) using intraoperative 3D fluoroscopy (io3DF) for spinal procedures and have recently acquired an intra-operative frameless spine navigation system to specifically optimize PPS implantation.

We aimed to compare the outcomes of utilizing io3DF alone versus its use in combination with spine navigation. We hypothesized that navigation-assisted PPS implantation provides a higher accuracy than conventional, io3DF-guided PPS implantation. Secondary endpoints were (1) exposure of patients and OR staff to radiation, (2) surgical duration, and (3) complications arising from the use of these modalities.

METHODS

Study design

This single-center cohort study had a total of 168 patients who were classified into two groups based on the usage of io3DF with or without the navigation system. Two senior surgeons performed the surgeries.

Participants

This study was conducted after receiving approval from our local ethics committee. All included patients provided informed consent. In group 1, a total of 102 patients with degenerative lumbar disc disease underwent surgery using the Artis Zeego® 3D fluoroscopy robotic system (Siemens, Erlangen, Germany) without any navigation. This setup is described in detail elsewhere.[26] These patients were operated on between October 2009 and December 2013. In group 2, the surgery was conducted on 66 patients who underwent PPS fixation between January 2014 and December 2016. The surgery in the latter group of patients utilized a new robotic multi-axis 3D Artis Zeego® Q along with an infrared tracking camera Curve® navigation system from Brainlab (BrainLAB, Munich, Germany). All patients in group 1, except two who only had PPS without an intervertebral cage, underwent

transforaminal lumbar interbody fusion (TLIF) access for placement of a cage filled with autogenous bone graft mixed with demineralized bone matrix followed by PPS instrumentation (Viper 2 System; DePuy Synthes Spine, Raynham, MA). In group 2, the procedure was performed using a combination of spinal navigation and io3D fluoroscopic image guidance. Based on our long-term experience in using these setups, we have established an HyOR that not only facilitates the PPS procedures but also various other surgical procedures that are not limited to brain tumors, deep brain stimulations, and intraparenchymal electroencephalogram electrode placement.

Patients operated for tumor, trauma, or deformities or using open access were not included in the study.

Surgical Procedure

We applied a surgical technique described in detail elsewhere [94, 115], with a few modifications. First, the patients were placed in the prone position on a Maquet OR table feet (with the ends of feet on the side of the base of Zeego®) after general anesthesia with endotracheal intubation. This was followed by intraoperative 2D fluoroscopy (io2DF) to delineate the region of interest. In group 1, projection of pedicle was marked on the skin using an io2DF. Appropriate lateral and anterior-posterior views were determined and stored in the Zeego® for automatic use during surgery. Using io2DF, each pedicle of interest was calculated for percutaneous insertion of a K-wire. After all K-wires were inserted, io3DF was performed again to verify the accuracy of implantation before screw placement into the pedicle. After the screw insertion, a final io3DF was performed as an ultimate check. In

group 2, the io2DF alone consisted of identifying the nearest spinous process to the region of interest. It was dissected through a 2-cm midline incision to allow a firm attachment of the navigation reference clamp, which was then oriented cranially to spare the field of view of the infrared camera. An io3DF was performed using the appropriate pre-set 3D program selected on the Zeego® Q console and Brainlab navigation software. After the navigation screen confirmed that the software had appropriately registered the position of C-arm, a short 6-s apnea was required during the 3D image acquisition (C-arm rotation around the patient), and the images were automatically transferred to the navigation system. The concordance between the 3D images and the patient was verified using a reference pointer. According to the size of each pedicle, the screw characteristics were planned, stored, and fine-tuned. A 2-cm skin incision was made 4–5 cm from the midline at the level of each targeted pedicle, and a metallic guide wire was then inserted through a pedicle finder. Due to the use of navigation system, there was no need for fluoroscopic control in this group before screw placement. The placement of corresponding screws was performed after manually drilling the pedicle entrance for non-self-drilling screws. In both groups, once the screws were placed, an ultimate 3D sequence was generated to grade the screw placement accuracy within the pedicles using the Zeego® workstation. Hemostasis was verified, and the two-layer closure of aponeurosis and skin was performed using dermal glue at the surface. When TLIF arthrodesis was necessary, an additional 2D fluoroscopy step was performed before the aforementioned steps to ensure a safe TLIF approach and adequate intervertebral cage insertion. Radiation exposure to the surgeon was limited in the aforementioned 2D fluoroscopy step, which required proximity between the surgeon and patient. Hence, the risk of

radiation exposure to the surgical team was limited by acquiring 3D images remotely from the patient with the manipulator standing behind a security screen far from the Zeego® Q X-ray source. The surgeon wore a dosimeter that was subsequently analyzed by the Department of Radio-Physiology. To avoid unnecessary radiation exposure, all members of the surgical team left the OR during the 6 s of 3D image acquisition.

Variables and Data Sources

To assess the accuracy of PPS placement, we employed a grading system based on 2-mm increments in pedicle violation, as described by Wang et al.,[95] which is commonly used for evaluating PPS placement accuracy [96]. Briefly, the violations were defined as grade 0, no pedicle breach; grade 1, violation ≤2 mm; grade 2, violation of 2–4 mm; and grade 3, violation ≥4 mm. Penetration of the internal, external, superior, or inferior cortical walls of the pedicles was measured in mm. As it was previously demonstrated that there is no clinical or structural difference between screws with a cortical violation <2 mm and those without perforation [97], we decided not to change the position of the screws with a grade 1 violation.

Therefore, for the analysis of the pedicle screw accuracy, grade 0 and grade 1 screws were combined. Similarly, grade 2 and grade 3 were combined as they both required intraoperative revision.

Table 3-1 : Distribution and accuracy of pedicle screws in operated vertebrae

Table 1. Distribution and Accuracy of Pedicle Screws Inserted at Various Spinal Levels Before and After Surgical Revision If Required and Pedicle Screw Accuracy in Groups 1 and 2

A. Distribution and Accuracy of Pedicle Screws Inserted at Various Spinal Levels Before and After Surgical Revision

	Before Surgical Revision									After Surgical Revision								
	L1	L2	L3	L4	L5	S1	Total	%	G0 + G1 (%)	L1	L2	L3	L4	L5	S1	Total	%	G0 + G1 (%)
Group 1																		
G0	0	1	20	110	154	74	359	82	93.5	0	1	20	112	159	76	368	84	97.9
G1	2	2	9	17	26	3	59	13.5		2	2	9	18	26	4	61	13.9	
G2	0	0	2	2	6	1	11	2.5		0	0	2	2	4	0	8	1.8	
G3	0	0	0	3	4	2	9	2.0		0	0	0	0	1	0	1	0.2	
Total	2	3	31	132	190	80	438	100		2	3	31	132	190	80	438	100	
Group 2																		
G0	0	2	5	66	124	64	261	94.6	97.1	0	2	6	67	128	64	267	96.7	99.6
G1	0	0	2	3	1	1	7	2.5		0	0	2	3	2	1	8	2.9	
G2	0	0	0	1	1	1	3	1.1		0	0	0	0	0	1	1	0.4	
G3	0	0	1	0	4	0	5	1.8		0	0	0	0	0	0	0	0.0	
Total	0	2	8	70	130	66	276	100		0	2	8	70	130	66	276	100	

B. Summary of Pedicle Screw Accuracy Assessment

	Group 1		Group 2	
	Before Revision (%)	After Revision (%)	Before Revision (%)	After Revision (%)
G0	82.0	84.0	94.6	96.7
G1	13.5	13.9	2.5	2.9
G2	2.5	1.8	1.1	0.4
G3	2.0	0.2	1.8	0.0
G0 + G1	95.5	97.9	97.1	99.6
G2 + G3	4.5	2.0	2.9	0.4

G0, screw perfectly in the pedicle; G1, 0 > screw pedicle violation ≤2; G2, 2 > screw pedicle violation ≤3; G3, screw pedicle violation ≥4.

A senior neurosurgeon evaluated the accuracy of PPS position on the Zeego® workstation immediately after the final io3DF was performed. Before the present manuscript was written, an independent physician not involved in the surgery reviewed all cases to double check the pedicle violation grades. The independent physician revised all the screws using the same concerted reading protocol that the surgeons used during intraoperative analysis. There were very few discrepancies. All discrepancies between the original evaluation of the surgeon and that of the independent physician were discussed until a consensus was achieved. Most often, the findings of the independent physician were used because he was not involved in the surgical procedure.

Table 3-2 : Demographic characteristics of our population

Table 2. Demographic Characteristics of Study Population

Variables	Group 1	Group 2	*P* Value
Number	102	66	
Sex			
Female	65 (63.7)	37 (56.1)	>0.05
Male	37 (36.3)	29 (43.9)	>0.05
Age, years, mean	57.9 (SD 14.2)	58.4 (SD 13.9)	>0.05
Min	20	23	
Max	83	85	
BMI, kg/m^2, mean	26.9 (SD 4.0)	26.8 (SD 3.9)	>0.05
Min	18.9	20.3	
Max	40.9	36.7	
Pain			
Lumbar	66 (64.7)	40 (60.6)	>0.05
Radicular	27 (26.5)	21 (31.8)	>0.05
Mix	9 (8.8)	5 (7.6)	>0.05
VAS	7.5 (SD 1.6)*	7.3 (SD 1.5)†	>0.05
Min	2	3	
Max	10	10	
Motor deficits	16 (15.7)	8 (12.1)	>0.05
Operative indications			
Spondylolisthesis	50 (49)	30 (45.5)	>0.05
Disc arthrosis	35 (34.3)	26 (39.4)	>0.05
Other	17 (16.7)	10 (15.1)	>0.05
Previous lumbar surgery	31 (30.4)	24 (36.4)	>0.05
Disc hernia	11 (10.8)	13 (19.7)	>0.05
Lumbar stenosis	13 (12.8)	4 (6.1)	>0.05
Other	7 (6.9)	7 (10.6)	>0.05
Screws per patient			
2	1 (1)	1 (1.5)	>0.05
4	87 (85.3)	59 (89.4)	>0.05
5	1 (1)	0 (0)	>0.05
6	11 (10.8)	5 (7.6)	>0.05
8	1 (1)	1 (1.5)	>0.05
9	1 (1)	0 (0)	>0.05
Screws per level	438 (100)	276 (100)	
L1	2 (0.5)	0 (0)	>0.05
L2	3 (0.7)	4 (1.4)	>0.05
L3	31 (7.1)	10 (3.6)	>0.05
L4	132 (30.1)	68 (24.6)	>0.05
L5	190 (43.4)	128 (46.4)	>0.05
S1	80 (18.3)	66 (23.9)	>0.05

Data in parentheses are percentages except where noted to be SD.
Min, minimum; Max, maximum; BMI, body mass index; VAS, visual analog scale.
*Data missing for 2 patients.
†Data missing for 1 patient.

After the accuracy analysis, we compared the precision of screw placement before and after surgical revision if required (Table 2).

Statistical Methods

We reported and compared the clinical characteristics between the two studied groups. The continuous variables were reported as mean ± standard deviation (SD). They were compared using the Student's unpaired t-test as well as maximum, and minimum. For qualitative variables, the Fisher's exact test was used. To analyze the learning curve, we used the Spearman correlation. A *P*-value less than 0.05 was considered to indicate statistical significance.

RESULTS

Participants

Demographic characteristics were similar between the two groups (Table 1).

A total of 438 screws were placed in group 1 and 276 screws were inserted in group 2. The L5 level was the most common site for pedicle screw placement in both groups.

Pedicle Screw Accuracy

In group 1, of the six screws with a grade 2 violation (L5), two were repositioned. In group 2, one screw with a grade 2 violation (L5) was replaced, and another (S1) was left in place as it did not endanger the nerve or its stability.

In each group, surgical revision decreased the rate of pedicle violation. Using the Fisher test, we found a statistically significant difference in group 2 (navigated) when comparing the combined grade 0 and grade 1 pedicle violations with the combined grade 2 and grade 3 violations ($P < 0.0001$). However, we found no significant difference in group 1 when analyzing the screw accuracy before and after intraoperative revision. Similarly, there was no difference between the two groups (group 1 vs group 2) before and after intraoperative revision.

After revision of screw placement, the overall pedicle screw accuracy (violation grade 0 or 1) increased from 93.5% to 97.9% in group 1 and from 97.1% to 99.6% in group 2.

Radiation Exposure

We observed a reduced level of radiation exposure not only to the patients but also to the surgeons and all OR staff. Radiation exposure was automatically evaluated using the io3DF device, Zeego®. During the procedure in group 1, the surgeon initially wore a badge dosimeter, which was subsequently analyzed by the Department of Radio-Physiology. The cumulative radiation exposure to the surgeon remained below measurable levels (<0 mSv). The average radiation exposure per patient was 571.6 ± 468.3 mGy in group 1, compared to only 365.6 ± 196.8 mGy in group 2 (Table 3), suggesting that PPS insertion using io3DF in conjunction with spine navigation is safer than using io3DF alone.

Table 3-3 : Mean radiation exposure

Table 3. Mean Radiation Exposure in Groups 1 and 2

	Group 1*	Group 2	*P* Value
Mean irradiation ($mGym^2$)	571.9 (SD 468.3)	365.6 (SD 196.8)	0.000088
Min	11.6	81.4	
Max	2570	1170	

Min, minimum; Max, maximum.
*Radiation data not available for 12 patients.

Operative Duration

The average surgical duration recorded by the anesthesiologist was defined as the time from infiltration and incision of the skin to the skin closure. The duration was recorded as 270 (SD 91) and 254 (SD 76) min in

groups 1 and 2, respectively demonstrates the evolution of our learning curve for the entire cohort of io3DF-navigated cases.

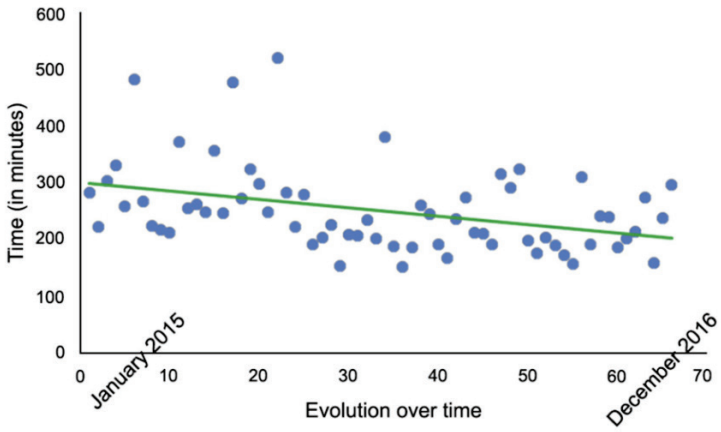

Figure 3-3 Learning curve.

Learning curve of the intraoperative three-dimensional fluoroscopy imaging guide associated with computer-assisted navigation for pedicle screw placement. Operative time displays a statistically significant ($P < 0.003$) negative linear trend over time, indicating a favorable learning curve.

Complications

We did not notice any permanent neurological injury due to pedicle breaches or misplacement of screws. The main complication observed was dural breach during surgery, with an incidence of 7.8% and 4.5% in groups 1 and 2, respectively; no significant difference was observed between the groups ($P > .05$). Of the 11 dural breaches, 9 occurred in patients who had undergone previous surgeries. It is well-established that reoperation on a previously operated spine increases the risk of dural breach. The dural breaches were diagnosed intraoperatively using the TLIF approach, most

often when the lumbar canal needed to be addressed. All were repaired immediately under a microscope. There were no breaches during pedicle screw placement. Apart from one patient who presented with postoperative ureteral perforation in group 1, all other complications were transient. These included one case of pulmonary embolism, one urinary incontinence/retention, one epidural hematoma requiring surgical evacuation, one superficial wound infection, and one intramuscular hematoma (not requiring an operation in one patient who was receiving anticoagulant therapy). In group 2, one patient complained of transient postoperative perineal hypoesthesia, urinary retention, and constipation and another suffered from cauda equine compression, which was due to early subsidence of the intervertebral cage (the cage shifted backwards), leading to cauda equine syndrome. The latter case was revised for cage replacement. Overall complications between the two groups did not show any statistical difference ($P > .05$). Table 4 summarizes the data on complications.

Table 3-4 : Overall complications

Table 4. Complications in Groups 1 and 2

Complications	Group 1	Group 2	*P* Value
Dura mater tear	8 (7.8)	3 (4.5)	>0.05
Other	6 (5.9)	2 (3.0)	>0.05
Ureteral perforation	1	0	
Pulmonary embolism	1	0	
Epidural hematoma	1	0	
Cage subsidence	0	1	
Urinary incontinence/retention	1	0	
Perineal hypoesthesia	0	1	
Superficial wound infection	1	0	
Intramuscular hematoma	1	0	
Total	14 (13.7)	4 (7.6)	>0.05

Data in parentheses are percentages.

DISCUSSION

Spinal fusion with pedicle screw insertion is an effective technique for stabilizing the spine. Its increasing use by multiple generations of surgeons yields a higher risk of misplacing the screw within the pedicle. Accurate placement of pedicle screw is important to avoid other complications with minor to major consequences, such as neurological impairments, postoperative radicular pain, dural tears, weakness, or even paralysis. In the initial report on the technique of pedicle screw insertion, Roy-Camille et al [147] reported up to a 10% occurrence of misplaced screws. Since then, a number of studies have reported inaccuracies in the placement of the pedicle screw ranging from 15 to 50% [35, 38, 43, 148-154]. In order to overcome this issue, computer-based image-guided systems have been introduced progressively

over the last two decades [39, 41, 43, 136, 137, 145, 155-157]. Computer-assisted technology aims to diminish pedicle breaches and hence minimize the risk of neurovascular injuries [57, 158-161]. In our department, we have been using io3DF since 2009 and have recently implemented a dedicated HyOR to ensure accurate spinal surgical procedures as well as other surgeries requiring io3DF and navigation facility. To the best of our knowledge, the results of using a similar HyOR (Zeego ® Q and Curve® navigation) have not been reported previously. To investigate whether navigation improves pedicle screw accuracy, Boon et al [162] evaluated the effect of using an O-arm and concluded that the device provided no noteworthy benefits in improving the accuracy of pedicle screw insertion or reducing complications in single-level spondylolisthesis patients compared to the free-hand technique. In the present study, we demonstrated that io3DF in conjunction with spinal navigation is helpful in increasing pedicle screw accuracy from 97.9 to 99.6% without major permanent complications. Navarro-Ramirez et al and Gelasis et al. [107, 127] showed that navigation makes spine surgery safer and more accurate. It is of note that if we had considered that grade 1 screw is a misplaced screw, then the Fisher test would reveal a statistically significant difference between the two groups before and after intraoperative revision. Nevertheless, non-significant difference would appear in each group when comparing before and after intraoperative revisions. In this setting, navigation appears to be associated with a theoretical statistical difference. The findings of the present study are consistent with the results of these previous studies.

PPS placement requires a minimally invasive spine surgery (MISS) technique. In MISS, targeted elements are hidden from the operator. Hence, during PPS procedures, the spine is unexposed and needs intraoperatively

acquired fluoroscopic images to be visualized. It has been well demonstrated that radiation time and doses increase while performing MISS [117, 163-166]. Similar to a study by Kim et al. [125], we found that navigation helps decrease radiation exposure to the surgeon, OR personnel, and even the patient. Our findings show that the radiation dose delivered to patients was significantly higher when io3DF was used alone than in conjunction with navigation ($P <$ .00008).

It is assumed that navigation increases the operative time because of the inevitable setup time of the device and the time needed to acquire and process the intraoperative images. To perform an easier comparison between the two groups, the mean surgical duration given above was considered for one-level procedures only, as TLIF at more than one level is likely to significantly prolong the surgical duration. Moreover, the given average time does not account for preparation time of the procedure in group 1 (non-navigated), which may be quite long because of the need to predetermine and save the Zeego® position in lateral and antero-posterior views before effectively starting the procedure. When using the navigation system, it was not necessary to pre-register the Zeego® Q position as screw implantation was completely based on spine navigation using the io3DF acquisition, which was automatically transferred to the Brainlab station. Nevertheless, we observed that the operative time was shorter in group 2. Furthermore, when we analyzed the surgical duration independently of the number of levels operated on, we observed that the difference between the two groups became statistically significant. In fact, when multiple levels were included, navigation appeared to reduce the operative time because of the need for practically acquiring lateral and antero-posterior views for all pedicles in non-

navigated cases. We also analyzed the effect of learning curve over time in our navigated cases. The mean time to process the first 33 cases was 280 (SD 84) min compared to 227 (SD 56) min for the next 33 cases ($P < .0013$). Meta-analysis of a few series in the literature did not reveal significant differences in the surgical duration by using navigation systems compared to control cases [160, 161]. Similar to Khanna et al. [167], we found that navigation helped reduce the operative time even after the learning curve phase. The same team analyzed the cost effectiveness of using minimally invasive TLIF performed at a single level with fluoroscopy versus CT navigation and showed similar clinical outcomes and costs at 6 months [168]. We did not evaluate the cost effectiveness in our study, but the findings of Khanna et al demonstrate that complex OR setup and the use of navigation does not necessarily increase cost to unacceptable levels. Due to our HyOR setting, a limited number of intraoperative image sets were required, and there was no need for the entire team to wear lead-shielded vests during surgery as the Zeego® could be activated remotely. A few authors have practiced similar protocols to reduce unnecessary radiation exposure to the surgeon and OR team [131, 139].

Limitations

This comparative study is partially retrospective (data from group 1) and therefore, suffers from some missing data. However, we believe that the overall results would not change significantly even if there were no missing data, as the relevant cases were widely distributed throughout the duration of this study. This eliminates, for example, the effect of learning curve of the device. Furthermore, we did not compare clinical outcomes with our excellent PPS placement rate. We plan to analyze this in future when we would have accumulated a sufficient follow-up time. Moreover, this comparative study

did not include financial aspects in terms of cost effectiveness analysis. Setting up a HyOR does cost money; however, this does not necessarily imply that the cost is substantially high. We work in a university environment and believe that a few complex cases referred to us deserve such investments for us to definitively offer acceptable therapeutic solutions to patients.

CONCLUSIONS

We aimed to compare the surgical effectiveness and safety of navigated and non-navigated PPS placement in degenerative lumbar disc disease. We demonstrated that the utilization of Brainlab Curve® spine navigation concurrently with the Siemens Zeego® Q io3DF for PPS placement provided an excellent PPS accuracy rate while significantly reducing radiation exposure to the patient, surgeon, and OR staff, with no increase in the operative time or rate of complications. Future studies are needed to corroborate these improvements in terms of clinical outcomes and to evaluate cost effectiveness.

Conflict of interest statement:

The authors declare that the article content was composed in the absence of any commercial or financial relationships that could be construed as a potential conflict of interest. Received 10 October 2017; accepted 13 December 2017 Citation: World Neurosurg. (2017). https://doi.org/10.1016/j.wneu.2017.12.080 Journal homepage: ww.WORLDNEUROSURGERY.org Available online: www.sciencedirect.com 1878-8750/$ - see front matter ª 2017 Elsevier Inc.

3.2.6 Highlights from this study

1. This cohort study compared PPS placement using io3DF alone or with spine navigation.

2. io3DF with spine navigation minimized radiation exposure in patients and OR staff.

3. The use of Brainlab Curve spine navigation concurrently with the Siemens Zeego Q io3DF system for PPS placement resulted in an excellent PPS accuracy rate.

4. No significant differences in efficacy, operating time, or complication rate were observed

3.3 APPLICATION OF A THREE-DIMENSIONAL GRAFT OF AUTOLOGOUS OSTEODIFFERENTIATED ADIPOSE STEM CELLS IN PATIENTS UNDERGOING MINIMALLY INVASIVE TRANSFORAMINAL LUMBAR INTERBODY FUSION: CLINICAL PROOF OF CONCEPT

Fomekong E, Dufrane D, Berg BV, André W, Aouassar N, Veriter S, Raftopoulos C.

3.3.1 The rationale of the study

Autologous bone is widely accepted as the gold standard graft material. It can be used in patients undergoing TLIF and intervertebral bone grafting [169, 170]. Unfortunately, the harvesting of autologous bone can be associated with persistent donor site pain, paresthesia, hematoma, and infection. Keller et al.[171] and Summers et al.[80] reported major complication rates ranging from 0.76% to 25%. Because of the risk of donor-site adverse events, a plethora of bone substitutes have been developed, including DBM, ceramics, and BMP [146, 172-174]. Their use is associated with complication rates ranging from 1% to 44% [40, 175-178], with reported complications including heterotopic bone formation, postoperative radiculitis, vertebral osteolysis, subsidence, and retrograde ejaculation [66, 178-181].

AMSCs have recently emerged as new bone graft source. Many authors have applied this source efficiently and safely as an alternative to bone tissue [89, 170, 182-185]. We developed a graft made of scaffold-free autologous AMSCs differentiated with DBM in a 3D osteogenic structure [87, 186]. We previously demonstrated the safety and efficacy of this graft in filling a critical-sized femoral bone defect in a preclinical pig non-union model at 6 months post-implantation, and in extreme clinical cases of bone tumor

resection and congenital/acquired bone nonunion up to 48 months post-transplantation [186, 187]. Complete stem cell differentiation in an osteogenic 3D structure improved the efficacy of bone reconstitution by promoting angiogenesis and osteogenesis and made the process safer by reducing the risk of growth factor release [89].

Encouraged by these results, we initiated this study to apply AMSCs to MI-TLIF in humans in the form of a scaffold-free osteogenic 3D graft. We hypothesized that AMSCs would achieve a good fusion rate in humans and could therefore be used as an alternative to other spinal fusion graft materials.

The specific methodology included fat tissue collection and graft manufacturing.

3.3.2 Fat tissue collection

Once a patient agreed to participate to the study and provided informed consent, a lipoaspiration procedure was scheduled. The aspiration was performed in the periumbilical area. The reference entry point was located 5–10 cm from the central point of the umbilicus (**Error! Reference source not found. Error! Reference source not found.**). From that point, stellar aspiration was performed until 10 ml of fat tissue was harvested. Care was taken not to perform aspiration too close to the umbilicus due to periumbilical innervation. To avoid inferior epigastric vessels and their perforating branches, aspiration was limited to the periumbilical zone.

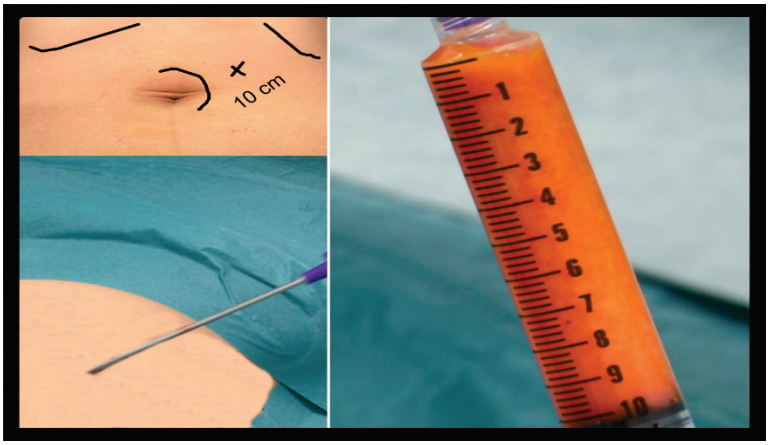

Figure 3-4: Lipo-aspiration

Subcutaneous fat tissue is harvested starting 5 to 10 cm from the center of the umbilicus. Suction should be avoided in the immediate area of the umbilicus because of innervation. A total of 10 mL is collected and sent to the local tissue bank for cell engineering.

3.3.3 Graft manufacturing

The fat tissue is transported to our local tissue bank for processing, which involves the following stages:

- Proliferation phase, during which adipose cells are isolated and seeded (human adipose stem cells are washed, rinsed, and expanded for 4 iterations) in the proliferation media
- Differentiation (cell osteogenic induction and differentiation)
- 3D induction phase by the addition of DBM
- Biopsy for quality control
- Visual inspection and preservation

The entire process requires 11 weeks: 4 weeks for cell growth, 3 weeks for cell differentiation and induction, and 4 weeks for cell preservation.

3.3.4 Summary of the study

We applied osteogenic 3D grafts made from autologous AMSCs in patients undergoing MI-TLIF. Of the nine patients from whom adipose tissue was collected, only three were implanted with a 3D graft. Six cell cultures failed due to unexpected hypercapnia in the proliferation medium. The final AMSC osteogenic product was stable, did not rupture with forceps manipulation, and was easily implanted directly into the cage with no marked change in operating time.

Clinical outcomes, including ODI and visual analog scale (VAS) scores, as well as fusion status, were assessed preoperatively and up to 12 months postoperatively. At 12 months, all operated levels treated with AMSCs (n= 4; two levels in one patient and one in one patient each) could be assessed. Grade 3 solid fusion (defined as the formation of a continuous bone bridge across the intervertebral space through or around the cage) was confirmed at two levels out of four. The mean pain score improved from 8.3 to 2, and ODI improved from 47% to 31%. These findings indicated a better quality of life for the index patient. No donor site complication was observed.

3.3.5 The published paper

Acta Neurochir
DOI 10.1007/s00701-016-3051-6

ORIGINAL ARTICLE - SPINE

Application of a three-dimensional graft of autologous osteodifferentiated adipose stem cells in patients undergoing minimally invasive transforaminal lumbar interbody fusion: clinical proof of concept

E. Fomekong ; D. Dufrane; B. Vande Berg ; W. André; N. Aouassar ; S. Veriter ; C. Raftopoulos

Abstract

BACKGROUND: The authors applied a scaffold-free osteogenic three-dimensional (3D) graft made of adipose derived mesenchymal stem cells (AMSCs) in patients undergoing minimally invasive transforaminal lumbar interbody fusion (MI-TLIF).

METHODS: Three patients (2 patients and 1 patient with 1 and 2 levels, respectively) with degenerative spondylolisthesis underwent MI-TLIF with 3D graft made of AMSCs. To obtain the AMSCs, fatty tissue was collected from the abdomen by lipoaspiration and differentiated afterwards in our Cell/Tissue bank. Clinical outcomes, including Oswestry Disability Index (ODI) and Visual Analog Scale (VAS) as well as fusion status were assessed preoperatively and up to 12 months postoperatively.

RESULTS: At 12 months, all four operated AMSC levels could be assessed (n=4). Grade 3 fusion could be confirmed at two levels out of four. Mean VAS score improved from 8.3 to 2 and ODI also improved from 47% to 31%. No donor site complication was observed. The final AMSC

osteogenic product was stable, did not rupture with forceps manipulation, and was easily implanted directly into the cage with no marked modification of operating time.

CONCLUSION: A scaffold-free 3D graft made of AMSCs can be manufactured and used as a promising alternative for spinal fusion procedures. Nevertheless, further studies of a larger series of patients are needed to confirm its effectiveness.

KEYWORDS: Adipose-derived mesenchymal stem cells, bone graft, spondylolisthesis, transforaminal lumbar interbody fusion, fusion rate.

Introduction

Spinal fusion procedures are widely used in the treatment of various morbidities, such as deformity, trauma, and degenerative disc disease, associated with instability.[188] Minimally invasive transforaminal lumbar interbody fusion (MI-TLIF) is now one of the most frequently used procedures.[189] Over the last few decades, autologous bone grafting has been used in patients undergoing MI-TLIF.[169, 190] This type of graft is considered the gold standard for spinal fusion, but it is associated with various adverse effects. The harvesting of autologous bone can be associated with persistent donor site pain, paresthesia, hematoma, and infection. Keller et al. and Summers et al. reported major complication rates ranging from 0.76% to 25%.[80, 171].

Bone substitutes, such as ceramics, bone morphogenic proteins (BMPs), and demineralized bone matrix (DBM), have been developed to prevent the problem of donor site morbidity. Ceramics are osteoconductive,

biodegradable bone graft scaffolds and should be combined with a local bone graft to enhance their osteoinductive and osteogenic potential.[172-174] BMP/INFUSE (Medtronic, Memphis, MN, USA), a potent stimulator of the differentiation of osteoprogenitor cells into osteoblasts, has been used as an iliac crest bone graft substitute in the spine, but many authors have reported complications associated with its application, ranging from 0.66% to 44%.[40, 175-178, 191] The rate or the nature of the complications differs according to the site of the fusion. Dysphasia and dysphonia have been reported for anterior cervical procedures whereas vertebral osteolysis, graft migration or subsidence, postoperative radiculitis and heterotopic or ectopic bone formation are more frequent in other spine regions. Other complications like retrograde ejaculations and hematoma formation have also been reported.[66, 178-181] Therefore, the Food and Drug Administration has issued a safety warning about the use of this product.[192] Derived from human allograft tissue, DBM has repeatedly shown osteoinduction power with fusion rates varying from 82.7% to 92.6% [193-195].

More recently, a new graft source, adipose-derived mesenchymal stem cells (AMSCs), has emerged and has proven to be more advantageous than autologous iliac crest bone. Zhu et al. showed that adipose tissue is more readily available and that stem cells can be obtained in large quantities. [185] Similarly, Whyles et al. recently published that the proliferation capacity was increased by fourfold in AMSCs compared with bone marrow-derived mesenchymal stem cells (BM-MSCs) after 20 days in culture.[183] Yang et al. demonstrated that one gram of abdominal fat tissue could yield up to around $1x10^6$ AMSCs.[184] In contrast, Pittenger et al. reported that of 6×10^6 cells aspirated from *bone marrow* only 0.001% to 0.01% appeared to be stem

cells.[182] Schubert et al. reported a shorter differentiation time for AMSCs than for BM-MSCs (6.1 ± 2.3 days vs. 9.0 ± 1.9 days, $P < 0.001$), similar immunomodulation capacities at the osteogenic differentiated and undifferentiated status, greater angiogenic properties in vitro and in vivo (19.6 ± 6.8 vessels/0.016 mm² vs. 10.9 ± 4.9 vessels/0.016 mm², $P < 0.005$), and greater osteogenic capacity (53.3 ± 7.9 cells/0.16 mm² vs. 19.1 ± 17.6 cells/0.16 mm², $P < 0.001$).[89] A review by Werner and coauthors highlighted the reliability and effectiveness of AMSCs as an alternative for bone tissue engineering.[170]

We developed a graft made of scaffold-free autologous AMSCs differentiated with DBM in a three-dimensional (3D) osteogenic structure.[87] We previously demonstrated the safety and efficacy of this graft in filling a critical-size femoral bone defect in a preclinical pig non-union model at six months post-implantation and in extreme clinical cases of bone tumor resection and congenital/acquired bone non-unions up to 48 months post-transplantation.[186, 187] Complete stem cell differentiation in an osteogenic 3D structure improved the efficacy of bone reconstitution by promoting angiogenesis and osteogenesis and made the process safer by reducing the risk of growth factor release.[89]

Encouraged by these results, we initiated the present study to apply AMSCs to neurosurgical spine procedures, namely MI-TLIF by using a scaffold-free osteogenic 3D graft (made of AMSCs) in humans. We hypothesized that AMSCs would achieve a good fusion rate in humans and would therefore, be used as an alternative to other spine fusion grafts.

Methods

Ethical approval was obtained from the Catholic University of Louvain Ethics Committee (N°B403201111681).

Patient population

From March 2012 through January 2014, we prospectively identified 58 patients eligible for TLIF. All patients had chronic low back and/or leg pain resulting from degenerative disc disease or isthmic spondylolisthesis and were refractory to medical treatment. The patients were divided into two groups, MI-TLIF (n = 28) or OPEN-TLIF (n = 30), based on the neurosurgeon's preference. MI-TLIF subjects were categorized according to whether or not they agreed to the AMSC protocol, and nine patients consented. Because of a technical problem during AMSC processing (hypercapnia of > 5% CO_2 in the incubator prevented cell growth), only three subjects (two females, one male) were implanted with AMSC during MI-TLIF procedures.

Patient' selection

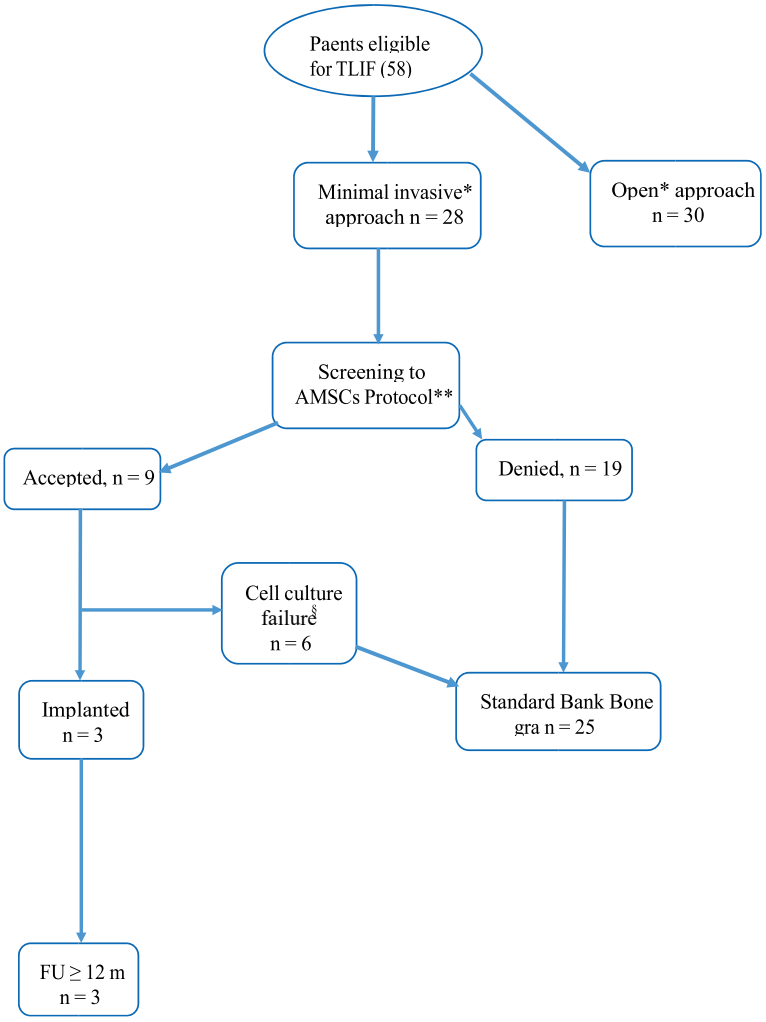

Figure 3-5 : Diagram showing the process of subjects selection

The outlined steps summarize the number of selected patients per group

*FU: follow-up; NA, not available; *, Depending on the surgeon; **, Patients were asked whether they agree to take part in the AMSC protocol or not. §, Insufficient quality of the native tissue harvesting and technical problem of cell incubator with abnormal CO_2 concentration.*

Table 1. Patient demographic data

Patient characteristics	*n* = 3
Gender	
Male	1 (33)
Female	2 (67)
Age (y) ± SD (range)	48.7 ± 14.3 (32-67)
Mean Pain duration (y, range)	2.3 (1-4)
< 1	0
1-2	2
> 2	1
TLIF level	*n* = 4
Single	2*
Two	1*
L4-L5	2 (50)
L5-S1	2 (50)
Diagnosis	
Lytic Spondylolisthesis	1 (33,3)
Degenerative Spondylolisthesis	1 (33,3)
DDD	1 (33,3)

DDD, degenerative disk disease
BB, bank bone
* , The figure refers to the number of patients undergoing TLIF in single or two level
SD, Standard deviation
TLIF, transforaminal lumbar interbody fusion
All figures in parenthesis are percentages if not indicated otherwise

Table 2. Fusion assessment at the operated

Nb of patients	n = 3
Total Nb of levels assessed (6 m and 12 m)	7
Nb of levels assessed at 6 months	3
Fusion grades (%)	
I	1 (33)
IIa	0
IIb	0
III	2 (67)
Nb of levels assessed at 12 months	4
Fusion grades (%)	
I	0
IIa	0
IIb	2 (50)
III	2 (50)

AMSCs, adipose-derived mesenchymal stem cells; Nb, number; m, month; BB, bank bone

Patients who refused the protocol as well as those who were not implanted because of the technical problem, underwent MI-TLIF with bank bone (BB) in the form of a combination of inactivated bone and DBM provided by the Cell/Tissue bank of our hospital (Center of Tissue and Cell Therapy, University Hospital Saint-Luc, Brussels, Belgium). The OPEN-TLIF subjects were not included in the study (Fig. 1).

Graft manufacturing

The tissue-engineered product is made of 2 major components: (a) allogenic demineralized bone matrix and (b) autologous adipose stem cells.

(a) Human DBM was provided by the musculoskeletal tissue bank and produced from multi-organ human donors. The diaphysis of femoral or tibial bone was cut and grounded into particles of size 200–700 μm for

demineralization. DBM was produced by grinding cortical bone from selected human donors (< 45 years old). First, human bone tissue was defatted in acetone (99%) bath overnight and then washed for 2 h in demineralized water. Decalcification was performed by immersion in 0.6N HCl for 3 h (20 mL solution per gram of bone) and agitation done at room temperature. The demineralized bone powder was then rinsed with demineralized water for 2 h and the pH measured. If the pH was too acidic, the DBM was buffered with 0.1 M phosphate solution again under agitation. Finally, the DBM was freeze-dried and weighed. The DBM was sterilized with 25 kGray by gamma irradiation at a temperature of −80°C.

The osteogenic properties of the DBM were assessed on representative batches by: (i) residual calcium concentration after the demineralization process (measured from the calcium contained in a mean of 1.3 g of DBM vs. non-demineralized bone powder from each donor) and (ii) osteoinduction one month after *in vivo* implantation in the para-vertebral musculature of nude rats (male, 6–8 weeks old) to quantify new bone formation (presence of bone marrow, osteoblast activity, and new bone formation) by histomorphometry (a standard 300 cross-grid for point counting under microphotography at 10× magnification; four non-overlapping areas per slide were studied) for demineralized vs. non-demineralized bone matrix.

(b) Autologous adipose stem cells were prepared as described by a cell bank [186, 187]. The Endocrine Cell Therapy Unit is recognized by the Belgian Federal Agency for Medicines and Health Products as a clinical laboratory for the processing of AMSCs. The AMSC expansion, and differentiation were performed in line with good manufacturing practices

(GMPs) and the ISO 9001-2008 quality management system. All AMSC isolation and expansion procedures were performed in grade A air-laminated flow located in a grade B clean room (validated annually by the ICCE SA, Elsene, Belgium) in accordance with Belgian Ministry of Health recommendations and European directives (regulation 1394/2007 for advanced cell therapy products). The environment for cell culture was checked by weekly particle counting (under static and dynamic conditions; Laser II Particle Counter, Particle Measuring Systems Germany GmbH, Darmstadt, Germany) and microbiological testing at each manipulation, as recorded in the "Graft Report".

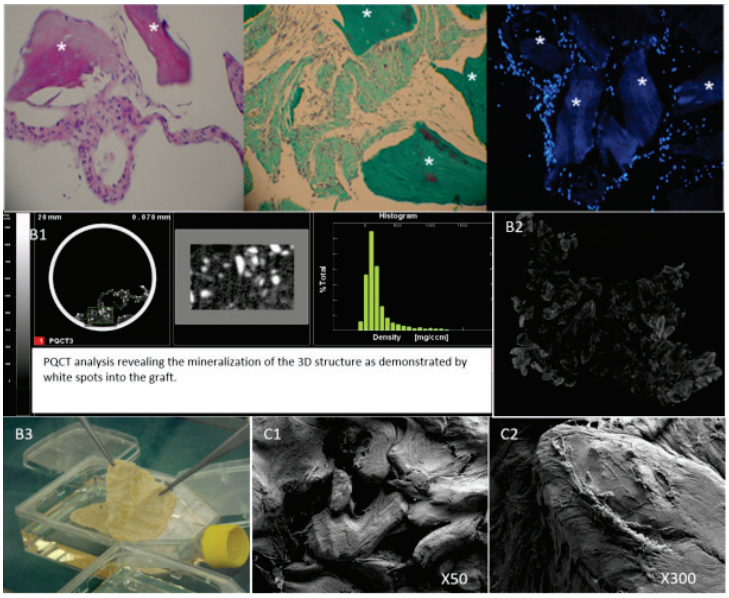

Figure 3-6 : Graft manufacturing steps

Fig. 2. **A.** The graft integrity (for the optimal 3D graft) was confirmed by an Hematoxylin-eosin staining (Left) with the integrity of the interconnective tissue (extracellular collagen matrix synthesized by adipose stem cells) between DBM (*) as shown by Masson's trichrome (Middle). The cellular viability of adipose stem cells inside the interconnective tissue was confirmed by DAPI staining (Right). B: The mineralization was confirmed pQCT (B1, white spot for calcium deposition). The 3D structure was confirmed by XCMT (B2). The final 3D structure is shown (B3) C: SEM demonstrated that DBM particles are linked by the interconnective tissue (C1) synthesized by adipose stem cells (surrounding DBM particles, C2).

The final 3-dimensional graft was obtained by multiple steps including:

The adipose tissue digestion and AMSC isolation.

For the isolation of human AMSCs, a mean of 4.4 g (range, 3.2–6.5 g) of fatty tissue was harvested under local anesthesia by lipoaspiration (following the Coleman technique in the abdominal region) from patients after informed consent and serologic screening. The adipose tissue was digested with GMP collagenase 0.075 g; 8000 PZ U/L; Serva Electrophoresis GmbH, Heidelberg, Germany. After sequential trypsinizations in a 75-cm^2 culture flask, AMSCs were then isolated and expanded in the proliferation media (Dulbecco's modified Eagle's medium supplemented with 10% heat-inactivated and viral-tested fetal bovine serum certified by the U.S. Department of Agriculture; Life Technologies, Grand Island, NY, USA) up to passage 5 (P5) within 50 ± 6 days to assess their properties in terms of in vitro mesenchymal differentiation capacity (adipogenesis, chondrogenesis, and osteogenesis) and surface markers (CD44, CD45, CD73, CD90, CD105) (see below).

The AMSC differentiation and constitution of the 3-dimensional graft.

At P5, AMSCs were incubated in 150-cm^2 culture flasks in osteogenic media composed of proliferation media supplemented with dexamethasone (1 µM), sodium ascorbate (50 µg/mL), and sodium dihydrophosphate (36 mg/mL). After 11 ± 0.6 days of incubation, DBM (10 mg/mL) was added to create a multi-dimensional structure that was ready to use for implantation straight from the plastic dish. The 3D graft was implanted after a mean of 40 ± 14 days of incubation in osteogenic media (after P5).

The 3D graft was rinsed three times with transplantation media (CMRL; Mediatec Inc., Manassas, VA, USA) without phenol red and without antibiotics or sera. The graft was finally placed in a sterile culture flask enclosed in three sterile plastic bags. The graft was then transferred at room temperature, in less than 15 min, to the operating room for implantation.

AMSCs (at P5) were tested in specific media to assess the capacity of differentiation towards the 3 main mesenchymal lineages. Confluent AMSCs cultures were induced to undergo osteogenesis by replacement of the proliferation medium with specific induction media for osteogenesis: proliferation medium supplemented with dexamethasone (1 µM), sodium ascorbate (50 µg/mL), and sodium dihydrophosphate (36 mg/mL). The medium was replaced every two days until differentiation could be demonstrated by alizarin red (for CaPO4 deposition) and osteocalcin (for bone phenotype).

The quality control testing of the cell therapy product.

A 20-mm^2 biopsy (on the day of transplantation) was fixed in 4% paraformaldehyde overnight. We normalized the integrity of the 3D-graft by the (DBM − ECM)/viable cell ratio (see above) between −1 and +1.

Cytogenetic stability was studied by karyotype and fluorescence *in situ* hybridization (FISH) analyses at P4 of the AMSCs (undifferentiated and differentiated) from the three patients, whose procedures were completed without technical problems, to assess the oncogenic safety of the cellular components of the 3D-graft. Metaphase chromosomes were obtained according to standard protocols from cultured AMSCs in the exponential growth phase after P4. Twenty Giemsa-Trypsin-Wright-banded metaphases were analyzed, and karyotypes were reported according to the 2013 International System for Human Cytogenetics Nomenclature.

A FISH experiment was performed using the P4 AMSCs (undifferentiated and differentiated) according to standard protocols to detect aneuploidy of chromosomes 7 and 8 using CEP7/D7Z1 (SpectrumGreen or SpectrumOrange) or CEP8/D8Z2 (SpectrumOrange or SpectrumGreen) probes (Abbot Molecular, Ottignies/Louvain-la-Neuve, Belgium).[196] At least 100 nuclei were counted, and the thresholds were calculated following the inverse beta law with a confidence interval of 99.9%.

Mycoplasma and endotoxin assays were also performed according to current GMP guidelines using TEXCELL SA (Evry, France) on cellular samples collected at P4 for undifferentiated and osteogenic cells (the last sample prior to graft delivery). Microbiological testing using BACTEC

assays was performed at each media change (twice a week during the manufacture of the graft) for aerobic, anaerobic, moisture, and yeast culture.

In-process controls (on cellular samples collected at P5 for undifferentiated and osteogenic cells up to the last sample prior to graft delivery) based on safety tests showed no microbiological or mycoplasmic contamination and no endotoxin content in any manufactured batch. Thus, all manufactured 3D grafts fulfilled the release criteria for implantation.

The characterization of the osteogenic 3-dimensional graft.

To assess the volumetric bone mineral density of the final 3D graft, peripheral quantitative computed tomography (pQCT, XCT Research SA, Sratec Pforzheim, Germany) and X-ray microtomography (Skyscan 1172 high-resolution desktop XCMT system; Skyscan, Aartselaar, Belgium) were performed on each sample. Two samples were analysed by SEM at magnification 50X and 300X to analyse the micro-architectural structure of the 3D graft. Interconnections between cells, ECM and DBM were observed and correlate to histomorphometrical analysis. Samples were fixed in Glutaraldehyde 2.5% and gradually dehydrated in an ethanol solution from 10% to 100%. Samples were then gold coated before observation.

Surgical procedure

Three months after AMSC graft manufacture, MI-TLIF was performed under general anesthesia. The patient was positioned prone on a radiolucent operating table. Localization and memorization of the vertebral segment and each targeted pedicle was performed by fluoroscopic Zeego 2D guidance (Siemens, Forchheim, Bavaria, Germany). An incision of 2 cm was

made 4–5 cm from the midline on the side where the most severe radicular compression was present. A tubular retractor (Pipeline; DePuy Spine, Johnson & Johnson, Arlington, USA) was docked to expose the targeted facet joint. After maximized discectomy, the disc space was filled with AMSC graft and a Concorde cage (DePuy Spine, Johnson & Johnson, Arlington, USA) filled with AMSCs was inserted into the disc space. Fluoroscopic Zeego 3D images were acquired to check for correct cage placement. Guide wires were then placed percutaneously into the pedicles under fluoroscopic Zeego guidance. Percutaneous pedicle screws (PPS) were inserted using the Viper 2 fixation system (DePuy Spine, Johnson & Johnson, Arlington, USA) and a Zeego 3D sequence confirmed their position. Rods were then slid into the screw heads and tightened. A para-midline "mirror image" incision was made on the contralateral side centered over the targeted pedicles. PPS and rods were connected by the same percutaneous system as that on the TLIF side.[94].

Clinical evaluation

Clinical outcomes were examined pre- and post-operatively and during follow-up visits using back and leg pain Visual Analogue Scales (VAS) and the Oswestry Disability Index (ODI).

Radiological evaluation of fusion

Multi-detector spiral CT images were obtained at 6 and 12 months after surgery in all patients implanted with AMSCs. A senior independent radiologist specializing in musculoskeletal radiology analyzed all images on a workstation using the multiplanar software from our Picture Archiving and Communication System. The fusion status of the relevant intervertebral disc

was graded: grade 3 (solid fusion) was defined as the formation of a continuous bone bridge across the intervertebral space through or around the cage; grade 2B was described as new trabecular bone extending from the end plates into the disc but without forming a continuous bone bridge; grade 2A was determined as relative prominence of the vertebral end plates due to subtle migration of the interbody space within the bony end plates; and grade 1 was given when there was no evidence of trabecular bone formation extending from the end plates.[197]

For the safety evaluation, the radiologist was asked to note any bone formation beyond the interbody cage and any bone resorption from the vertebral end plates.

Statistical analysis

Because of the small sample size, it seemed more statistically appropriate to use descriptive than inferential statistics. We accordingly report proportions of the interbody level disc fused, means (age, pain duration, VAS and ODI), and standard deviations. No statistical tests were performed.

Results

Graft characteristics

At P4, the characteristics of the human AMSCs were confirmed by differentiation into adipose, osteogenic, and chondrogenic phenotypes and by a significant shift in the mean fluorescence intensity curve (FACS) for CD44 (>99.9%), CD73 (>96%), CD90 (>98%) and CD105 (>97%). CD45 antigen expression was negative (<6%).

The quality of the human DBM was confirmed by significant reduction in calcium content (by a mean demineralization of 98%, $p < 0.005$) and by significantly higher *in vivo* osteogenesis (+11% of the explanted graft with osteoinductivity in representative DBM batches, $p < 0.05$) compared to non-demineralized cortical bone matrix.

A mean of 20 ± 4 million AMSCs per patient was available by the end of P4 and were sufficient for seeding into three culture flasks of 150 cm^2 for P5. Osteogenic differentiation was then induced at P5 for 15 days (when AMSCs were confluent) before supplementation with DBM at 10 mg/mL to create the 3D structure. All grafts showed a 3D structure prior to implantation. The 3D graft was implanted 89 ± 9 days after adipose tissue procurement. Two to three grafts of 3 × 3 cm^2 (one graft per 150 cm^2 flask) per patient were produced from AMSCs supplemented with 10 mg/mL DBM. The final product was stable and did not rupture with forceps manipulation (Fig. 2B3). The integrity of the 3D graft was assessed at the end of manufacturing by the histomorphometric potency score. A score between −1 and +1 (in terms of cellular content, inter-connective tissue integrity, and DBM content) was obtained for optimal 3D graft integrity (Fig. 2A).

According to pQCT, a significantly degree of mineralization was observed for ASCs incubated with DBM. The optimal concentration of DBM was adjusted with the anticipated function of the 3D construction to produce a sufficiently stable graft for manipulation with forceps and integration in a lumbar cage (Fig 2B1). The 3D structure of ASCs incubated with DBM, which was observed macroscopically, was confirmed by X-ray microtomography (Fig. 2B2). The characterization of the ultrastructure of the 3D graft, by scanning electron microscopy, demonstrated that the

interconnective tissue (synthesized by adipose stem cells) promotes the connection between DBM particles (Fig. 2C).

No complex numerical or structural clonal chromosomal aberrations were detected in the AMSCs developed for each graft at P1 and P4 (in both undifferentiated and differentiated status). Minor clones with structural aberrations detected in the undifferentiated AMSCs at P4 were absent from the differentiated AMSCs. Minority tetrasomies of both probes by FISH, suggesting tetraploidy, were found for undifferentiated AMSCs. Initial trisomy 8 was not detected, but minority tetraploidy (detected by the tetrasomies of both probes by FISH) was found after osteogenic differentiation.

Participants

Three patients received AMSCs. The average age of the population was 48.7 years, with an average pain duration of 2.3 years (Table 1).

No complications associated with surgery were reported. All of the cages were implanted successfully. After surgery, none of the patients showed neurological deterioration. All patients treated with AMSCs were followed up for at least twelve months.

Clinical and Radiographic outcomes

The mean VAS score improved from a preoperative value of 8.3 ± 0.5 to 2 ± 1.4 postoperatively. The mean preoperative ODI score was 47 ± 23 and decreased to 31 ± 5 twelve months postoperatively.

In total, four levels were implanted with AMSCs. Single-level implantation was performed in 67% (2/3) of the patients. The last patient had two levels implanted (Table 1). At six months post-surgery, fusion could be assessed with CT scan in two patients. One patient (with one operated level) had standard X-Ray instead of CT scan imaging and therefore, fusion characteristics could not be evaluated adequately. Two out of the 3 levels evaluated at this time period showed characteristics of solid fusion. At 12 months, 2 assessed levels demonstrated grade 3 fusion (Table 2). On CT imaging, no adverse local effects, such as bone formation away from the interbody cage or bone resorption in vertebral end plates, were noted (Fig. 3).

Fig. 3 Sagittal CT scan comparing bridging bone of a patient treated with AMSCs.

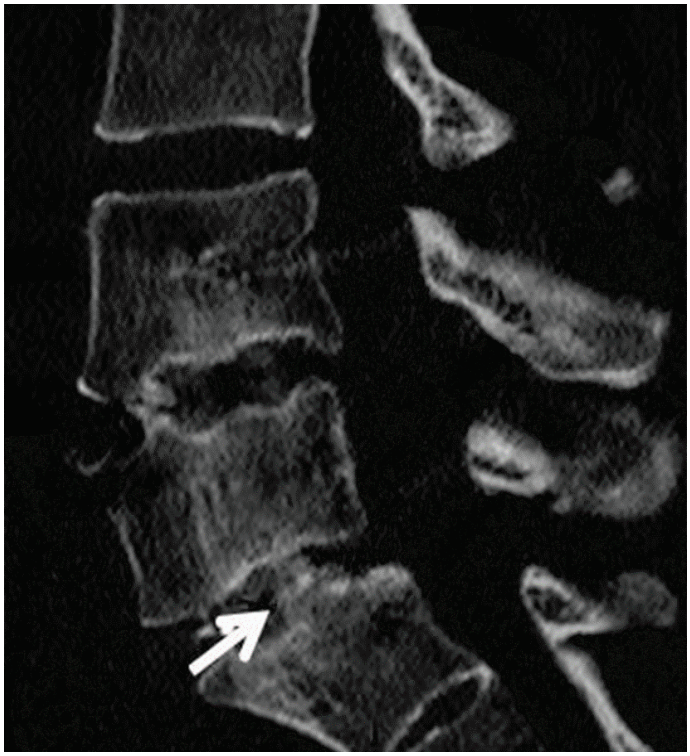

Figure 3-7 : View of fusion after AMSCs graft application

Discussion

The objective of the present study was to preliminary apply scaffold-free osteogenic 3D grafts from stem cells from abdominal fat tissue in human's spine during interbody fusion and stabilization procedures. As said earlier, we previously demonstrated the safety and efficacy of this graft in filling a critical-size femoral bone defect animal model at six months post-implantation and in extreme clinical cases of bone tumor resection and congenital/acquired bone non-unions up to 48 months post-transplantation.[187] Our results show that the procedure is applicable in human's spine without

complications. There were no donor site complications and the amount of fat tissue that could be collected was unlimited. Fischgrund et al. and Vaccaro et al. reported morbidity associated with the use of autologous iliac crest, including nonunion, in up to 55% of cases.[198, 199] Iliac crest autogenous bone grafting is associated with pain, paresthesia, hematoma, and even infection at the donor site in more than 60% of cases.[200, 201] None of our patients showed any of these symptoms after abdominal fat collection, and no complications were observed near the implantation site on post-operative CT imaging.

Mean VAS and ODI scores were improved in all patients at 12 months compared with preoperative values.

There was a period of 30 days between the decision that surgery was indicated and abdominal fat cell harvesting, and implantation was performed 89 days later. Thus, the whole process took 119 days, in contrast to 111 days for patients receiving bank bone. The duration of this new process should not, therefore, be considered a barrier to using stem cells from abdominal fat, especially since the period between the decision to undergo surgery and harvesting could be reduced. Currently, the improvement of the manufacturing significantly reduced the time to obtain the final 3-dimensional scaffold free-graft (from adipose stem cells after the native adipose tissue procurement) by 1.5 month.

Another important issue remains the risk of oncogenicity following the use of growth factors and stem cells to promote osteogenesis. BMP-2, the main growth factors contained in DBM and used to control important features of stem cells osteoblastic differentiation through WNT signaling-activating ligands, demonstrated controversial effects on osteogenic differentiation and

tumor growth. Luo et al.[202] reported that BMP-2 failed to induce bone formation and instead efficiently promoted tumor growth, while Wang et al.[203] conversely showed that BMP-2 treatment induced the up-regulation of terminal osteogenic markers inhibiting their tumorigenic potential. Recently, Rubio et al.[204] confirmed that the in vivo osteoblastic sarcoma developed by a synergistic effect of 40 mg of calcium substrates (hydroxyapatite and tricalciumphosphate) and 35 μg of BMP-2 on 1 × 106 cells human MSCs. In our study, the final product was characterized by a significantly lower concentration of BMP-2 (after protein extraction a mean of 54 ± 13 ng of BMP-2/g of DBM in comparison to 5.5 ± 13.4 ng/g of Tissue-engineered product (from adipose stem cells)) in comparison to those reported by Rubio et al.[204] Indeed, one 3D graft is constituted by the addition of 10 mg/ml of DBM (170 mg of DBM reconstituted in 17 ml of osteogenic media in a 150-cm2 flask corresponding to 5.8 ng of BMP-2 since 34.4 ng of BMP-2 is extracted per 1 g of DBM) to a mean of 5.3 × 106 AMSCs (number of cells per flask of 150 cm2 exposed to 170 mg of DBM at P4). It was also noted that the concentration of BMP-2 per gram of tissue was significantly reduced (by 85.2%) by the in vitro osteogenic maturation of AMSCs (in combination of DBM in the final 3D graft) in comparison to the equivalent amount of DBM. Although human MSC (deficient for p53 and/or Rb) failed to induce tumor formation in vivo, suggesting the safety of these cells in clinical application, Perrot et al.[205] postulated a risk associated with autologous fat graft implantation in a post-neoplasic context, especially for osteosarcoma. Controversy exists concerning the potential for spontaneous transformation of MSCs after prolonged ex vivo culture, but several studies reported that MSCs have limited tendencies to develop tumors.[206-208] Our results could indicate (i) the absence of adverse events in patients up to four years after

implantation for the first implanted patient; (ii) AMSCs delivery after a shorter in vitro culture (P4), thus avoiding the selection of tumor cell clones; (iii) the stabilization of the genome by osteogenic differentiation and (iv) the reduction of the concentration of BMP-2 in the final graft in comparison to DBM alone. But of course, the present series is limited and should be considered as a "proof of concept".

Another objective of this study was to assess the quality of the fusion using AMSCs. Our results show that this alternative source can achieve lumbar interbody fusion in humans (Fig. 3). The apparent reduction in the fusion rate observed over time (at twelve months compare to six) was due to a difference in the number of levels assessed during the two periods (Table 2), which could lead to this variation in fusion rate in a small population. Our results were analyzed by a blinded independent radiologist who distinguished between grades 3 and 2B.

We are unaware of any other studies using AMSCs in TLIF surgical procedures in humans. Studies of TLIF procedures using local bone grafts have found fusion rates ranging from 76% to 93% [209-212] in a follow-up evaluation period extending from six to twenty-four months. Larger series are needed to confirm that the use of AMSCs in interbody fusion is not inferior to the use of local bone graft.

From these early results in this limited group of patients, AMSCs appear to provide an attractive alternative to iliac crest bone graft, providing a safe source of stem cells and avoiding the morbidity associated with autologous bone graft harvest.

Conclusion

The implantation of stem cells derived from adipose tissue in humans' spine has never been reported in the literature. In this preliminary study, use of AMSCs was reproducible and associated with no major complications. This initial experience represents a promising alternative to current graft materials and needs to be confirmed in future and extensive investigations.

3.3.7 Highlights from this study

This study represents the first application of a scaffold-free 3D graft made of AMSCs to the human spine. The findings suggest that AMSCs may be a promising alternative graft material for spinal fusion procedures. Further studies involving larger series of patients are needed to confirm its effectiveness.

After this study was performed, a multicenter RCT study was initiated to confirm the safety and specific surgical effectiveness of AMSC grafts in patients with symptomatic grade I and grade II spondylolisthesis, which is currently ongoing

Chapter 4 GENERAL DISCUSSION, STRENGTHS AND LIMITATIONS

4.1 DISCUSSION

Treatment of CLBP due to lumbar spine degeneration remains challenging to health care providers. The standard first-line treatments for CLBP are optimally conservative medical and physical managements. Nevertheless, some patients remain refractory to this type of management, at which point surgery becomes an option.

In this era of rapid development of new technologies and their application in medical fields, spine surgeons are using different devices and techniques to address spine surgery. Spinal fusion with pedicle screw insertion is an effective technique for stabilizing the spine. Increasing use of this technique by surgeons of various skill and experience levels yields a higher risk of screw misplacement within the pedicle. Accurate pedicle screw placement is important for avoiding both minor and major complications. A number of studies have reported rates of inaccuracy in the placement of pedicle screws ranging from 15% to 50% [35, 43, 147, 148, 154]. To overcome this issue, computer-based image-guided systems have been introduced and progressively refined over the last two decades [39, 41, 43, 136, 137, 145, 155, 157]. Computer-assisted technology aims to diminish pedicle breaches and hence minimize the risk of neurovascular injuries [42, 57, 158-160]. Our studies show that the use of computer-assisted navigation to implant PPSs based on intraoperatively acquired 3D fluoroscopic images can provide an accuracy rate of nearly 100% and dramatically reduce the radiation exposure to surgeons and patients without significant major downsides. Of course,

learning takes time. Implementing new technologies must be accompanied with leaning new procedures. The learning curve may be very steep, and some surgeons may be reluctant to use new tools

New technologies are now becoming widespread as more institutions modernize their spine surgery facilities. In as study analyzing the learning curve of io3DF image-guided pedicle screw placement int thoracolumbar spine, Ryang et al. [213] found that io3DF can improve pedicle screw accuracy and reduce radiation exposure of the surgeon and patient once the learning curve is overcome and a normal workflow is established. The only way to overcome the learning curve and restore a normal workflow in spinal procedures is to use navigation routinely in every spinal instrumentation.

New devices must be evaluated, as it cannot be assumed that they are all relevant. Our research contributes to these necessary assessments and confirms the impact of these new technologies on surgical procedures. We have demonstrated that utilization of io3DF and navigation helps to reduce radiation to patients and OR staff. Use of io3DF allows to perform limited number of intraoperative fluoroscopies compared to conventional 2D fluoroscopy. Villard et al. [128] found from a prospective randomized comparison of navigated versus non-navigated freehand techniques that radiation exposure to the surgeon during pedicle screw insertion with the latter technique was up to 9.96 times greater than with navigation. In the present research, we demonstrated that there was no radiation to the surgeon at all. In a cadaveric study, Kim et al. compared surgeon exposure and fluoroscopy time without dosimetry in a patient series using conventional fluoroscopy and 2D fluoroscopy-based navigation. They found that fluoroscopic time was significantly reduced by navigation, whereas operating

time showed no significant difference[125]. During the C-arm orbital rotation of a 3D fluoroscopic device around the patient, a set of 100 images is obtained. One can therefore expect this will contribute to a higher dose for the patient than the images necessary during the freehand technique in the non-navigated procedure. In fact, this proved not to be the case, because most fluoroscopic images in the non-navigated technique are acquired in the lateral projection. In the lateral projection a higher dose is necessary to produce images of sufficient quality [132]. Therefore, less images could contribute to a higher radiation dose to the patient.

New technologies include biotechnology. Our study also aimed to demonstrate the feasibility of an alternative to bone grafting with important potential benefits. Over the past decade, adipose tissue has been the subject of intense research. Many studies have demonstrated that AMSCs appear to be an excellent candidate for tissue engineering due to ease of access and low rates of harvesting site-related comorbidities. Furthermore, the production of osteodifferentiated autologous grafts is a reproducible and simple procedure, although the length of time necessary to obtain a final implantable graft is currently still prohibitive. In fact, the tissue culture time ranges from 2.5 to 3 months to obtain a graft ready for implantation, and it may be difficult for patients to accept such a long waiting time before surgery. We applied scaffold-free 3D AMSCs to the human lumbar spine and demonstrated that fusion was possible. While only a few patients were included in this study, it serves as proof that the concept is feasible.

An important ongoing concern for AMSCs is the risk of oncogenicity following the use of growth factors and stem cells to promote osteogenesis. Luo et al. [202] reported that BMP-2 failed to induce bone formation and instead

efficiently promoted tumor growth in osteosarcoma cells, while Wang et al. [203] conversely showed that BMP-2 inhibits the tumorigenic potential of terminal osteogenic markers, by inducing their upregulation. Recently, Rubio et al. [204] confirmed that 40 mg of calcium substrates (hydroxyapatite and tricalcium phosphate) and 35 µg of BMP-2 had a synergistic effect to promote the differentiation of 1×10^6 human MSCs into osteoblastic sarcoma. In our study, the final product was characterized by a significantly lower concentration of BMP-2 (after protein extraction, a mean of 54 ± 13 ng of BMP-2/g of DBM vs. 5.5 ± 13.4 ng/g of tissue-engineered product from AMSCs) in comparison to those reported by Rubio et al. The potential for spontaneous transformation of MSCs after prolonged *ex vivo* culture remains controversial, but several studies have reported that MSCs show limited tendencies to develop tumors [206-208]. Our results indicate (i) the absence of adverse events up to 4 years after implantation in our patients; (ii) AMSC delivery after a shorter *in vitro* culture (P4), thus avoiding the selection of tumor cell clones; (iii) the stabilization of the genome by osteogenic differentiation; and (iv) the reduction of BMP-2 concentration in the final graft in comparison to DBM alone.

4.2 STRENGTHS AND LIMITATIONS

This PhD project evaluated the influence of using Zeego 3DF intraoperative images for pedicle screw placement and also compared the utilization of the device alone with its concurrent use in spine navigation. We found that pedicle screw accuracy could be increased while minimizing the irradiation of OR staff. As an additional avenue to improving patient outcomes, we further explored the feasibility of using autologous scaffold-

free osteogenic grafts of stem cells derived from adipose tissue for spinal fusion surgery, which avoids the harvesting site complications associated with bone grafts.

Nevertheless, some limitations to this research should be noted. The research outlined in this thesis evaluated only technical and radiological immediate outcomes but did not assess patient's long-term clinical outcomes. Second, the number of patients included in the study involving AMSCs is very small, and their follow-up period was short. While the study serves as proof of concept for the application of AMSCs to the human spine, a number of issues remain to be clarified before we can consider the technique as a definitive alternative for spinal fusion. Another limitation of our study is that we used radiation doses as given by the fluoroscopy without any attempt to translate them into clinical potential deterministic or stochastic effects. Nonetheless, we did not observe acute lesions in patients attributable to deterministic effects of radiation. Finally, our research did not include financial considerations in terms of a cost-effectiveness analysis. Setting up a hybrid operating room costs money; however, while equipping a dedicated spine OR is expensive, the cost is not necessarily prohibitive for high-volume hospitals. In a university-affiliated hospital, the referral of complex cases warrants such investment in order to offer acceptable therapeutic solutions to these patients.

Chapter 5 CONCLUSIONS AND PERSPECTIVES

5.1 CONCLUSIONS

Among the many therapeutic options for the treatment of CLBP, surgery is deemed appropriate in carefully selected patients. The main surgical procedures are decompression, fusion, and occasionally arthroplasty. The work reported here contributes to improve the management of this major socioeconomic burden.

Using io3DF concurrently with spine navigation eliminates the need for fluoroscopy in up to 75% of cases in the series reported by Laine et al. [38]. We achieved a very high accuracy rate of pedicle screw placement utilizing this total navigation system and drastically reduced radiation exposure to OR staff. Although clinical benefits are not apparent during the short-term postoperative period, we believe that long-term studies will elucidate further benefits of io3DF-ioNAV. The system is relatively easy to learn and makes spinal surgery under minimally invasive conditions safer and more efficient.

Lumbar spine stabilization for CLBP involves not just pedicle screw placement using the devices and techniques reported in the present thesis, but also good intervertebral fusion, which necessitates having adequate implants. Tissue engineering has led to the development of osteogenically differentiated AMSCs. Autologous bone grafting of AMSCs has been used in animal models and humans for indications including femoral and maxillofacial grafting. We used this graft for the first time in lumbar spine surgery without any adverse events at the 4-year follow-up. The concept proved to be feasible and reproducible. Nevertheless, studies involving a

larger series of patients and long-term follow-up are necessary to shed light on this promising autologous graft source.

5.2 PERSPECTIVES

As described earlier, this work has some limitations in spite of the encouraging findings reported. Although we have demonstrated that io3DF along with spine ioNav is effective in increasing the pedicle screw placement rate while markedly decreasing radiation exposure to OR staff, larger, multicenter RCTs are needed to confirm these findings and promote the advancement of these new technologies in spine surgery. It is likely that intraoperative full navigation will replace standard fluoroscopy in the coming decades. With that trend in mind, our research should be expanded to include other centers that wish to participate.

Comparative series with regards to radiation are mandatory to find out the exact radiation effects of the new devices. It may be interesting to compare a freehand open TLIF technique with a fully navigated one to help demonstrate the added value of the io3DF and navigation in terms of learning curve, operating duration, and hospital stay in a cohort of patients.

Robotics have increasingly penetrated the medical field as a whole, and spinal surgery in particular. Today, pedicle screw placement using io3DF and navigation requires surgeon active intervention at all steps. It may be easier to combine navigation and imaging hardware to automate the workflow of registration and insertion of pedicle screws. We imagine that in such a setting, a screw trajectory will be indicated by a laser, and the robot will move to the index pedicle to implant a previously calibrated screw without any

human intervention. This possibility must be discussed with developers from device companies.

It is noteworthy that since our study on the application of a scaffold-free 3D graft from AMSCs, a phase 1, multicenter RCT has been initiated and is now ongoing, which aims to evaluate the safety (local and systemic) of a specific surgical intervention with the use of grafts from AMSCs in patients with symptomatic low-grade degenerative spondylolisthesis grade I or II who undergo surgery for spinal fusion of one vertebral lumbar segment. The second objective of this RCT is to determine the clinical efficacy of lumbar interbody fusion with an AMSC-derived graft.

To build upon the present work, clinical studies must be initiated to evaluate the impact of applying the described new technologies via radiological and clinical follow-up. It will be of particular interest to assess whether outcomes differ between patients operated on with or without the combined use of intraoperative imaging and spine navigation.

Finally, due to the cost of implementation of a dedicated OR with advanced technologies, cost-effectiveness studies are critical to determine whether the investment is justified.

Concurrently with technical development, clinical research will remain necessary to assess engineers' findings and determine the hardware technologies and bioengineering to be offered to patients.

Chapter 6 APPENDICES

Other peer-review papers associated to the study

6.1 An unusual case of ureteral perforation in minimally invasive pedicle screw instrumentation and review of the literature. **Fomekong E**, Pierrard J, Danse E, Tombal B, Raftopoulos C. *World Neurosurg. 2017* Dec 8. pii: S1878-8750(17)32108-3. doi: 10.1016/j.wneu.2017.11.175. PMID: 29229340

6.2 Percutaneous Pedicle Screws: Application Under Intraoperative Robotic 3D Fluoroscopic Navigation. **Fomekong E**, Labeau J, Raftopoulos C. Current Progress in Neurosurgery Volume 2 – 2017 by Basant K Misra (Editor) (Author), Edward R Laws Editor) (Author), Andrew H Kaye (Editor) (Author)

6.3 Percutaneous pedicle screw implantation for refractory low back pain: from manual 2D to fully robotic intraoperative 2D/3D fluoroscopy. Raftopoulos C, Waterkeyn F, **Fomekong E**, Duprez T.Adv Tech Stand Neurosurg. 2012 38:75-93. doi: 10.1007/978-3-7091-0676-1_4. PMID: 22592412.

6.1 COMPLICATIONS OF MINIMALLY INVASIVE PEDICLE SCREW PLACEMENT

Fomekong E, Pierrard J, Danse E, Tombal B, Raftopoulos C.

6.1.1 Introduction

In this thesis, the surgical technique utilizes for osteosynthesis involves MISS. Special care must be taken when using MISS because the usual anatomical landmarks are concealed.

We report a rare case of ureteral rupture occurring as a complication of percutaneous pedicle screw placement. This complication is most often reported in gynecologic, colorectal, and vascular pelvic surgery or endoscopic procedures for ureteric pathologies.

6.1.2 Summary

A 60-year old man complained of unbearable abdominal pain on the day after right L4-L5 transforaminal intervertebral fusion and percutaneous pedicle screw placement. A computed tomography workup revealed contrast media extravasation outside the excretory system consistent with a left ureteral traumatic perforation. The patient underwent left nephrostomy and a double-J stent insertion and subsequently fully recovered. The ureter completely healed, enabling stent removal 5 months later.

We performed a review of the literature indexed in PubMed and EMBASE, which were screened for cases of ureteral injury caused by posterior lumbar surgery. We found a total of 27 reports, with only one other case following MI-TLIF

An Unusual Case of Ureteral Perforation in Minimally Invasive Pedicle Screw Instrumentation: Case Report and Review of the Literature

Edward Fomekong[1], Julien Pierrard[4], Etienne Danse[2], Bertrand Tombal[3], Christian Raftopoulos[1]

Key words
- Complication
- K-wire
- Lumbar spine operation
- Minimally invasive operation
- Ureteral injury

Abbreviations and Acronyms
CT: Computed tomography
K-wire: Kirschner wire
MISS: Minimally invasive spine surgery
MI-TLIF: Minimally invasive transforaminal lumbar interbody fusion
TLIF: Transforaminal lumbar interbody fusion

From the Departments of [1]Neurosurgery, and [2]Radiology Cliniques Universitaires Saint-Luc Bruxelles, Brussels; [3]Medical Student (MS), Université Catholique de Louvain, Brussels; [4]Department of Urology, Cliniques Universitaires Saint-Luc Bruxelles, Brussels, Belgium

To whom correspondence should be addressed: Christian Raftopoulos, M.D., Ph.D. [E-mail: christian.raftopoulos@uclouvain.be]

Citation: World Neurosurg. (2018) 111:28-35.
https://doi.org/10.1016/j.wneu.2017.11.175

Journal homepage: www.WORLDNEUROSURGERY.org

Available online: www.sciencedirect.com

BACKGROUND: **Injury of the ureter is a potentially devastating complication most often reported in gynecologic, colorectal, or vascular pelvic surgery or endoscopic procedures for ureteric diseases. We report a rare case of ureteral rupture occurring as a complication of percutaneous pedicle screw placement.**

CASE DESCRIPTION: **A 60-year-old man reported unbearable abdominal pain on the day after right L4-L5 transforaminal intervertebral fusion and percutaneous pedicle screw placement. A computer tomography workup showed contrast media extravasation outside the excretory system consistent with a left ureteral traumatic perforation. The patient underwent left nephrostomy and a double-J stent insertion and subsequently fully recovered. The ureter completely healed, enabling stent removal 5 months later.**

METHODS: **PubMed and EMBASE were screened for ureteral injury caused by posterior lumbar surgery.**

RESULTS: **We found 27 other reports with only 1 other case after minimally invasive transforaminal lumbar interbody.**

CONCLUSIONS: **Complications of minimally invasive pedicle screw placement are often described as dural tear of neurologic impairment. This report shows that unexpected side effects are still possible and spine surgeons should be aware especially when performing minimally invasive procedures, in which, by definition, pedicles are concealed from direct visualization.**

BACKGROUND

Lumbar fusion is a reliable neurosurgical modality widely used in the treatment of degenerative lumbar disease.[1] There are multiple pathways for this type of surgery including transforaminal lumbar interbody fusion (TLIF) developed in 1998 by Harms et al.,[2] which we practice in our center. This operation has been performed by minimal access for more than 10 years.[3] The drawbacks of minimally invasive spine surgery (MISS) are the loss of the usual anatomic landmarks and a greater dependence on intraoperative imaging.[4]

MISS complications are rarely reported and often limited to neurologic impairment or vascular insult. Visceral complications are even rarer and this scarcity can lead to late diagnosis and increase related morbidity.[5,6] We report an unusual case of ureteral rupture after minimally invasive TLIF (MI-TLIF) and percutaneous pedicle screw placement with utilization of Kirschner wire (K-wire). Then, we present a review of literature for ureteral injury after posterior spinal surgery.

METHODS

For the review of the literature, 2 independent investigators screened PubMed and EMBASE until August 2017 for the following terms: "spine surgery AND ureteral injury," "spine surgery AND urinoma," and "ureteric injury AND lumbar spine surgery." We found 118 references. Only articles that reported ureteral injury after a lumbar posterior spinal surgery were included. After, we screened the bibliography of the included articles to find missing articles. A total of 27 articles met the inclusion criteria.

The patients provided informed consent for publication of the case.

CASE DESCRIPTION

A 60-year-old man was admitted for surgical treatment of L4-L5 spondylodiscarthrosis. He presented with a history of many years of predominant lumbar pain radiating to the right lower limb, which was unsuccessfully treated with conservative optimal medical management. His past medical history showed type II diabetes mellitus, hypertension, left calf muscle leiomyosarcoma, gastric ulcer, and hypercholesterolemia. He reported severe lumbar pain (8/10 on a visual analog scale) and evaluated his Oswestry Disability Index to be 46%. Clinical examination showed a body mass index of 28.7 kg/m^2. Preoperative computed tomography (CT), magnetic resonance imaging, and single-photon emission CT showed a spondylodiscarthrosis at the L4-L5 level. Because of symptoms refractory to optimal medical treatment, surgery was suggested to the patient.

Under general anesthesia, with the patient in a prone position, we performed a right MI-TLIF and a percutaneous pedicle screw stabilization using a K-wire pedicle technique. The technique has already been reported in other publications.[7,8] Through a 2-cm incision made 4–5 cm lateral to the midline between the projection of the L4 and L5 pedicle, a cannulated pedicle finder was docked against the bone at the junction of the base of the transverse process and facet joint over the lateral wall of the targeted pedicle. The pedicle finder was then slowly advanced with gentle taps of a mallet and then, a K-wire was placed through the cannula. We used two-dimensional fluoroscopy to check the adequate insertion. The same process (Figure 1) was repeated for the 4 pedicles and once all the guidewires were in place, we proceeded to insertion of the cannulated screws through the pedicle finder. The final placement of the K-wire and the screws was verified with three-dimensional fluoroscopy to ensure adequate positioning. The incision was then closed with skin glue. The surgery proceeded uneventfully with no apparent complications.

The day after surgery, the patient started reporting abdominal pain. On postoperative day 2, he could walk in the corridor with no more lumbar or radicular pain but still had abdominal pain. Despite adequate postoperative pain management, abdominal pain worsened. On postoperative day 4, an abdominal CT showed a large (70 × 40 × 190 mm) left retroperitoneal collection compatible with a fresh urinoma not present on preoperative images. On multiplanar CT views performed 45 minutes after intravenous iodine injection, we observed a moderate left-side kidney hydronephrosis and an iodine diffusion in the left retroperitoneal space. This iodine effusion was coming from the midpart of the lumbar ureteral segment (Figure 2).

The following day, with the patient under general anesthesia because of intense unbearable pain, we performed a percutaneous nephrostomy with immediate resolution of pain. During the same anesthesia, of retrograde ureteral catheterization failed. The next day, an anterograde insertion of a double-J catheter. The nephrostomy catheter was subsequently removed after a successful occlusion test not leading to recurrence of urinoma. The double-J catheter was kept for 5 months before successful removal after ultrasonography that did not show urine extravasation.

We hypothesize that the ureteral partial tear occurred when the K-wire was inserted into the pedicle, perforating the anterior wall of the vertebra and penetrating the retroperitoneal space. To insert pedicle screws, a 2-cm skin incision was made 4–5 cm from the midline at the level of each targeted pedicle. A metallic guidewire (K-wire) was then inserted through a pedicle finder toward the index pedicle and advanced in the vertebral body using two-dimensional fluoroscopy verification. The screws were then placed after manually drilling the pedicle entrance if the screw was not self-drilling. We left the K-wire in place during the screw insertion and removed it only when we were sure that the screw traversed the anterior wall of the pedicle. It is likely that the K-wire perforated the anterior wall of the vertebra either during its insertion or during screw placement, which may have inadvertently advanced the metallic guidewire into the retroperitoneal space and subsequently injured the ureter.

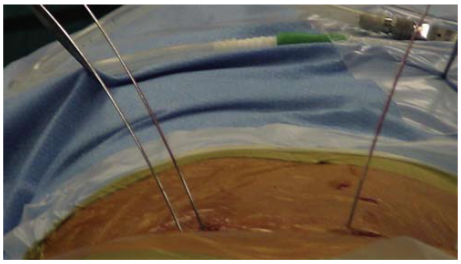

Figure 1. A Kirschner wire inserted in the pedicles.

DISCUSSION

MISS has become increasingly popular for a variety of indications close to that of open surgical access to the spine. Before performing MI-TLIF and percutaneous placement of pedicle screws for spine stabilization, a surgeon must be well trained with good experience in open procedures. Unlike conventional open access, the MISS approach uses transmuscular access to the spine and is reputed to significantly decrease iatrogenic soft tissue damage, intraoperative blood loss, postoperative pain and analgesic consumption, hospital stays, and overall cost.[9-12] Nevertheless, MISS, especially using K-wire for pedicle screw implantation, can yield complications such as neurologic, visceral, and vascular injuries. Only minimal literature is available reporting these complications. Chung et al.[13] reported a case of extensive epidural hematoma causing paraplegia in a patient undergoing MISS surgery using a K-wire. Smythe et al.[14] reported a case of suprarenal abdominal aortic injury and an associated pseudoaneurysm with intraoperative bleeding and transient systolic pressure decrease because of anterior K-wire perforation. In a series of 525 percutaneous pedicle screws, Mobbs et al.[15] reported 7 perforations of the anterior wall of the vertebra by the K-wire, only 2 of which caused retroperitoneal hemorrhage and ileus, which improved with conservative treatment.

Our PubMed and EMBASE research found 27 well-described ureteral complications after posterior spinal surgery (Table 1).[16-42] Eight other identical complications were found but 2 were mentioned with no details and others were published in languages other than English.[43-50]

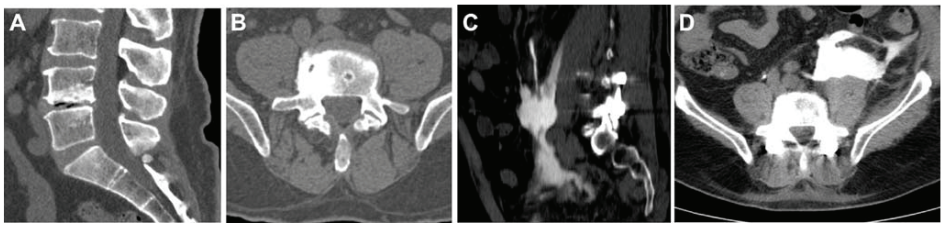

Figure 2. Preoperative sagittal (**A**) and axial (**B**) computed tomography images showing L4-L5 degenerative disc disease without visualization of retroperitoneal mass. (**C** and **D**) A multiplanar view of the computed tomography scan obtained 45 minutes after an intravenous injection of iodine. Moderate hydronephrosis in the left kidney and iodine diffusion in the left retroperitoneal space are observed. The iodine effusion is coming from the midpart of the lumbar ureteral segment.

Few articles (14/27) report the mechanism of ureteral injury. Most of the lesions were caused by use of a pituitary rongeur.[17-19,21-23,26-28,35,40] De Quintana-Schmidt et al.[45] described 2 principal mechanisms to wound the ureter during posterior lumbar surgery. The most frequently reported is the perforation of the anterior longitudinal spinal ligament, especially by a rongeur.[23,26,30,40] The second type of lesion occurs when the instruments inadvertently pass through the intertransverse space.[20,35] To our knowledge, this is the first time that ureteral tear caused by a K-wire pedicular perforation has been described. There is only 1 report of ureteral injury after an MI-TLIF, described by Tsai et al.[40] In this case, the ureteral avulsion was caused by the rupture of the anterior longitudinal spinal ligament and the removal of soft tissue by the pituitary rongeur, which probably contained the ureter.

In 4 of 14 well-described reports, the patients had a history of previous lumbar surgery. Revision surgery increases the risk of iatrogenic complications as a result of adhesions of tissues, blood vessels, and other structures such as the ureter. The challenge is particularly increased in revision spinal surgery by the presence of foreign devices such as pedicle screws and intervertebral cages. We found no report relative to ureteral complication rate after posterior lumbar revision surgery. However, in some studies of anterior spinal revision, ureteral complications occur in 1.55%–8.00%.[51-54] To avoid ureteral laceration during spinal revision surgery, some investigators recommend the preoperative placement of a double-J catheter through the ureter.[51-54] During surgery, this strategy allows the manual palpation of the ureter and the intraoperative fluoroscopic control of the ureteral location. However, despite the use of this device, Flouzat-Lachaniette et al.[54] still reported 2 cases of ureteral injury in patients who underwent anterior lumbar revision.

Co-occurring complications are mentioned in 6 cases. Most (5/6) are vascular injuries from vessels near the ureter and the operative site such as the inferior vena cava, common iliac vessels, and hypogastric artery.[18-20,22,23] This situation is explained by the close relation between the ureter and the large vessels and by the prone position, which induces compression of the ureters and the great vessels against the vertebral bodies, especially at the L4-L5 level.[18] Furthermore, Noyes et al.[26] reported a case of abscessed urinoma.

The initial presentation of ureteral injury is nonspecific and, because of the rarity of this complication, neurosurgeons are not able to recognize immediately when ureteral violation occurs. Moreover, the delay between surgery and the first symptoms is variable: from immediate postoperative symptoms to 5 months after lumbar disc surgery in a report by Sarikaya et al.[31] Intraoperative diagnosis is difficult but possible: for example, in a case of oblique lumbar interbody fusion procedure reported by Lee et al.,[55] the anesthesiologist signaled the sudden onset of gross hematuria, which allowed intraoperative reconstruction of the ureter by a urologist. The most reported symptoms are, in order of frequency, abdominal pain or distension (92.6%), fever (66.7%), ileus (29.6%) nausea and vomiting (18.5%), oliguria/anuria (18.5%), macroscopic hematuria (14.8%), initial sepsis or shock (7.4%), and right lower extremity numbness (3.7%). Generally, after laboratory tests, initial investigations consist of imaging studies, such as sonography or CT, and in rare cases, magnetic resonance imaging. These imaging findings commonly include unilateral hydronephrosis and a retroperitoneal fluid collection in the area of the operative zone. In the past, the diagnosis was concluded with intravenous pyelography and retrograde ureteropyelography. Since 1980, abdominal CT has been the recommended procedure with intravenous iodine injection, and with the acquisition, the first at the portal phase (70–90 seconds after injection), and the second at a delayed time (at least 30–45 minutes after the injection). The fluid collection initially detected at the portal phase is near the kidney or the ureteral pathway; it is partially or completely filled with iodine contrast more precisely at the delayed phase, leading to the suggestive diagnostic of an urinoma or hematoma.[56-58] In cases of an uncertain diagnosis, an exploratory operation with concomitant repair of the ureter was performed by surgeons.

Of our 27 reported cases, 14 ureters were completely sectioned, 11 were partially injured, 1 was entrapped by the lumbar instrument, and 1 was

Table 1. Summary of the 27 Cases of Ureteral Injury Found in the English Literature

Reference	Sex	Age (years)	Previous Lumbar Operation	Type of Surgery	Levels	Location of Ureteral Injury	Type of Injury	Delay from Operation	Investigations	Treatment	Outcome
McKay et al., 1954[6]	M	30	—	Laminectomy	—	Left ureteral injury just above the crossing of the iliac vessels	Complete ureteral section	2 weeks	IVP and surgical exploration	End-to-end anastomosis	Uneventful
Borski and Smith, 1960[17]	F	30	No	Laminectomy	L4-L5	Left L4-L5 posterior level	Partial tear	Immediate postoperative symptoms	IVP, combined anterograde and retrograde ureteropyelolagraphy, and surgical exploration	End-to-end anastomosis	Uneventful
Sandoz and Hodges, 1965[8]	M	35	No	Hemilaminectomy	L4-L5-S1	Right L4 level	Complete ureteral section	Immediate postoperative symptoms	IVP and retrograde pyelography	Unsuccessful end-to-end anastomosis with downward displacement of the kidney and then nephrectomy	—
Moore and Cohen, 1968[18]	M	33	No	Partial hemilaminectomy and microdiscectomy	L5-S1	Left posterior middle ureter	Partial tear	5 weeks	IVP and cystoscopy	Ureteral splinting	Infection in the interspace of L5-S1 and 3 episodes of meningitis
Holscher, 1988[20]	M	34	—	Laminectomy	L4-L5	Left ureter	Partial tear	—	Surgical exploration	Ureteratomy with end-to-end anastomosis	Epidural abscess, meningitis (*Pseudomonas*) with spinal fluid fistula treated by long-term antibiotics; the fistula closed spontaneously; normal renal function
Kern et al., 1989[2]	M	30	No	Partial hemilaminectomy	L5-S1	Right middle ureter	Partial tear	Immediate postoperative symptoms	Abdominal radiography, IVP, cystoscopy, retrograde ureteropyelolagraphy, and surgical exploration	Ureteratomy, drainage of the abscess, and splinting	Uneventful
Parker, 1971[22]	M	20	—	Hemilaminectomy	L4-L5	Right ureteropelvic junction	Complete ureteral section	2 days	IVP and cystoscopy	Nephrectomy	—
Gangal, 1972[23]	F	34	—	Hemilaminectomy and discectomy	L4-L5	Left L4-L5 posteromedial level	Partial tear	4 days	IVP	Ureteral splinting	Uneventful

—, no data available; M, male; IVP, intravenous pyelography; F, female; US, ultrasonography; CT, computed tomography; MRI, magnetic resonance imaging; PLIF, posterior Lumbar Interbody fusion; MI-TLIF, minimal invasive transforaminal lumbar interbody fusion; Lx, vertebral lumbar level where x is the numeric number of the vertebra; Sx, vertebral sacral level where x is the numeric number of the vertebra; AB, antibiotics.

Continues

Table 1. Continued

Reference	Sex	Age (years)	Previous Lumbar Operation	Type of Surgery	Levels	Location of Ureteral Injury	Type of Injury	Delay from Operation	Investigations	Treatment	Outcome
Zinman et al., 1978[24]	M	43	No	Laminectomy	L4-L5	Left posterolateral middle third	Partial tear	3 days	IVP and retrograde ureteropyelography	End-to-end anastomosis	Uneventful
Altebarmakian et al., 1981[75]	F	16	—	Laminectomy	L4-L5	Right proximal ureter	Partial tear	3 days	IVP and retrograde ureteropyelography	Ureteral splinting with drainage	Uneventful
Noyes and Morrisseau, 1982[26]	F	58	No	Laminectomy	L4-L5	Left L4 level	Complete ureteral section	Immediate postoperative symptoms	Surgical exploration, US, and arteriography	Drainage of the urinoma and then nephrectomy	—
Krone et al., 1985[27]	F	42	—	Discectomy	L5-S1	Right L5-S1 level	Complete ureteral section	Immediate postoperative symptoms	IVP and retrograde ureteropyelography	End-to-end anastomosis	Urinoma caused by leakage from anastomosis treated by reinsertion of the catheter and AB then uneventful
Defay et al., 1986[28]	F	58	—	Laminectomy	L4-L5	Left L4-L5 level	Partial tear	6 weeks	CT and IVP	End-to-end anastomosis	Uneventful
Bec, 1989[29]	M	53	Yes	—	—	Left distal ureter	Complete ureteral section	—	Retrograde ureteropyelography	End-to-end anastomosis	Uneventful
Flam, 1992[30]	F	60	No	Percutaneous nucleotomy	L4-L5	Left ureter	Complete ureteral section	2 days	US, CT, and retrograde ureteropyelography	End-to-end anastomosis	Uneventful
Sarikaya and Asci, 1996[31]	F	45	—	Hemilaminectomy and discectomy	L5-S1	Left ureter 7 cm from the ureteropelvic junction	Necrosis and strangulation	5 months	US, cystoscopy, retrograde ureteropyelography, and IVP	End-to-end anastomosis	Uneventful
Tainio and Kylmala, 1999[32]	F	54	No	Microdiscectomy	L4-L5	Right ureter	Complete ureteral section	Immediate postoperative symptoms	US, CT, and anterograde pyelography	End-to-end anastomosis	Uneventful
Trinchieri et al., 2001[33]	M	29	—	Lumbar disc operation	—	Left upper ureter	Complete ureteral section	2 weeks	US, CT, IVP, and retrograde ureteropyelography	Unsuccessful splinting and then unsuccessful downward displacement of the kidney with end-to-end ureteroureterostomy, and autotransplantation of the kidney	Uneventful
Demirkesen et al., 2006[34]	F	49	—	Discectomy	L3-L4-L5	Left upper ureter	Complete ureteral section	8 days	US, IVP, MRI, drainage and combined anterograde, and retrograde ureteropyelography	Ureterotomy with end-to-end anastomosis	Uneventful
Cho et al., 2008[35]	M	28	Yes	Microdiscectomy	L4-L5	Right distal ureter	Partial tear	Immediate postoperative symptoms	MRI, CT, cystoscopy, and retrograde ureteropyelography	End-to-end anastomosis	Uneventful

Hekal et al., 2008[36]	F	38	—	Discectomy	—	Right iliac ureter	Complete ureteral section	—	Abdominal radiography, US, and MRI	Percutaneous drainage by nephrostomy and ureteral replacement	Uneventful
Bjurlin et al., 2009[37]	F	24	Yes	Removal of the lumbar plate and broken screws with unirod spanning placement	L1-L2-L3	Right L2 level	Entrapment by lumbar instrumentation	14 days	CT, drainage, and simultaneous and combined anterograde and retrograde ureteropyelography	Unsuccessful splinting and then mobilization of the kidney with end-to-end ureteroureterostomy	Uneventful
Kaffenberger et al., 2010[38]	F	63	—	Discectomy and facetectomy with cage placement	L4-L5	Left L4 level	Partial tear	2 days	CT, retrograde ureteropyelography, IVP, and (after 3 months) combined anterograde and retrograde ureteropyelography	2 unsuccessful stent placements and then end-to-end anastomosis with renal mobilization	At 3 months: 30% left renal function without evidence of obstruction
Pillai et al., 2013[39]	F	33	No	Laminectomy and microdiscectomy with PLIF	L5-S1	Right middle ureter	Partial tear	2 weeks	US, CT, drainage, and ureterorenoscopy	Unsuccessful ureteral splinting and then vesical flap implantation	Uneventful
Tsai et al., 2013[40]	F	60	No	MI-TLIF	L4-L5	Right proximal ureter	Complete ureteral section	1 day	CT and retrograde ureteropyelography	Ureterotomy with end-to-end anastomosis	Uneventful
Akpiner et al., 2015[41]	M	44	Yes	—	—	Left middle ureter	Complete ureteral section	1 month	US and CT	End-to-end anastomosis	Uneventful
Garg et al., 2017[42]	M	44	—	Microdiscectomy	L5-S1	Left upper border of the sacral ala	Complete ureteral section	2 days	CT, drainage, retrograde ureteropyelography, and IVP	Percutaneous nephrostomy and then Boari flap implantation	Uneventful

—, no data available; M, male; IVP, intravenous pyelography; F, female; US, ultrasonography; CT, computed tomography; MRI, magnetic resonance imaging; PLIF, posterior lumbar interbody fusion; MI-TLIF, minimal invasive transforaminal lumbar interbody fusion; Lx, vertebral lumbar level where x is the numeric number of the vertebra; Sx, vertebral sacral level where x is the numeric number of the vertebra; A3, antibiotics.

strangulated and necrosed over a length of 1 cm. The strategies of reparation depend on the ureteral avulsion is partial or complete. If there is a simple tear without complete section, ureteral splinting can be performed through a double-J catheterization but it is not always reliable and a second attempt at end-to-end anastomosis is sometimes unavoidable.[33,37-39] End-to-end anastomosis is the first-line surgical procedure in cases of complete ureteral section. If the distance between the extremities of the ureter is important or if a partial ureterotomy is necessary because of stump fibrosis or necrosis, a dissection associated with a downward displacement of the kidney can be performed to allow appropriate end-to-end anastomosis.[18,33,37,38] In a few cases, there is no way to achieve correct repair and a nephrectomy should be considered.[18,22,26]

CONCLUSIONS

Ureteral injury is a rare complication of posterior lumbar surgery but with serious potential consequences, such as nephrectomy. When urinary tract leakage is suspected, CT with iodine injection is the recommended diagnostic method. We report 27 cases described in the English literature but this is only the second report of a ureteral injury after an MI-TLIF and the first case described caused by K-wire perforation.

REFERENCES

1. Gaines RW Jr. The use of pedicle-screw internal fixation for the operative treatment of spinal disorders. *J Bone Joint Surg Am*. 2000;82-A:1458-1476.
2. Harms JG, Jeszenszky D. Die posteriore, lumbale, interkorporelle Fusion in unilateraler transforaminaler Technik. *Oper Orthop Traumatol*. 1998;10:90-102 [in German].
3. Foley KT, Gupta SK. Percutaneous pedicle screw fixation of the lumbar spine: preliminary clinical results. *J Neurosurg*. 2002;97(1 suppl):7-12.
4. Schwender JD, Holly LT, Rouben DP, Foley KT. Minimally invasive transforaminal lumbar interbody fusion (TLIF): technical feasibility and initial results. *J Spinal Disord Tech*. 2005;18(suppl):S1-S6.
5. Brandes SB, Chelsky MJ, Buckman RF, Hanno PM. Ureteral injuries from penetrating trauma. *J Trauma*. 1994;36:766-769.
6. Ghali AM, El Malik EM, Ibrahim AI, Ismail G, Rashid M. Ureteric injuries: diagnosis, management, and outcome. *J Trauma*. 1999;46:150-158.

7. Fomekong E, Dufrane D, Berg BV, André W, Aouassar N, Veriter S, et al. Application of a three-dimensional graft of autologous osteodifferentiated adipose stem cells in patients undergoing minimally invasive transforaminal lumbar interbody fusion: clinical proof of concept. *Acta Neurochir (Wien)*. 2017;159:527-536.

8. Raftopoulos C, Waterkeyn F, Fomekong E, Duprez T. Percutaneous pedicle screw implantation for refractory low back pain: from manual 2D to fully robotic intraoperative 2D/3D fluoroscopy. *Adv Tech Stand Neurosurg*. 2012;38:75-93.

9. Assaker R. Minimal access spinal technologies: state-of-the-art, indications, and techniques. *Joint Bone Spine*. 2004;71:459-469.

10. Harris EB, Massey P, Lawrence J, Rihn J, Vaccaro A, Anderson DG. Percutaneous techniques for minimally invasive posterior lumbar fusion. *Neurosurg Focus*. 2008;25:E12.

11. Holly LT, Schwender JD, Rouben DP, Foley KT. Minimally invasive transforaminal lumbar interbody fusion: indications, technique, and complications. *Neurosurg Focus*. 2006;20:E6.

12. Oppenheimer JH, DeCastro I, McDonnell DE. Minimally invasive spine technology and minimally invasive spine surgery: a historical review. *Neurosurg Focus*. 2009;27:E9.

13. Chung T, Thien C, Wang YY. A rare cause of postoperative paraplegia in minimally invasive spine surgery. *Spine (Phila Pa 1976)*. 2014;39:E228-E230.

14. Smythe WR, Carpenter JP. Upper abdominal aortic injury during spinal surgery. *J Vasc Surg*. 1997;25:774-777.

15. Mobbs RJ, Raley DA. Complications with K-wire insertion for percutaneous pedicle screws. *J Spinal Disord Tech*. 2014;27:390-394.

16. McKay HW, Baird H, Justis HR. Management of ureteral injuries. JAMA. 1954;154:202-205.

17. Borski Major AA, Smith Major RA. Ureteral injury in lumbar-disc operation. *J Neurosurg*. 1960;17:925-928.

18. Sandoz I, Hodges CV. Ureteral injury incident to lumbar disk operation. *J Urol*. 1965;93:687-689.

19. Moore CA, Cohen A. Combined arterial, venous, and ureteral injury complicating lumbar disk surgery. *Am J Surg*. 1968;115:574-577.

20. Holscher EC. Vascular and visceral injuries during lumbar-disc surgery. *J Bone Joint Surg Am*. 1968;50:383-393.

21. Kern HB, Barnes W, Malament M. Lumbar Laminectomy and associated ureteral injury. *J Urol*. 1969;102:675-677.

22. Parker JM. Ureteral injury secondary to lumbar disk operation. *J Urol*. 1971;105:85.

23. Gangai MP. Ureteral injury incident to lumbar disc surgery. Case report. *J Neurosurg*. 1972;36:90-92.

24. Zinman LM, Libertino JA, Roth RA. Management of operative ureteral injury. *Urology*. 1978;12:290-303.

25. Altebarmakian VK, Davis RS, Khuri FJ. Ureteral injury associated with lumbar disk surgery. *Urology*. 1981;17:462-464.

26. Noyes DT, Morrisseau PM. Ureteral transection secondary to lumbar disk surgery. *Urology*. 1982;19:651-652.

27. Krone A, Heller V, Osterhage HR. Ureteral injury in lumbar disc surgery. *Acta Neurochir (Wien)*. 1985;78:108-112.

28. Defay P, L'Hermite J, Wiederkehr P, Raul P, Guillemin P. An unusual ureteric injury. *Br J Urol*. 1986;58:567.

29. Bec A. Ureteric injury during laminectomy for a prolapsed disc. *Br J Urol*. 1989;63:552-553.

30. Flam TA, Spitzenpfeil E, Zerbib M, Steg A, Debre B. Complete ureteral transection associated with percutaneous lumbar disk nucleotomy. *J Urol*. 1992;148:1249-1250.

31. Sarikaya S, Asci R. Ureteral injury secondary to lumbar disc operation in a patient with solitary kidney. *Ondokuz Mayis Universitesi Tip Dergisi*. 1996;13:163-164.

32. Tainio H, Kylmala T. Rupture of the ureter: an unexpected complication of microdiskectomy. *BJU Intl*. 1999;84:369-370.

33. Trinchieri A, Montanari E, Salvini P, Berardinelli L, Pisani E. Renal autotransplantation for complete ureteral avulsion following lumbar disk surgery. *J Urol*. 2001;165:1210-1211.

34. Demirkesen O, Tunc B, Ozkan B. A rare complication of lumbar disk surgery: ureteral avulsion. *Int Urol Nephrol*. 2006;38:459-461.

35. Cho KT, Im SH, Hong SK. Ureteral injury after inadvertent violation of the intertransverse space during posterior lumbar diskectomy: a case report. *Surg Neurol*. 2008;69:135-137.

36. Hekal IA, Mohsen T, Nabeeh A. Ureteric injury after lumbosacral discectomy: a case report and review of the literature. *J Trauma*. 2008;64:1387-1391.

37. Bjurlin MA, Rousseau LA, Vidal PP, Hollowell CM. Iatrogenic ureteral injury secondary to a thoracolumbar lateral revision instrumentation and fusion. *Spine J*. 2009;9:e13-e15.

38. Kaffenberger S, Tomaszewski JJ, Tsao AK, Jackman SV. Hand-assisted laparoscopic ureteroureterostomy with renal mobilization for delayed recognition of a proximal ureteral injury after lumbar disk surgery. *Can Urol Assoc J*. 2010;4:E82-E85.

39. Pillai SB, Hegde P, Venkatesh G, Iyyan B. Ureteral injury after posterior lumbar discectomy with interbody screw fixation. *BMJ Case Rep*. 2013;2013. https://doi.org/10.1136/bcr-2013-200383.

40. Tsai P-J, Wang H-YJ, Lin Y-S, Yang T-M. Laparoscopic ureteral repair for iatrogenic ureteral injury following lumbar disc surgery. *Formosan J Surg*. 2013;46:217-220.

41. Akpinar S, Yilmaz G, Celebioglu E. Cystic retroperitoneal mass due to ureteral injury as an outcome of lumbar disc hernia operation. *Urol J*. 2015;12:2291-2292.

42. Garg N, Panwar P, Devana SK, Ravi Mohan SM, Mandal AK. Ureteric injury after lumbosacral microdiscectomy: a case report and review of literature. *Urol Ann*. 2017;9:200-203.

43. Desaussure RL. Vascular injury coincident to disc surgery. *J Neurosurg*. 1959;16:222-228.

44. Gangai MP, Agee RB, Spence CR. Surgical injury to ureter. *Urology*. 1976;8:22-27.

45. de Quintana-Schmidt C, Clavel-Laria P, Bartumeus-Jené F. Lesión del uréter tras una cirugía lumbar posterior. Caso clínico [Ureteral injury after posterior lumbar surgery. Case report]. *Neurocirugía*. 2011;22:162-166 [in Spanish].

46. Faye R, Buzelin JM, Le Coguic G, Thebaut Y, Auvigne J. [A rare complication of disk surgery: ureteral fistula. Apropos of a case following counter-lateral laminectomy]. *J Urol (Paris)*. 1983;89:273-275 [in French].

47. Heller V, Osterhage HR, Heckl W, Frohmuller H. [Ureteral injuries in intervertebral lumbar disk surgery]. *Urologe A*. 1986;25:347-350 [in German].

48. Rios Gonzalez E, Ramon de Fata Chillon F, Tabernero Gomez A, Nunez Mora C, Hidalgo Togores L, de la Pena Barthel JJ. [Iatrogenic injury of the lumbar ureter and iliac vessels after lumbar discectomy: urologic treatment using kidney autotransplantation]. *Actas Urol Esp*. 2002;26:504-508 [in Spanish].

49. Turunc T, Kuzgunbay B, Gul U, Ozkardes H. Ureteral avulsion due to lumbar disc hernia repair. *Can J Urol*. 2010;17:5478-5479.

50. Steg A, Boccon-Gibod L, Vialatte J, Arvis G, Evrard J. [Ureteral complications of orthopedic surgery]. *Rev Chir Orthop Reparatrice Appar Mot*. 1974;60:169-174 [in French].

51. Brau SA, Delamarter RB, Kropf MA, Watkins RG 3rd, Williams LA, Schiffman ML, et al. Access strategies for revision in anterior lumbar surgery. *Spine*. 2008;33:1662-1667.

52. Santos ER, Pinto MR, Lonstein JE, Denis F, Garvey TA, Perra JH, et al. Revision lumbar arthrodesis for the treatment of lumbar cage pseudoarthrosis: complications. *J Spinal Disord Tech*. 2008;21:418-421.

53. Schwender JD, Casnellie MT, Perra JH, Transfeldt EE, Pinto MR, Denis F, et al. Perioperative complications in revision anterior lumbar spine surgery: incidence and risk factors. *Spine*. 2009;34:87-90.

54. Flouzat-Lachaniette CH, Delblond W, Poignard A, Allain J. Analysis of intraoperative difficulties and management of operative complications in revision anterior exposure of the lumbar spine: a report of 25 consecutive cases. *Eur Spine J*. 2013;22:766-774.

55. Lee HJ, Kim JS, Ryu KS, Park CK. Ureter injury as a complication of oblique lumbar interbody fusion. *World Neurosurg*. 2017;102:693.e7-693.e14.

56. Flynn DE, Caroline DF, Gembala RB, Ball DS, Radecki PD, Cohen GS. Urinoma secondary to surgical spinal fusion: radiologic diagnosis and treatment. *Abdom Imaging*. 1993;18:292-294.

57. Gayet G. Urinomas caused by ureteral injuries: CT appearance. *Abdom Imaging*. 2002;27:88-92.

58. Mitty HA. CT for diagnosis and management of urinary extravasation. *AJR Am J Roentgenol*. 1980; 134:497-501.

Conflict of interest statement: The authors declare that the article content was composed in the absence of any commercial or financial relationships that could be construed as a potential conflict of interest.

Received 18 September 2017; accepted 30 November 2017

Citation: World Neurosurg. (2018) 111:28-35.
https://doi.org/10.1016/j.wneu.2017.11.175

Journal homepage: www.WORLDNEUROSURGERY.org

Available online: www.sciencedirect.com

6.1.3 Highlights from the case study

1. This report shows that unexpected side effects are possible, and spine surgeons should use extra caution, particularly while performing MISS procedures, in which, by definition, the pedicles are concealed from direct visualization.

2. A review of the literature identified a total of 27 well-described ureteral complication following posterior spinal surgery.

3. Our case is the only reported ureteral perforation after lumbar surgery to be caused by a K-wire.

6.2 PERCUTANEOUS PEDICLE SCREWS: APPLICATION UNDER INTRAOPERATIVE ROBOTIC 3D FLUOROSCOPIC NAVIGATION

Fomekong E, Labeau J, Raftopoulos C.

6.2.1 Summary of the study

Spine surgeons are familiar with standard open surgical approaches to the spine, although they are associated with significant morbidity from blood loss, muscle trauma, increased postoperative pain and recovery times, and impaired spinal function [214-216]. Although minimally invasive surgery limits direct visualization of certain key anatomical landmarks, strategies have been developed in order to reduce complications. However, minimally invasive surgery requires more frequent use of intraoperative fluoroscopy, which is associated with various disadvantages. In particular, the entire surgical team (surgeon, assistant surgeon, and scrub nurse) and patients are exposed to X-rays, and the surgical team must wear uncomfortable protective equipment such as lead aprons and thyroid shields. To address these drawbacks, computer-assisted navigation (CAN) techniques have been developed [39, 109-111]. This chapter presents our strategy for reducing radiation in the operating room using CAN based on robotic 3D fluoroscopic images acquired intraoperatively [94, 217]. Subsequently, we describe the impact of this strategy to increase the precision of PPS placement, particularly in lumbar surgery.

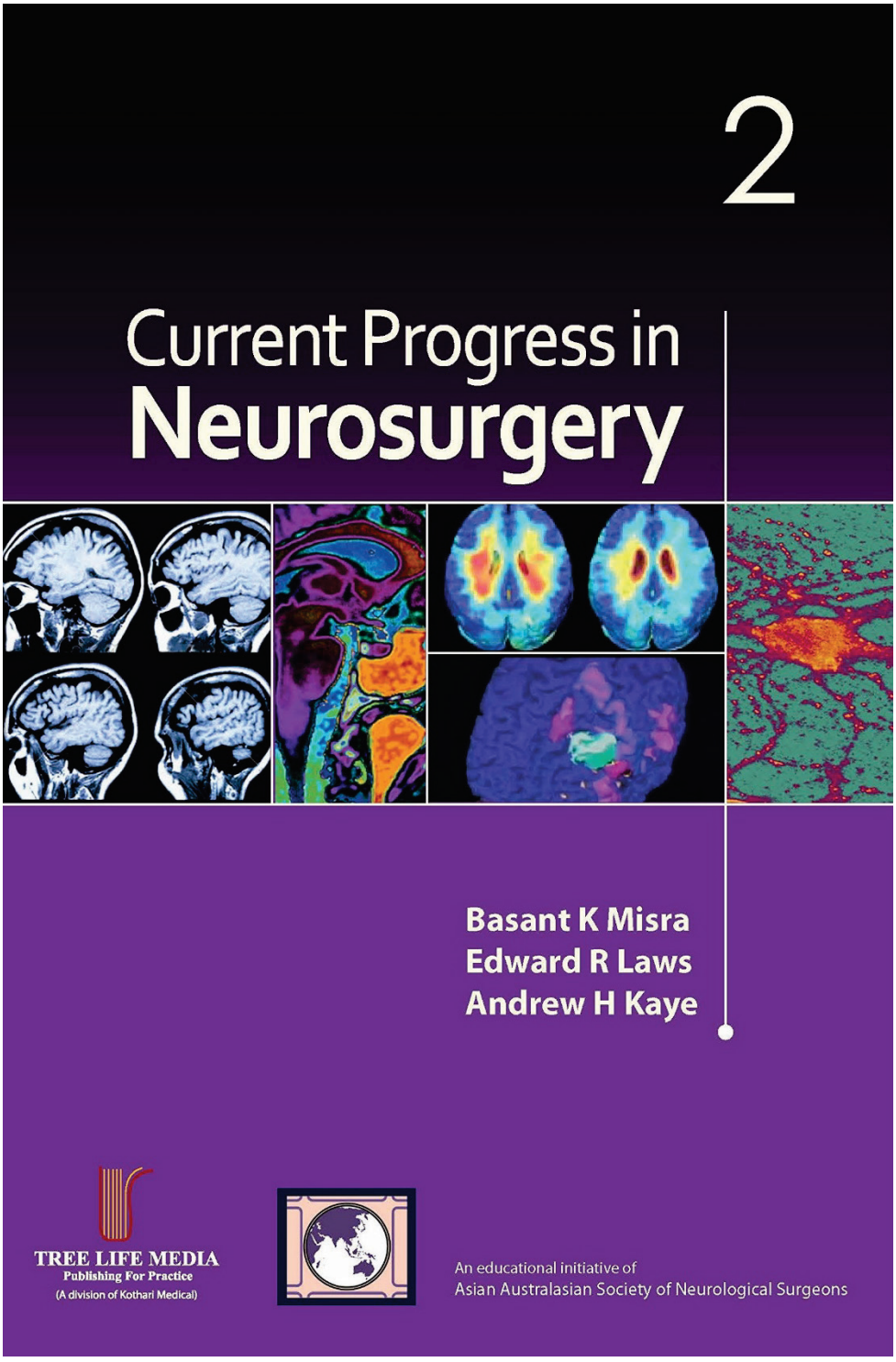
2
Current Progress in
Neurosurgery
Basant K Misra
Edward R Laws
Andrew H Kaye
TREE LIFE MEDIA
Publishing For Practice
(A division of Kothari Medical)
An educational initiative of
Asian Australasian Society of Neurological Surgeons

CHAPTER 7

Percutaneous Pedicle Screws: Application Under Intraoperative Robotic 3D Fluoroscopic Navigation

Edward Fomekong, Jason Labeau, and Christian Raftopoulos

INTRODUCTION

Spine surgeons are familiar with standard open surgical approaches to the spine, although these are associated with significant morbidity from blood loss, muscles trauma, increased postoperative pain and recovery times, and impaired spinal function.[1–3] Thus, although minimal invasive surgery (MIS) limits direct visualization of certain key anatomic landmarks, these strategies have been developed in order to reduce complications. However, MIS requires a more frequent use of intraoperative fluoroscopy which is associated with various disadvantages. In particular, the entire surgical team (surgeon, assistant surgeon, and scrub nurse) and the patient are exposed to the X-ray source and the surgical team must wear uncomfortable heavy protective equipment such as lead aprons and thyroid shields. To address these drawbacks, computer assisted navigation (CAN) techniques have been developed.[4–7] In this chapter, we present our strategy of reducing radiation into

Department of Neurosurgery, St. Luc University Hospital Brussels, UCL, Avenue Hippocrate, B-1200 Brussels, Belgium

the operating room using CAT based on intraoperative acquired robotic 3D fluoroscopic images.[8,9] Subsequently we describe the impact of this strategy to increase the precision of the percutaneous placed screws (PPSs), in particular in lumbar surgery.

Radiation in Spinal Surgery

With the development of MIS, radiation image guidance techniques were more used to reach satisfactory surgical results, decreased morbidity, and improved outcomes for selected patients. However, radiation exposure of surgeons and theater personnel has become a particular concern.[10,11] As the number of radiation-related procedures increases, international regulations aiming to control radiation exposure have been created. These guidelines are designed to prevent acute radiation exposures and to limit chronic radiation exposure to "acceptable" levels. All operators using ionizing radiation are advised to conform to the international principle of "As Low As Reasonably Achievable" (ALARA).

According to Rampersaud et al.,[10] fluoroscopically assisted pedicle screw placement exposes the spine surgeon to significantly greater (10–12 times) radiation levels than non-spinal procedures.[12,13] Consequently, both patients and surgeons are at a higher risk of developing radiation-induced malignancy. From a series of patients followed up by serial radiographies for idiopathic scoliosis, reviews showed malignancy rates of 17–239 per 100,000.[14,15]

Navigation in Spinal Surgery

Image guidance systems were introduced to cranial neurosurgery during the 1990s, and were applied to spinal surgery after the initial problem of reference array attachment to the spine was solved. Subsequently, a report of the first patient series with PPS was published in 1995.[16–18] Since then several studies have demonstrated advantages of image guidance, particularly in pedicle placement using this technique.[19–27] Hence, intraoperative CT and 3-dimensional (3D) image-guidance have recently become available to improve the accuracy of pedicle screw placement.[9,28–30] Most related studies have reported the use of standard open techniques in conjunction with these image-guidance tools. The ensuing accuracy of pedicle screw placement is considered quite good to excellent, and 99% accuracy rates have been reported in a limited pediatric patient series.[31] However, radiation exposure of the surgical team remains a major consideration with this technique. Further, CT-based intraoperative techniques are costly and time consuming. Nonetheless, the disadvantages of 3D intraoperative fluoroscopy can be circumvented using separated spine CAN modules.

MATERIALS AND METHODS

The robotic 3D Artis ZeeGo I image-guidance system has been used for many years in our institution, and although we have reported our experience with PPS using this device,[9] our use of combined extra separated navigation has not been reported. We recently acquired a new robotic multi-axis 3D Artis ZeeGo, named ZeeGO II (Fig. 1a, Siemens, Germany)

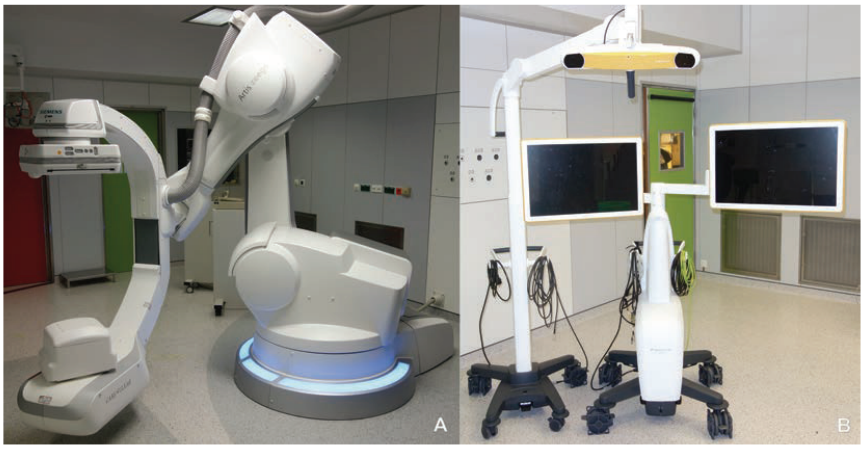

Figure 1: Zeego II from Siemens (A) and curve navigation system from BrainLab (B).

combined to a CAN system (Curve, BrainLab, Germany, Fig. 1b) to increase the accuracy of PPS while decreasing radiation exposure of the surgical team and the patient. In the present study, we report our preliminary experience using the Artis Zeego II in combination with Brainlab spine navigation for accurate placement of PPS in patients with refractory low back pain. Based on several years of experience with the Zeego 3D fluoroscoppy and more than 2 years' experience in combination with Curve navigation, we have implemented an operating room (OR) arrangement that facilitates appropriate spinal procedures when instrumentation is required (Fig. 2).

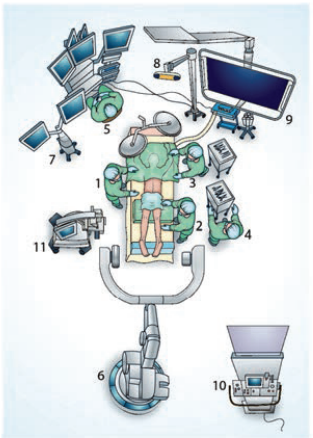

Our Study Population

PPS placement was performed in 28 consecutive patients using a combination of spine navigation and 3D image-guidance between January 2014 and December 2014 among the 11 male and 17 female patients with an average age of 58.6 years (range, 19–91 years). The mean body mass index (BMI) was 26.5 (range, 17.6–35.4; Table 1). The main indication among these patients was severe spondylodiscarthrosis with lumbar radicular pain that was refractory to conservative management (24 patients)

Figure 2: OR setup. 1, surgeon; 2, assistant surgeon; 3, scrub nurse; 4, technician; 5, anesthesiologist; 6, Zeego unit; 7, navigation unit; 8, infrared camera; 9, Zeego control screen; 10, Zeego control console; 11, surgical microscope.

Table 1: Clinical characteristics of 28 patients before percutaneous pedicle screw placement using 3D fluoroscopy and spine navigation.

Mean age (years)	58.6
Min.	19
Max.	91
Sex	
Female	17
Male	11
Mean BMI	26.5
Min.	17.6
Max.	35.4
Preoperative symptoms (pain)	
Lumbar radicular	22
Lumbar	6
Mean VAS	5.5
Min.	2
Max.	9
Mean ODI	44.4
Previous surgery	
Lumbar disk hernia	6
Canal stenosis	1
Scoliosis	1
Preoperative diagnosis	
Spondylolisthesis	11
Severe discarthrosis	22
Scoliosis	4
Other*	10

Fractures (n = 4), canal stenosis (n = 6) in association with severe discarthrosis in all cases and also with spondylolisthesis in two cases.

or unstable post-traumatic spine fractures (4 patients). The PPS procedure was performed after transforaminal lumbar interbody fusion (TLIF) in 20 patients, and without arthrodesis in 8 patients. All patients, after full explanation, signed an informed consent (Raftopoulos 2010).[8]

Step-by-step Surgical Procedure

PPS insertion was performed in all patients as follows: (1) After general anesthesia with endotracheal intubation, patients were installed in a prone position on the Maquet table feet first (end of feet at the side of the base of the Zeego II; Fig. 2); (2) A 2D fluoroscopy was performed to delineate the region of interest, and critically, the nearest spinous process was identified for the insertion of the navigation reference clamp; (3) Through a 2 cm midline incision, the spinous process was dissected and the reference clamp was firmly attached to it. It was then oriented cranially to spare the field of view of the infrared camera; (4)

Subsequently, Brainlab navigation software was used to prepare 3D image-acquisition, and the appropriate pre-set program was selected for 3D on the Zeego II console; (5) On the Zeego console, the Zeego was sent to the region of interest to perform the automatic 3D test procedure, and a final check of the navigation screen confirmed that the software appropriately registered the position of the C arm. A short 6-s apnea is required during the 3D images acquisition (c-arm rotation around the patient), and the images were automatically transferred to the navigation system; (6) Verification of the concordance between the 3D images and the patient with a reference pointer followed by planification, storage, and fine-tuning of all screw characteristics (length and diameter) according to the size of each pedicle (Fig. 3); (7) A 2-cm skin incision was made 4–5 cm from the midline at the level of each targeted pedicle, and a metallic guide-wire was then inserted through a pedicle finder; (8) A double-check step was then performed using 2D fluoroscopy after insertion of all the guide-wires to avoid insertion of multiple guide-wires into the same pedicle in patients with severe degenerative deformities; (9) Placement of corresponding screws was performed after manual drilling of the pedicle entrance; (10) Final 3D sequence analyses were performed to grade the screw placement within the pedicles using the Zeego workstation; (11) Rod measurements, insertion, and finalization of the instrumentation were then conducted; and (12) hemostasis was verified and closure of the aponeurosis and finally the skin in two layers was performed using dermo-glue for the surface. When TLIF arthrodesis was necessary, an additional 2D fluoroscopy step was usually performed prior to the above steps to ensure a safe TLIF approach. Radiation exposure of the surgeon was limited to the above 2D fluoroscopy steps (2) and (8), which required proximity of the surgeon and patient. Hence, the risk of radiation exposure to the surgical team was limited by acquiring 3D images remotely to the

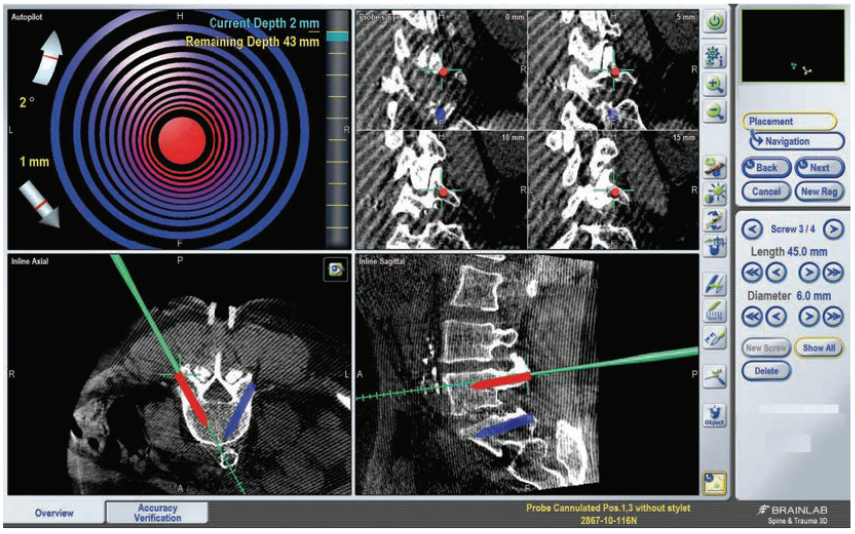

Figure 3: Virtual planning and navigation of all PPS.

patient and Zeego II X-ray source and being a security screen. The surgeon wore a dosimeter that was subsequently analyzed by the radio physical department.

RESULTS

Pedicle Screw Accuracy

A total of 128 consecutive PPSs were placed using the above surgical procedure. All patients were able to walk on the second postoperative day and were discharged before the sixth day. In agreement with previous reports, preoperative CTscans were performed for difficult cases with severe degenerative deformities and the imaging data was introduced into a Dextroscope (Volumes Interactions, Bracco, Singapore) for virtual surgery the day before. Operative levels extended from Th10 to S1 vertebrae (Table 2).

Table 2: Operative data from 28 patients after PPS placement using CAN based on preoperative acquired robotic 3D fluoroscopic images.

Levels operated	**%**
Th10-Th11	6
L1-L2	6
L2-L3	6
L3-L4	20
L4-L5	15
L5-S1	47
Total number of screws	128
Number of screw related to vertebra	**n**
Th10	4
Th11	4
L1	4
L2	8
L3	18
L4	16
L5	42
S1	32
Associate procedures	**%**
TLIF	68
Recalibration	4.7
Mean surgical duration (min.)	
Min.	167
Max.	482
Mean radiation dose to patient	**µGym²**
Overall	21,3
Per 3D scan	8,6

Only 2 of 128 PPSs were misplaced (1.5%), and were subsequently corrected after intraoperative 3D control. An additional 3D scan was performed for each of these two cases, and final analyses of all screws demonstrated perfect intrapedicular insertion (100% grade 0 of Wang classification, Fig. 4).

Radiation

Cumulative radiation exposure of surgeons remained below measurable levels [<0 millisievert (mSv)]. The cumulative radiation exposure per patient was only 22.3 μGym^2, and the average radiation exposure per case during 3D image acquisition was 21.62 μGym^2. The

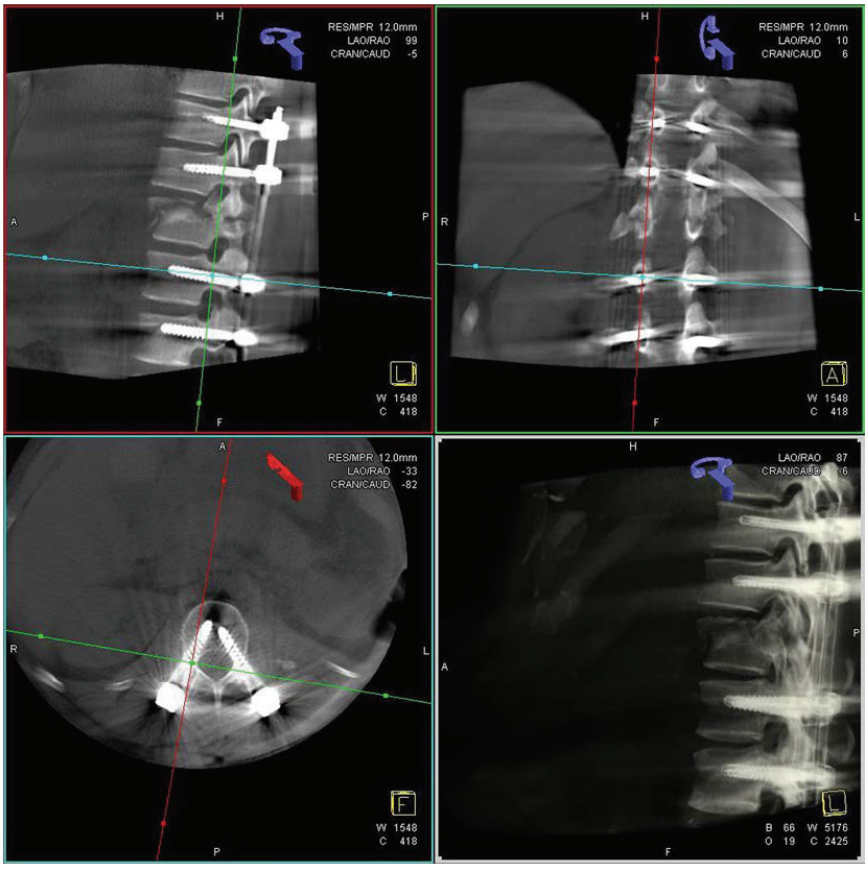

Figure 4: Preoperative acquired robotic 3D fluoroscopic image showing Wang grade 0 for all PPS.

mean exposure time to radiation was 1.2 minutes. In total, the final average radiation dose per patient for the entire procedure was 22.3 μGym^2.

Complications

Complications included only one dural breach during a TLIF procedure, which was sutured immediately without any further events.
Overall, 98.5% of this preliminary series had Wang evaluations of grade 0 at 3D intraoperative scan control, and 100% had grade 0 before the end of surgery.

DISCUSSION

The present study demonstrates that the use of CAN to implant our PPS based on preoperative acquired 3D fluoroscopic images can provide up to 100% accuracy and dramatically reduces radiation exposures of surgeons and patients. Specifically, total radiation exposure times for patients were reduced by performing the main surgical procedure using a virtual 3D interface on a navigation system, and radiation exposure of the surgeon was undetectable. Because the long-term effects of chronic exposure to X-rays remain unclear,[32–34] this technical development is of vital importance. Use of CT-based guidance for percutaneous procedures has been demonstrated in spinal biopsy,[35] percutaneous discectomy,[36] kyphoplasty,[37] aspiration of spinal cysts,[38] and during implantation of pedicle screws.[4,7,12,39–42] In agreement with the present observations, Villard et al.[43] showed that 3D fluoroscopy-based spinal navigation for lumbar fusion significantly reduced radiation exposure of surgeons by up to 9.96-fold compared with freehand techniques.

In a systematic review of literature published between 1980 and 1993, Yu and Khan[44] found that radiation exposure was higher during MIS spine procedures than for open procedures. However, use of a CAN system with 3D virtual pedicle screw planning circumvented the disadvantage of obscured spine anatomic landmarks, and hence, extra X-ray exposure during surgery was no longer required to improve accuracy. In a study of four cadavers, Smith et al.[45] compared surgeon radiation exposure during C-arm fluoroscopy and computer-assisted image guidance for implantation of pedicle screws, and showed no measurable radiation exposures using navigation, and no differences in the accuracy of screw placement between the techniques.

In agreement, the present observations suggest that, in experienced hands, omission of the final 3D imaging step further reduces radiation doses, and the present calculations demonstrate that one 3D image step delivers 8.6 μGym^2 to the patient. In the present study, no dosimeter was applied to the surgeon's face to measure eyes exposure, representing a limitation of the study. However, because the present dosimetric measurements showed undetectable exposures, eye exposures were likely negligible also.

In the present procedure, performance of spine navigation based on Zeego II 3D fluoroscopy reduced the numbers of required preoperative fluoroscopic acquisitions. Although 3D scans require greater patient radiation exposures than 2D acquisition, only two 3D scans were required for the entire procedure, thus reducing total radiation exposure. In contrast,

assessment of screw positions were performed using additional 3D fluoroscopy at the end of surgery in cases in which navigation was not performed, and most fluoroscopic images were taken in lateral view, which requires higher doses for image quality.[46] Therefore, the present navigation technique favorably reduces radiation exposures of patients during percutaneous PPS implantation.

CONCLUSION

The use of CAN based on preoperative robotic 3D fluoroscopic images increases accuracy of PPS implantation and decreased total radiation doses to undetectable levels for the staff in the operating theater. Moreover, Wang grade 0 was achieved in 100% of the cases at the end of surgery without complications in this preliminary series. However, further studies are required to this strategy on a larger population.

KEY LEARNING POINTS

1. PPS implantation with or without intervertebral cages (TLIF) are globally accepted interventions to address spinal degenerative or traumatic spine pathologies that are refractory to conservative management.
2. MIS approaches help to minimize tissue damage and lead to better and faster recovery.
3. Minimizing surgical invasiveness requires increased image guidance often associated to increase radiation exposures of patients and spine surgeons.
4. Use of spinal CAN based on preoperative acquired 3D fluoroscopic images helps to improve PPS implantation while minimizing exposure of surgical team members and patients to radiation.
   With careful planning, the rate of PPS precisely located intrapedicular reached 100% in this preliminary series.

REFERENCES

1. Foley KT, Lefkowitz MA. Advances in minimally invasive spine surgery. *Clin Neurosurg* 2002;49:499–517.
2. Kawaguchi Y, Matsui H, Tsuji H. Back muscle injury after posterior lumbar spine surgery. A histologic and enzymatic analysis. *Spine (Phila Pa 1976)* 1996;21(8):941–4.
3. Kawaguchi Y, Yabuki S, Styf J, et al. Back muscle injury after posterior lumbar spine surgery. Topographic evaluation of intramuscular pressure and blood flow in the porcine back muscle during surgery. *Spine (Phila Pa 1976)* 1996;21(22):2683–8.
4. Foley KT, Simon DA, Rampersaud YR. Virtual fluoroscopy: computer-assisted fluoroscopic navigation. *Spine (Phila Pa 1976)* 2001;26(4):347–51.
5. Kalfas IH. Image-guided spinal navigation. *Clin Neurosurg* 2000;46:70–88.

6. Merloz P, Tonetti J, Pittet L, et al. Computer-assisted spine surgery. *Comput Aided Surg* 1998;3(6):297–305.
7. Schlenzka D, Laine T, Lund T. Computer-assisted spine surgery. *Eur Spine J* 2000;9 Suppl 1:S57–S64.
8. Raftopoulos C. Spine neurosurgery in Belgium. *World Neurosurg* 2010;74(4–5):430–1.
9. Raftopoulos C, Waterkeyn F, Fomekong E, Duprez T. Percutaneous pedicle screw implantation for refractory low back pain: from manual 2D to fully robotic intraoperative 2D/3D fluoroscopy. *Adv Tech Stand Neurosurg* 2012;38:75–93.
10. Rampersaud YR, Foley KT, Shen AC, et al. Radiation exposure to the spine surgeon during fluoroscopically assisted pedicle screw insertion. *Spine (Phila Pa 1976)* 2000;25(20):2637–45.
11. Smith ZA, Fessler RG. Paradigm changes in spine surgery: evolution of minimally invasive techniques. *Nat Rev Neurol* 2012;8(8):443–50.
12. Kim CW, Lee YP, Taylor W, et al. Use of navigation-assisted fluoroscopy to decrease radiation exposure during minimally invasive spine surgery. *Spine J* 2008;8(4):584–90.
13. Theocharopoulos N, Damilakis J, Perisinakis K, et al. Occupational gonadal and embryo/fetal doses from fluoroscopically assisted surgical treatments of spinal disorders. *Spine (Phila Pa 1976)* 2004;29(22):2573–80.
14. Bone CM, Hsieh GH. The risk of carcinogenesis from radiographs to pediatric orthopaedic patients. *J Pediatr Orthop* 2000;20(2):251–4.
15. Goldberg MS, Mayo NE, Levy AR, et al. Adverse reproductive outcomes among women exposed to low levels of ionizing radiation from diagnostic radiography for adolescent idiopathic scoliosis. *Epidemiology* 1998;9(3):271–8.
16. Nolte LP, Visarius H, Arm E, et al. Computer-aided fixation of spinal implants. *J Image Guid Surg* 1995;1(2):88–93.
17. Nolte LP, Zamorano L, Visarius H, et al. Clinical evaluation of a system for precision enhancement in spine surgery. *Clin Biomech (Bristol, Avon)* 1995;10(6):293–303.
18. Nolte LP, Zamorano LJ, Jiang Z, et al. Image-guided insertion of transpedicular screws. A laboratory set-up. *Spine (Phila Pa 1976)* 1995;20(4):497–500.
19. Assaker R, Reyns N, Vinchon M, et al. Transpedicular screw placement: image-guided versus lateral-view fluoroscopy: in vitro simulation. *Spine (Phila Pa 1976)* 2001;26(19):2160–4.
20. Han W, Gao ZL, Wang JC, et al. Pedicle screw placement in the thoracic spine: a comparison study of computer-assisted navigation and conventional techniques. *Orthopedics* 2010;33(8).
21. Ishikawa Y, Kanemura T, Yoshida G, et al. Clinical accuracy of three-dimensional fluoroscopy-based computer-assisted cervical pedicle screw placement: a retrospective comparative study of conventional versus computer-assisted cervical pedicle screw placement. *J Neurosurg Spine* 2010;13(5):606–11.
22. Kelleher MO, McEvoy L, Nagaria J, et al. Image-guided transarticular atlanto-axial screw fixation. *Int J Med Robot* 2006;2(2):154–60.
23. Kosmopoulos V, Schizas C. Pedicle screw placement accuracy: a meta-analysis. *Spine (Phila Pa 1976)* 2007;32(3):E111–E120.
24. Laine T, Lund T, Ylikoski M, et al. Accuracy of pedicle screw insertion with and without computer assistance: a randomised controlled clinical study in 100 consecutive patients. *Eur Spine J* 2000;9(3):235–40.
25. Rajasekaran S, Vidyadhara S, Ramesh P, et al. Randomized clinical study to compare the accuracy of navigated and non-navigated thoracic pedicle screws in deformity correction surgeries. *Spine (Phila Pa 1976)* 2007;32(2):E56–E64.
26. Richter M, Cakir B, Schmidt R. Cervical pedicle screws: conventional versus computer-assisted placement of cannulated screws. *Spine (Phila Pa 1976)* 2005;30(20):2280–7.
27. Ughwanogho E, Patel NM, Baldwin KD, et al. Computed tomography-guided navigation of thoracic pedicle screws for adolescent idiopathic scoliosis results in more accurate placement and less screw removal. *Spine (Phila Pa 1976)* 2012;37(8):E473–E478.

28. Larson AN, Santos ER, Polly DW Jr., et al. Pediatric pedicle screw placement using intraoperative computed tomography and 3-dimensional image-guided navigation. *Spine (Phila Pa 1976)* 2012;37(3):E188–E194.
29. Santos ER, Ledonio CG, Castro CA, et al. The accuracy of intraoperative O-arm images for the assessment of pedicle screw postion. *Spine (Phila Pa 1976)* 2012;37(2):E119–125.
30. Silbermann J, Riese F, Allam Y, et al. Computer tomography assessment of pedicle screw placement in lumbar and sacral spine: comparison between free-hand and O-arm based navigation techniques. *Eur Spine J* 2011;20(6):875–81.
31. Larson AN, Polly DW Jr., Guidera KJ, et al. The accuracy of navigation and 3D image-guided placement for the placement of pedicle screws in congenital spine deformity. *J Pediatr Orthop* 2012;32(6):e23–e29.
32. Dewey P, Incoll I. Evaluation of thyroid shields for reduction of radiation exposure to orthopaedic surgeons. *Aust N Z J Surg* 1998;68(9):635–6.
33. Mroz TE, Abdullah KG, Steinmetz MP, et al. Radiation exposure to the surgeon during percutaneous pedicle screw placement. *J Spinal Disord Tech* 2011;24(4):264–7.
34. Ul Haque M, Shufflebarger HL, O'Brien M, Macagno A. Radiation exposure during pedicle screw placement in adolescent idiopathic scoliosis: is fluoroscopy safe? *Spine (Phila Pa 1976)* 2006;31(21):2516–20.
35. Leschka SC, Babic D, El Shikh S, et al. C-arm cone beam computed tomography needle path overlay for image-guided procedures of the spine and pelvis. *Neuroradiology* 2012;54(3):215–23.
36. von Jako RA, Cselik Z. Percutaneous laser discectomy guided with stereotactic computer-assisted surgical navigation. *Lasers Surg Med* 2009;41(1):42–51.
37. Izadpanah K, Konrad G, Sudkamp NP, Oberst M. Computer navigation in balloon kyphoplasty reduces the intraoperative radiation exposure. *Spine (Phila Pa 1976)* 2009;34(12):1325–9.
38. Takahashi S, Saruhashi Y, Odate S, et al. Percutaneous aspiration of spinal terminal ventricle cysts using real-time magnetic resonance imaging and navigation. *Spine (Phila Pa 1976)* 2009;34(6):629–34.
39. Gebhard F, Weidner A, Liener UC, et al. Navigation at the spine. *Injury* 2004;35 Suppl 1:S-A35-45.
40. Hofstetter R, Slomczykowski M, Sati M, Nolte LP. Fluoroscopy as an imaging means for computer-assisted surgical navigation. *Comput Aided Surg* 1999;4(2):65–76.
41. Holly LT, Foley KT. Three-dimensional fluoroscopy-guided percutaneous thoracolumbar pedicle screw placement. Technical note. *J Neurosurg* 2003;99(3 Suppl):324–9.
42. Tjardes T, Shafizadeh S, Rixen D, et al. Image-guided spine surgery: state of the art and future directions. *Eur Spine J* 2010;19(1):25–45.
43. Villard J, Ryang YM, Demetriades AK, et al. Radiation exposure to the surgeon and the patient during posterior lumbar spinal instrumentation: a prospective randomized comparison of navigated versus non-navigated freehand techniques. *Spine (Phila Pa 1976)* 2014;39(13):1004–9.
44. Yu E, Khan SN. Does less invasive spine surgery result in increased radiation exposure? A systematic review. *Clin Orthop Relat Res* 2014;472(6):1738–48.
45. Smith HE, Welsch MD, Sasso RC, Vaccaro AR. Comparison of radiation exposure in lumbar pedicle screw placement with fluoroscopy vs computer-assisted image guidance with intraoperative three-dimensional imaging. *J Spinal Cord Med* 2008;31(5):532–7.
46. Perisinakis K, Theocharopoulos N, Damilakis J, et al. Estimation of patient dose and associated radiogenic risks from fluoroscopically guided pedicle screw insertion. *Spine (Phila Pa 1976)* 2004;29(14):1555–60.

6.2.2 Highlights from this paper

1. PPS implantation via MISS with or without intervertebral fusion is globally accepted to address spinal degenerative or traumatic spine pathologies that are refractory to conservative management.

2. MISS approaches help to minimize tissue damage and lead to better and faster recovery.

3. MISS requires increased image guidance often associated with increased radiation exposure to patients and surgeons.

4. Use of spinal CAN based on 3D fluoroscopic images acquired preoperatively can improve PPS implantation while minimizing the radiation exposure of surgical team members and patients.

5. With careful planning, the rate of precise intrapedicular PPS placement reached 100% in this preliminary series

6.3 PERCUTANEOUS PEDICLE SCREW IMPLANTATION FOR REFRACTORY LOW BACK PAIN: FROM MANUAL 2D TO FULLY ROBOTIC INTRAOPERATIVE 2D/3D FLUOROSCOPY

Raftopoulos C., Waterkeyn F., **Fomekong E.**, Duprez T.

6.3.1 Summary of this paper

Spinal fusion with interbody cages filled with bone graft is a treatment option for CLBP refractory to medical treatments. Reported fusion rates range from 72% to 91% depending on the complexity of the surgical procedure. The more complex the surgical procedure, the higher the complication rate, varying between 6 and 31% depending on the surgical technique. The paper reports the use of a robotic multi-axis 2D/3D fluoroscopy system to enhance the accuracy of PPS placement and reviews other strategies and results reported in the literature.

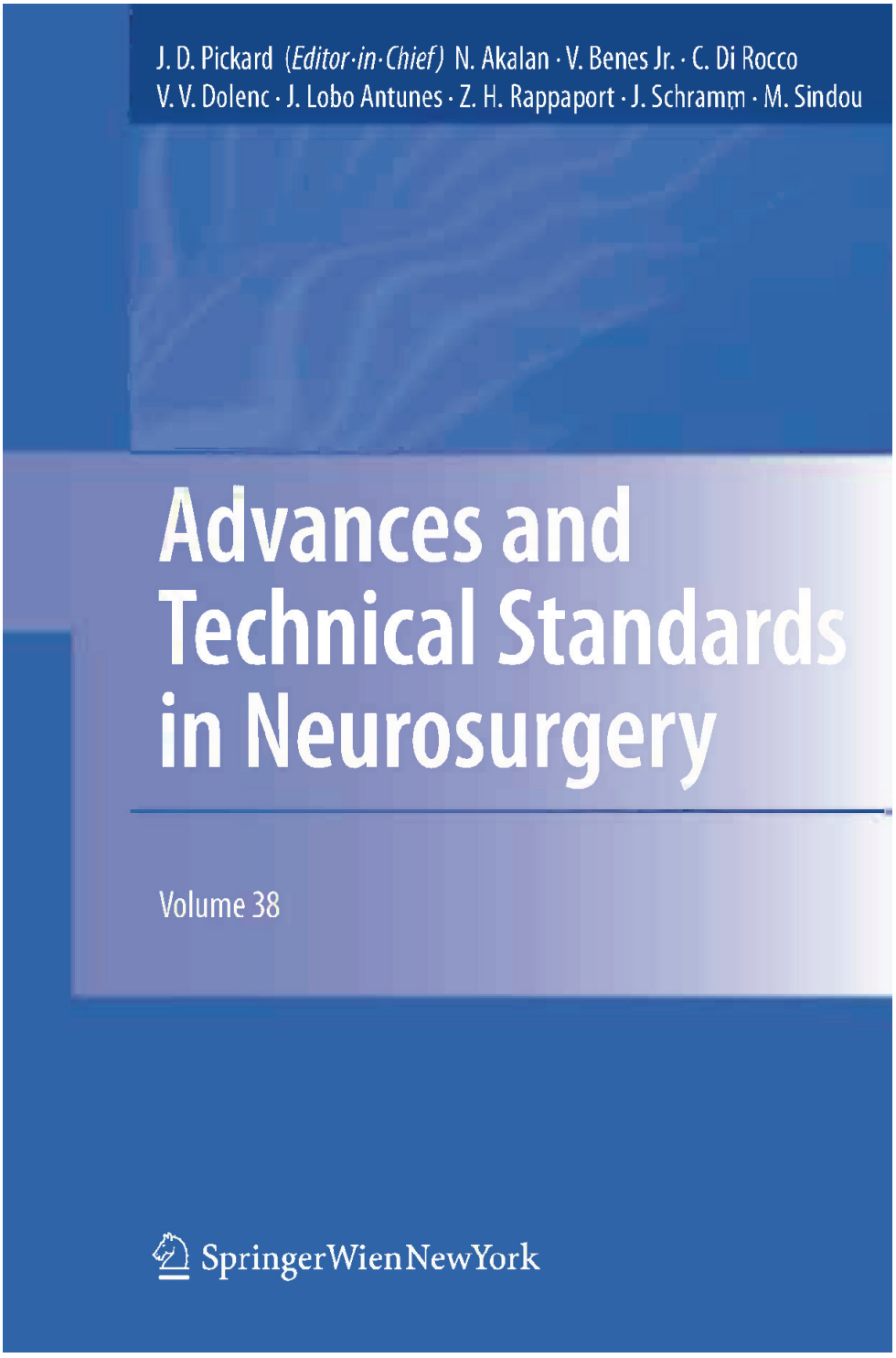
J. D. Pickard (Editor-in-Chief) N. Akalan · V. Benes Jr. · C. Di Rocco
V. V. Dolenc · J. Lobo Antunes · Z. H. Rappaport · J. Schramm · M. Sindou
Advances and Technical Standards in Neurosurgery
Volume 38
SpringerWienNewYork

Percutaneous pedicle screw implantation for refractory low back pain: from manual 2D to fully robotic intraoperative 2D/3D fluoroscopy

C. RAFTOPOULOS, F. WATERKEYN, E. FOMEKONG, and T. DUPREZ

Department of Neurosurgery and Neuroradiology, Clinique Universitaire St-Luc, Brussels, Université catholique de Louvain, Louvain-la-Neuve, Belgium

With 5 Figures and 7 Tables

Contents

J. D. Pickard et al. (eds.), *Advances and Technical Standards in Neurosurgery*

Abstract

Many surgical treatments for chronic low back pain that is refractory to medical treatments focus on spine stabilization. One of the main surgical procedures consists of placing an interbody cage with bone grafts associated with pedicle screws [2, 25, 30]. This technique can be performed using different approaches: a large open posterior approach, tubular approaches (minimal open) or percutaneously (minimally invasive percutaneous or MIP) [5, 28]. One of the main difficulties is to precisely locate the screws into the pedicle avoiding especially infero-medial pedicle breaches. This difficulty is even greater when working percutaneously. This paper focuses on percutaneously placed pedicle screws (PPS), reports the use of a robotic multi-axis 2D/3D fluoroscopy to enhance the accuracy of pedicle screw placement and reviews other strategies and results reported in the literature.

Keywords: Pedicle screw; percutaneous; fluoroscopy; 3D fluoroscopy; C-arm, robotic; pedicle breach; intraoperative imaging; low back pain; radiation.

Abbreviations

i2DF	intraoperative two-dimensional fluoroscopy
i3DF	intraoperative three-dimensional fluoroscopy
CAN	computer assisted navigation
CT	computerized tomography
OR	operating room
PPS	percutaneously placed pedicle screw
TLIF	transforaminal lumbar interbody fusion

Pedicle screws for better fusion rate

Many surgical treatments for chronic low back pain that is refractory to medical treatments focus on spine stabilization. This treatment is most often applied when dealing with spondylolisthesis, painful discopathy, post lumbar canal recalibration, and disc hernia recurrence. One of the main surgical treatments consists of applying bone grafts taken from the pelvis or from a bone bank to the area to be treated in the hope that these will fuse with the underlying

vertebrae. To obtain a higher rate of intervertebral fusion, an interbody cage may be placed with bone grafts associated with pedicle screws and, sometimes, with bone grafts also placed posteriorly around the screws and connecting rods [2, 25, 30]. These procedures achieve different fusion rates, ranging from 72% for a simple postero-lateral fusion technique to 91% for more complex interbody fusion with pedicle screws [7]. However, the more complex the surgical procedure is, the higher is the complication rate, varying between 6 and 31%, depending on the surgical technique.

From open to percutaneously placed pedicle screws (PPS)

Large open posterior approach

In the majority of centres, most procedures performed for the surgical treatment of resistant low back pain require a large open posterior approach to the lumbar region, which is associated with clear disadvantages, including extensive dissection of the paravertebral muscles, considerable blood loss and, over a longer follow-up period, muscular denervation with atrophy, persistent chronic low back pain and depression [1, 4, 5, 17, 23, 24, 26, 34].

Less aggressive posterior approaches

Since around 1990, various pioneering surgical teams have developed techniques aimed at reducing the iatrogenic injury to the dorsal neuromuscular ligamentous complex and its associated blood loss [1, 4, 5, 17, 23, 24, 26, 34]. This evolution has been characterized by the development of minimally invasive techniques using smaller surgical corridors or even percutaneous approaches [17, 20]. The two most significant advances in this field are minimal exposure tubular retractors, such as the METRx system (Medtronic, Memphis, USA) or the Pipeline system (Depuy Spine, Johnson & Johnson, Arlington, USA), and percutaneously placed pedicle screws (PPS), for example using the Sextant device (Medtronic, Memphis, USA) or the Viper system (DePuy Spine, Johnson & Johnson, Arlington, USA). Minimal exposure tubular retractors are now used by a growing number of surgical teams for the treatment of lumbar disc hernias, spine canal recalibration or transforaminal lumbar interbody fusion (TLIF). We started to use PPS using the Sextant system in association with computer assisted navigation (CAN) from BrainLab (Germany) in June 2008. More than one year later, however, we changed to the Viper system from DePuy Spine (Johnson & Johnson, Arlington, USA) because of its greater versatility, particularly for performing osteosynthesis at multiple levels and implanting the connection rods.

Table 1. *General characteristics of 2D/3D fluoroscopic systems available for spine surgery compared to the 2DF OEC 9800 from GE*

Model	Company	Arm gantry size (cm)	Weight (kg)	Fluoroscopy		Robotised	Flat-panel	CAN	3D acquisition time (s)	Price (K€)
				2D	3D					
OEC 9800	GE	84	227	+	−	−	−	+	−	110
FD Vario 3D	Ziehm	89.5	270	+	+	P	+	+	45	300
O-arm	Medtronic	96.5	885	+	+	P	+	+*	13–26	500
Arcadis Orbic 3D	Siemens	78	348	+	+	P	−	+	30–60	250
Artis zeego	Siemens	52–81.5	1850	+	+	F	+	−	5–8	1200

+*, compatible only with Medtronic navigation.
CAN computer-assisted navigation; *F* fully; *P* partially.

Percutaneous: three main problems

When performing PPS implantation, three problems are evident: The first is the loss of anatomical landmarks with, as a result, reduced accuracy which could lead to neurovascular complications and less stable osteosynthesis. This loss of accuracy can be corrected by using a CAN system. The second problem is an increased intraoperative use of the two dimensional fluoroscopy (i2DF) (OEC 9800 from GE, USA; Table 1), with an increase in ionizing radiation doses delivered to the patient and *repetitively to* the medical team. The third problem is that manipulating the conventional i2DF, which is already difficult, becomes an even greater burden for everyone in the OR.

Need for better intraoperative control

CT outside the OR

Briefly, our goal was to find a procedure that offered better intraoperative disclosure of possible implant misplacement than i2DF. As a first strategy, after the surgical procedure we took the anaesthetized patient to the computerized tomography (CT) room located outside the OR. This approach placed considerable extra demands on everyone by increasing the length of the procedure by about 30 minutes. Although it allowed us to correct any mistakes before awaking the patient, the inconvenience of this procedure highlighted the need to be able to perform a CT-like quality control inside the OR.

Intraoperative 2D/3D fluoroscopic systems

We, therefore, started to test different intraoperative three dimensional fluoroscopy (i3DF) systems (Table 1). One of the first we tested was the O-arm Surgical Imaging System from Medtronic. This system was rather cumbersome and could be used only with the CAN from the same company but it was effective. [11, 29]. The second system tested was the Arcadis Orbic system from Siemens (Siemens AG, Forchheim, Germany). The Arcadis Orbic isocentric C-arm was less cumbersome to manipulate and also compatible with different CAN systems [16, 33], so we believed it could be a good choice. However, as soon as we started to use the Artis Zeego, again from Siemens, we were convinced that this was the system best adapted to our needs. Indeed, the Zeego is a robotic multi-axis fluoroscopy device that delivers not only 2D images but also fast CT-like 3D views and was coupled to a motorized surgical table [14]. Although, a CAN cannot yet be integrated with this robotic C-arm fluoroscopy, our main requirements were met by the greater ease of manipulation and the high quality of the images. The aim of this manuscript is to report our preliminary experience using the Artis Zeego for the accurate placement of PPS in the treatment of refractory low back pain.

Does i2D/3DF mean fewer complications?

Our experience with the Artis Zeego

Our population

We report the results from our first 24 patients with refractory low back pain related to degenerative lumbar disease who were treated using percutaneous osteosynthesis (Table 2). The mean age of our population was 59 years a, 50%

Table 2. *Clinical data of 24 patients in whom PPS were placed using i3DF (Zeego)*

Mean age (years)	59
Min.	21
Max.	84
Sex	
Female	14 (58)
Male	10 (42)
Mean BMI (kg/m^2)	26.5
Min.	19
Max.	33
Lumboradicular pain (%)	24 (100)
Lumbar predominant	12 (50)
Radicular predominant	5 (21)
Lumbar/radicular pain similar	7 (29)
Mean VAS (/10)	7
Min.	5
Max.	9
Motor deficit[a] (%)	4 (17)
Mean ODI[b] (%)	48
Min.	20
Max.	84
Previous surgery (%)	9 (37)
LDH	6 (25)
LCS	3 (12.5)
Osteosynthesis	2 (8.3)
Main pathology	
Spondylolisthesis	12 (50)
Severe discopathy	10 (41.7)
Scoliosis	2 (8.3)

BMI body mass index; *i3DF* intraoperative 3-dimensional fluoroscopy; *LCS* lumbar canal stenosis; *LDH* lumbar disc hernia; *ODI* Oswestry disease index; *PPS* percutaneous pedicle screw; *VAS* visual analogue scale.

[a]4/5 on the NFIP (national foundation for infantile paralysis) scale.

[b]not reported for 2 patients.

Table 3. *Characteristics of the surgical procedures*

Lumbar level	*n* (%)
L3-L4	1 (4)
L4-L5	11 (46)
L5-S1	7 (29)
L4-L5-S1	3 (13)
L3-L4-L5-S1	1 (4)
L2-L3-L4-L5	1 (4)
TLIF (%)	20 (84)
One level	19 (80)
Two levels	1 (4)
MBDUA (%)	9 (38)
LDH (%)	1 (6)
Number of PPS	106
L2	2 (1.9)
L3	4 (3.7)
L4	30 (28.3)
L5	46 (43.4)
S1	24 (22.7)
Mean duration of surgery (min)	254
Min.	122
Max.	548

LDH Lumbar disc hernia; *MBDUA* microsurgical bilateral decompression via unilateral approach; *PPS* percutaneous pedicle screw; *TLIF* transforaminal lumbar interbody fusion.

had predominantly lumbar pain and 37% had had previous surgery. The characteristics of the operative procedures are shown in Table 3. One hundred and six PPS were implanted using the Viper 2 fixation system (DePuy Spine, Johnson & Johnson, Arlington, USA) associated when necessary with a TLIF procedure (84%; cage plus allograft bone) or a posterior lumbar fusion procedure (one case) performed through a tubular retractor. The PPS were most frequently implanted at the L4-L5 spinal level (46%). Three main degenerative lumbo-sacral pathologies were treated alone or in combination: spondylolisthesis (12 cases), severe discopathy (10 cases), and degenerative scoliosis (2 cases).

2D/3D Artis Zeego

The Artis Zeego system (Siemens, Germany) is characterized essentially by the association of robotic multi-axis C-arm fluoroscopy and a translucent robotic table. This system can be positioned in whichever way the surgeon wants. Different positions can be memorized and repeated as often as necessary, and the quality of the 3D sequences is near that of a traditional CT scan.

Fig. 1. Panoramic view of our operating room equipped with the Artis Zeego (robotic C-arm fluoroscopy), its synchronized translucent table (covered by sterile drapes) and different control screens

Figure 1 shows a panoramic view of our OR equipped with the Artis Zeego, its translucent operating table and different control screens.

The CT scan remained our gold standard for checking the accuracy of PPS placement during this preliminary experience so each patient had a control CT during postoperative week one.

Our surgical process

The surgical process, using the Viper system (DePuy Spine, Johnson & Johnson, Arlington, USA) was characterized by the following steps: (1) memorization with the Zeego 2D function of one profile (more in scoliosis cases) and multiple antero-posterior views, one for each targeted pedicle; (2) two cm skin incisions at four to five cm from the midline at the level of each targeted pedicle, starting on one side; (3) percutaneous placement of guide-wires using the Zeego 2D function and the owl's eye technique followed again by steps two and three on the other patient side; (4) all the guide-wires positions were checked using a Zeego 3D sequence followed by correction of any misplaced guide-wires; (5) pedicles taping; (6) placement over the guide-wires of cannulated polyaxial screws down into each pedicle; (7) all the pedicle screws locations were checked using an additional Zeego 3D sequence followed, if required, by relocation of misplaced screws; (8) rods measuring and insertion; (9) screws insertion and tightening and at last, (10) screws extensions removal, bone graft placement when necessary and closure.

Pedicle breach quantification

To compare the i3DF images obtained with the Zeego and those of the postoperative CT scan, we used a specific classification to quantify the severity of the PPS pedicle breach. This scale was reported by Wang et al. and has four grades [32]: Grade 0 for no pedicle breach, grade 1 for a breach less than two mm, grade 2 for a breach between two and four mm and, finally, grade 3 for a breach of more than four mm. The postoperative CT images were analyzed independently by a neuroradiologist.

Preoperative virtual surgery for the difficult cases

Recently, for more difficult cases, we have performed a preoperative CT and introduced the data into our Dextroscope system (Volumes Interactions, Bracco, Singapore) [21]. This system gives surgeons a preoperative virtual 3D view of the lumbar spine being operated on, allowing the surgeon to plan his surgery better by operating virtually using a control hand for orientation and a stylus for access to the different functions of the program, for example, virtual drilling. This virtual 3D planning device was, in particular, used in the management of the two patients with lumbar degenerative scoliosis.

Our results: fewer complications

We implanted 106 consecutive PPS. A summary of the results is shown in Tables 4a and 4b. Pedicle breaches were analyzed at the two main stages of the surgical procedure. The percentage of guide-wire pedicle breaches (guide-wire out of the pedicle) was very low at 5.7%. Figure 2 shows an example of guide-wires correctly positioned in the pedicles. All the misplaced wires were corrected. The rate of PPS pedicle breach disclosed by the i3DF was higher, at 11.4% (Fig. 3). However, only five PPS, which were considered as too misplaced (all the grade 3 and the two grade 2), were relocated. Of all the PPS pedicle breaches, only 20% were medial and all were corrected. Figure 4 shows correctly placed PPS (grade 0) and illustrates that the analysis involved not only the coronal section, but also sagittal and axial ones.

Finally, the percentage of PPS pedicle breaches disclosed on the postoperative CT images appeared to be 4.7%, with all the breaching PPS of grade 1 except for one grade two (intraoperatively accepted) and two grade 3 (lateral breaches), which were in fact already visible on the i3DF images with a more careful analysis and better knowledge of the Zeego software (Fig. 5). As these two grade 3 PPS were lateral, one associated with a TLIF and neither symptomatic, it was not necessary to reposition them. Intraoperative 3DF using the Artis Zeego showed a sensitivity of 95% and a specificity of 80% for PPS grade 0 breach; for grade 0 plus grade 1 breach, the sensitivity and specificity increased to 100%.

Table 4a. *Guide-wire and PPS pedicle breach grading[a] observed on Zeego i3DF images and on a postoperative CT-scan*

Patient	*n* of PPS	i3DF										CT discrepancy				
		K-wire (left/right)					PPS (left/right)					PPS				
		L2	L3	L4	L5	S1	L2	L3	L4	L5	S1	L2	L3	L4	L5	S1
1	4					in/out→→in[b]	–	–	–	0/0	0/0					
2	4						–	–	0/0	0/0	–					
3	4						–	–	0/0	0/0	–					
4	4						–	–	–	0/0	0/0					
5	4						–		0/3→→0[b]	1/3→→0[b]	–			1/	3[c]/	
6	4						–	0/0	0/0	–	–					
7	6						–	–	0/2→→0[b]	0/0	0/0					
8	5						–	–	/0	0/0	0/0					
9	6						–	–	0/0	0/1	0/0				/0	
10	4						–	–	–	1/0	0/0				0/	
11	4						–	–	–	0/0	0/0					
12	4						–	–	1/0	0/0				0/		
13	4						–	–	–	1/0	0/0				0/	
14	7		out→→in[b]/in			in/out→→in[b]	–	1/	0/0	0/0	0/0		3[c]/			
15	4						–	–	–	0/0	0/0					
16	4						–	–	–	0/0	0/0					
17	4						–	–	2/0	2→→3→→0[b]/0	–					
18	4						–	–	0/0	0/0	–					
19	4					in/out→→in[b]	–			0/0	1/0					
20[d]	6						0/1	0/	/0	0/0		/0				
21	4						–	–	0/0	0/0	–					
22	4				out→→in[b]/out→→in[b]		–	–	3→→0[b]/0	0/0	–					

23	4			– –	0/0	0/0 –
24	4			– –	0/0	0/0 –

	Before correction	After correction	Before correction	After correction	
Total: *n* (%)	106	106	106	106	106
Grade 0 (or in)	100 (94.3)	106 (100)	94 (88.6)	98 (92.5)	101 (95.3)
Grade 1	0	0	7 (6.6)	7 (6.6)	2 (1.9)
Grade 2	0	0	2 (1.9)	1 (0.9)	1 (0.9)
Grade 3 (or out)	6 (5.7)	0	3 (2.9)	0	2 (1.9)

	Not using i3DF	With i3DF
Total: *n* (%)	106	106
Grade 0 (or in)	91 (85.8)	101 (95.3)
Grade1	2 (1.9)	2 (1.9)
Grade 2	3 (2.8)	1 (0.9)
Grade 3 (or out)	10 (9.4)	2 (1.9)

CT Postoperative computerized tomography; *i3DF* intraoperative three-dimensional fluoroscopy; *PPS* percutaneous pedicle screw.
[a]grade 0, no breach; I, <2 mm; II, 2 – 4 mm; III, >4mm.
[b]repositioning and validation after a new i3DF.
[c]retrospective analysis of the i3DF imagery reveals a grade 3 breach; the poor peroperative interpretation was related to previous surgery in these 2 patients and an inadequate knowledge of the imaging system.
[d]patient with two hemivertebrae.

Table 4b. *Pedicle breach rate (%) and screw repositioning in our consecutive series of 106 percutaneously placed pedicle screws (PPS) using i2DF/3DF*

PPS $N-106$	Intra-op (i2DF → i3DF control)		Post-op (CT)
	Guide-wire (out)	PPS	PPS
Pedicle Breach	6 (5.7)	12 (11.4)	5 (4.7)
Repositioning	6	5	0

CT postoperative computerized tomography was used as the ultimate control.

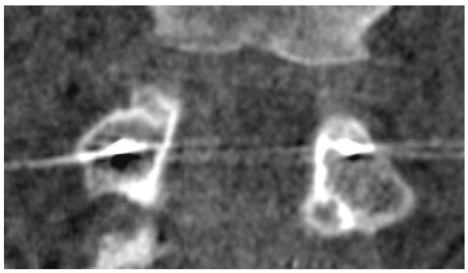

Fig. 2. Zeego intraoperative coronal view of two pedicles (from a i3D sequence) disclosing precisely guide-wires location; no pedicle breach

In terms of complications, we therefore only had 4.7% pedicle breaches, none of which required revision because they were asymptomatic. There were no nerve root injuries or other complications.

Other experiences

Regarding PPS breach rates

We reviewed the PPS breach percentage reported in the literature (Table 5a and 5b) and observed that using only i2DF, the pedicle breach rate was high at around 25% [6, 15, 26, 27]. This rate decreased to around 20% when a CAN system was used with the i2DF [22, 31]. However, using i3DF, even without a CAN system, was associated with a markedly lower pedicle breach rate of 9% [6]. When a CAN system was added to the i3DF for implanting PPS, the pedicle breach rate was even lower, varying between 5.3% and 7.3% [9, 15], similar to our experience without CAN (4.7%). These results compare favourably with those obtained using a classical open technique: pedicle breach rate of 9.7% without CAN and 4.8% if a CAN system was used (meta-analysis of 130 studies) [12].

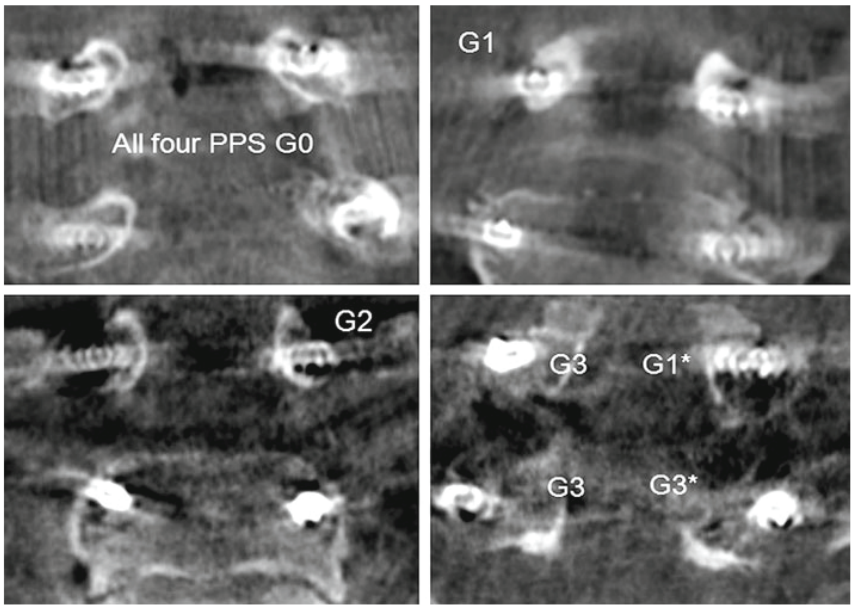

Fig. 3. These four Zeego intraoperative coronal views (from a i3DF sequence) show the possible grades of pedicle breach in different patients. G1* and G3* were initially misanalyzed as G0 and G1, respectively (patient 5, Table 3). G0, no breach; G1, <2 mm; G2, 2–4 mm; G3, >4 mm; PPS, percutaneous pedicle screw

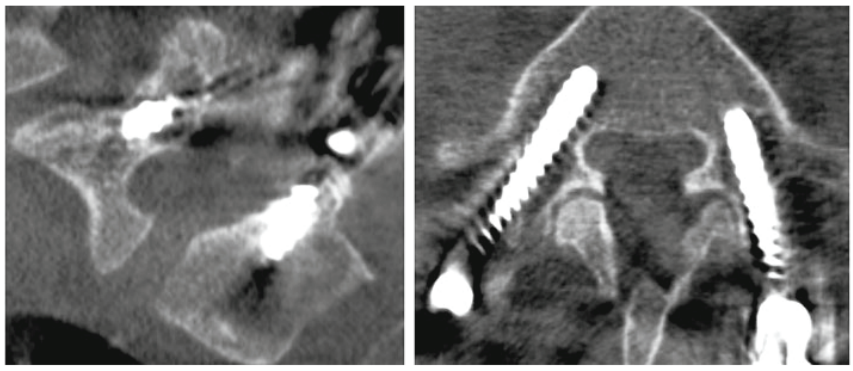

Fig. 4. Vertebral sagittal and axial views from a Zeego intraoperative three dimensional fluoroscopy (i3DF) sequence showing percutaneously placed pedicle screws (PPS)

All complications using PPS

Regarding the complication rates reported in the literature (Table 5a and 5b), rates of nerve root injury vary from 0 to 6.7%, of additional surgery from 0 to

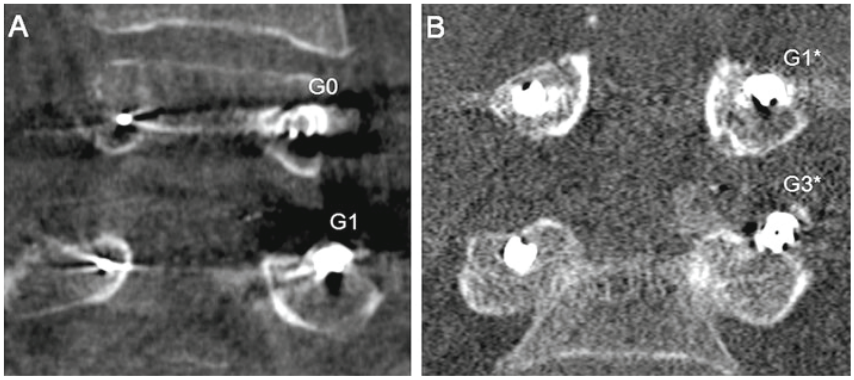

Fig. 5. Patient 5. (A) *Zeego* intraoperative coronal view from a three dimensional fluoroscopy (i3DF) sequence incorrectly analyzed and considered as showing a left L4 G0 and a left L5 G1; (B) the *postoperative CT* confirmed what could be already seen on the Zeego i3DF sequence: there was in fact a left L4 G1* and a left L5 G3*. G0, no breach; G1, <2 mm; G2, 2–4 mm; G3, >4 mm

6.7%, and of other complications, such as haematoma or infection, from 0 and 7.8% [10, 22, 26]. What is remarkable is that surgical teams using at least i3DF reported no complications (Table 5a).

Few exceptional good results: analysis method related?

It is important to note that results outside the general ranges have been reported using PPS implantation without CAN. For example, Powers et al. reported a 0.7% pedicle breach rate with a 0.7% infection rate if we consider only their patients with a control postoperative CT. However, these authors did not describe the method they used to define the pedicle breach [12, 19]. The same observations can be applied to the results of Schwender et al., who reported only 4.1% misplaced PPS, all requiring repositioning [28]. Although the experience and expertise of these surgical teams is high, it is likely that an independent radiologist, or three observers as in some studies [22, 26], may have disclosed a larger number of pedicle breaches on postoperative CTs.

Potential problem: higher radiation doses

Performing i3DF control images for PPS may involve higher ionizing radiation doses not only for patients but in particular for the medical staff due to repeated exposures. Several teams have analyzed this potential problem. Some reported that the association of CAN with CT enabled intraoperative radiation doses to be reduced [8]. Other teams using two fluoroscopes placed

Table 5a. *Review of the literature for lumbosacral PPS placement*

Study	N of patients	N	CAN	i3DF	Pedicle breach grade on CT (%)				Complications n (%)		
					0	I	II	III	NRI	New surgery	Other[b]
Wiesner[a], 00	51	408	–	–	383 (93.8)	13 (3.2)	10 (2.4)	2 (0.4)	2 (3.9)	1 (1.9)	4 (7.8)
Villavicencio, 05	46	220	+	Arcadis	217 (98.6)	2 (0.9)	0	1 (0.5)	2 (2.9)	1 (2.2)	3 (4.3)
Schizas, 07	15	60	–	–	55 (91.6)	3 (5)	0	2 (3.3)	1 (6.7)	1 (6.7)	–
Nakashima, 09	67	150	+	Arcadis	139 (92.7)	11 (7.3)	0		1 (1.5)	1 (1.5)	2 (3)
		150	–	–	127 (84.6)	18 (12)	5 (3.3)				
Eric, 10	15	36	+	O-Arm	36 (100)	0	0	0	–	–	–
Park, 10	11	40	+	O-Arm	37 (92.5)	3 (7.5)	0	0	–	–	–
Wood, 11	67	110	+	–	103 (93.6)		7 (6.4)		–	–	–
		186	+	O-Arm	183 (98.4)		3 (1.6)		–	–	–
Ravi, 11	41	161	+	–	124 (77)	31 (19.2)	5 (3.1)	1 (0.6)	1 (2.4)	1 (2.4)	–
Current, 11	24	106	–	Zeego	101 (95.3)	2 (1.9)	1 (0.9)	2 (1.9)	–	–	–

CAN computer-assisted navigation; *CT* postoperative computerized tomography; *i2DF* intraoperative 2-dimensional fluoroscopy; *i3DF* intraoperative 3-dimensional fluoroscopy; *N* number of screws; *NR* not reported; *NRI*, nerve root injury; *pCT* pre-operative computerized tomography; *PPS* percutaneous pedicle screw.

[a]External fixation via PPS.

[b]Liquid leak, haematoma or infection.

Table 5b. *Summary of pedicle breach rates reported in the literature when using percutaneously placed pedicle screws (PPS) with or without computer assisted navigation (CAN) or with a robotic device*

PPS	i2DF		i3DF			Symptomatic
	–	CAN	–	CAN	Robotic Insertion	
Pedicle breach rate %	25	20	5	5	10	0–6.7

Symptomatic, percentage of symptomatic pedicle breaches

in orthogonal planes demonstrated that a ring dosimeter placed on the surgeon's right hand received about 10.3 mREM per screw placed and concluded that the placement of PPS could be considered as safe but required optimal protection against radiation [13]. Because systems and surgical strategies vary, we recently felt compelled to initiate another prospective study focused on the radiation dose received by the patient and the surgeons during our surgical protocol. *Conscious of this problem, Siemens implemented on our Zeego system in June 2011, a new software allowing to reduce of more than 50% the delivered radiation doses while keeping a good image quality.*

And robotic PPS insertion?

Finally, regarding robotic PPS insertion, slightly higher pedicle breach rates have been reported, based on i3DF control images, compared to those obtained with a free-hand technique [3, 18]. Indeed, the reported rates of pedicle breach with robotic insertion are around 10%. Devito et al reported the results from a multicentre study (14 centres) in which 646 pedicle screws were placed by SpineAssist robots and assessed postoperatively with a CT. These authors reported a 10.7% pedicle breach rate and four neurological deficits requiring surgical revision [3]. Pechlivanis et al reported their experience of implanting 133 pedicle screws using the Hexapod robot mounted on a spinous process [18]; their pedicle breach rate was 8.3%. It therefore appears that results using robotic PPS implantation are no better than and not even as good as the results reported when using i2DF/3DF with or without a CAN system. The robotic strategy is also associated with potential neurological deficits.

Conclusions

In conclusion, performing minimally invasive percutaneous techniques under control of i3DF images allows surgeons to drastically reduce the rate of PPS pedicle breach (4.7% instead of 14.2%), with or without a CAN system. It is

clear that carrying out this kind of minimally invasive procedure necessitates considerable involvement of the medical team, particularly in terms of becoming familiar with the new technologies, hardware as well as software, and of the initially longer surgical procedures because of the learning curve. However, our ultimate aim must be that our patients benefit from the most stable osteosynthesis possible with a minimal risk of additional surgery or permanent nerve root injury. The reduced rate of complications that we demonstrated will be of benefit not only to the patient but also to the medical teams and may be associated with improved cost-effectiveness, although this remains to be demonstrated. In the future, percutaneous surgery for lumbar degenerative processes that cause refractory low back pain should be performed with an intraoperative CT-like system to ensure the best possible accuracy. Finally, we should remember that better surgery also means better surgical indications and, probably, also less surgery through improved patient and doctor education.

References

[1] Anand N, Baron EM, Thaiyananthan G, Khalsa K, Goldstein TB (2008) Minimally invasive multilevel percutaneous correction and fusion for adult lumbar degenerative scoliosis: a technique and feasibility study. J Spinal Disord Tech 21: 459–67

[2] Anjarwalla NK, Morcom RK, Fraser RD (2006) Supplementary stabilization with anterior lumbar intervertebral fusion – a radiologic review. Spine (Phila Pa 1976) 31: 1281–87

[3] Devito DP, Kaplan L, Dietl R, Pfeiffer M, Horne D, Silberstein B, Hardenbrook M, Kiriyanthan G, Barzilay Y, Bruskin A, Sackerer D, Alexandrovsky V, Stuer C, Burger R, Maeurer J, Gordon DG, Schoenmayr R, Friedlander A, Knoller N, Schmieder K, Pechlivanis I, Kim IS, Meyer B, Shoham M (2010) Clinical acceptance and accuracy assessment of spinal implants guided with SpineAssist surgical robot: retrospective study. Spine (Phila Pa 1976) 35: 2109–15

[4] Dickerman RD, Reynolds AS, Tackett J, Winters K, Alvarado C (2008) Percutaneous pedicle screws significantly decrease muscle damage and operative time: surgical technique makes a difference! Eur Spine J 17: 1398–1400

[5] Foley KT, Gupta SK (2002) Percutaneous pedicle screw fixation of the lumbar spine: preliminary clinical results. J Neurosurg 97: 7–12

[6] Fraser J, Gebhard H, Irie D, Parikh K, Hartl R (2010) Iso-C/3-dimensional neuronavigation versus conventional fluoroscopy for minimally invasive pedicle screw placement in lumbar fusion. Minim Invasive Neurosurg 53: 184–90

[7] Fritzell P, Hagg O, Wessberg P, Nordwall A (2002) Chronic low back pain and fusion: a comparison of three surgical techniques: a prospective multicenter randomized study from the Swedish lumbar spine study group. Spine (Phila Pa 1976) 27: 1131–41

[8] Gebhard FT, Kraus MD, Schneider E, Liener UC, Kinzl L, Arand M (2006) Does computer-assisted spine surgery reduce intraoperative radiation doses? Spine (Phila Pa 1976) 31: 2024–27

[9] Holly LT, Foley KT (2003) Three-dimensional fluoroscopy-guided percutaneous thoracolumbar pedicle screw placement. Technical note. J Neurosurg 99: 324–29

[10] Idler C, Rolfe KW, Gorek JE (2010) Accuracy of percutaneous lumbar pedicle screw placement using the oblique or "owl's-eye" view and novel guidance technology. J Neurosurg Spine 13: 509–15
[11] Kim S, Chung J, Yi BJ, Kim YS (2010) An assistive image-guided surgical robot system using O-arm fluoroscopy for pedicle screw insertion: preliminary and cadaveric study. Neurosurgery 67: 1757–67
[12] Kosmopoulos V, Schizas C (2007) Pedicle screw placement accuracy: a meta-analysis. Spine (Phila Pa 1976) 32: E111–20
[13] Mroz TE, Abdullah KG, Steinmetz MP, Klineberg EO, Lieberman IH (2010) Radiation exposure to the surgeon during percutaneous pedicle screw placement. J Spinal Disord Tech 24: 264–67
[14] Murayama Y, Irie K, Saguchi T, Ishibashi T, Ebara M, Nagashima H, Isoshima A, Arakawa H, Takao H, Ohashi H, Joki T, Kato M, Tani S, Ikeuchi S, Abe T (2011) Robotic digital subtraction angiography systems within the hybrid operating room. Neurosurgery 68: 1427–32; discussion 1433
[15] Nakashima H, Sato K, Ando T, Inoh H, Nakamura H (2009) Comparison of the percutaneous screw placement precision of isocentric C-arm 3-dimensional fluoroscopy-navigated pedicle screw implantation and conventional fluoroscopy method with minimally invasive surgery. J Spinal Disord Tech 22: 468–72
[16] Nottmeier EW, Crosby T (2009) Timing of vertebral registration in three-dimensional, fluoroscopy-based, image-guided spinal surgery. J Spinal Disord Tech 22: 358–60
[17] Oppenheimer JH, DeCastro I, McDonnell DE (2009) Minimally invasive spine technology and minimally invasive spine surgery: a historical review. Neurosurg Focus 27: E9
[18] Pechlivanis I, Kiriyanthan G, Engelhardt M, Scholz M, Lucke S, Harders A, Schmieder K (2009) Percutaneous placement of pedicle screws in the lumbar spine using a bone mounted miniature robotic system: first experiences and accuracy of screw placement. Spine (Phila Pa 1976) 34: 392–98
[19] Powers CJ, Podichetty VK, Isaacs RE (2006) Placement of percutaneous pedicle screws without imaging guidance. Neurosurg Focus 20: E3
[20] Raftopoulos C (2011) Spine neurosurgery in Belgium. World Neurosurgery 74: 430–31
[21] Raftopoulos C, Vaz G (2011) Surgical indications and techniques for failed coiled aneurysms. Adv Tech Stand Neurosurg 36: 199–226
[22] Ravi B, Zahrai A, Rampersaud R (2011) Clinical accuracy of computer-assisted two-dimensional fluoroscopy for the percutaneous placement of lumbosacral pedicle screws. Spine (Phila Pa 1976) 36: 84–91
[23] Regev GJ, Lee YP, Taylor WR, Garfin SR, Kim CW (2009) Nerve injury to the posterior rami medial branch during the insertion of pedicle screws: comparison of mini-open versus percutaneous pedicle screw insertion techniques. Spine (Phila Pa 1976) 34: 1239–42
[24] Ringel F, Stoffel M, Stuer C, Meyer B (2006) Minimally invasive transmuscular pedicle screw fixation of the thoracic and lumbar spine. Neurosurgery 59: ONS361–66
[25] Rivet DJ, Jeck D, Brennan J, Epstein A, Lauryssen C (2004) Clinical outcomes and complications associated with pedicle screw fixation-augmented lumbar interbody fusion. J Neurosurg Spine 1: 261–66
[26] Schizas C, Michel J, Kosmopoulos V, Theumann N (2007) Computer tomography assessment of pedicle screw insertion in percutaneous posterior transpedicular stabilization. Eur Spine J 16: 613–17

[27] Schulze CJ, Munzinger E, Weber U (1998) Clinical relevance of accuracy of pedicle screw placement. A computed tomographic-supported analysis. Spine (Phila Pa 1976) 23: 2215–20

[28] Schwender JD, Holly LT, Rouben DP, Foley KT (2005) Minimally invasive transforaminal lumbar interbody fusion (TLIF): technical feasibility and initial results. J Spinal Disord Tech 18(Suppl): S1–S6

[29] Silbermann J, Riese F, Allam Y, Reichert T, Koeppert H, Gutberlet M (2011) Computer tomography assessment of pedicle screw placement in lumbar and sacral spine: comparison between free-hand and O-arm based navigation techniques. Eur Spine J 20: 875–81

[30] Tokuhashi Y, Ajiro Y, Umezawa N (2008) Follow-up of patients with delayed union after posterior fusion with pedicle screw fixation. Spine (Phila Pa 1976) 33: 786–91

[31] von JR, Finn MA, Yonemura KS, Araghi A, Khoo LT, Carrino JA, Perez-Cruet M (2011) Minimally invasive percutaneous transpedicular screw fixation: increased accuracy and reduced radiation exposure by means of a novel electromagnetic navigation system. Acta Neurochir (Wien) 153: 589–96

[32] Wang MY, Kim KA, Liu CY, Kim P, Apuzzo ML (2004) Reliability of three-dimensional fluoroscopy for detecting pedicle screw violations in the thoracic and lumbar spine. Neurosurgery 54: 1138–42

[33] Watkins RG, Gupta A, Watkins RG (2010) Cost-effectiveness of image-guided spine surgery. Open Orthop J 4: 228–33

[34] Wiesner L, Kothe R, Schulitz KP, Ruther W (2000) Clinical evaluation and computed tomography scan analysis of screw tracts after percutaneous insertion of pedicle screws in the lumbar spine. Spine (Phila Pa 1976) 25: 615–21

6.3.2 Highlights from this paper

1. Intraoperative 3D fluoroscopy drastically reduced the rate of PPS breach (from 4.7% to 14.2%) in minimally invasive percutaneous techniques.

2. The procedure necessitates involvement of the entire medical team to become familiar with these new technologies.

3. The reduced rate of complications is beneficial to patients and medical staff and may be associated with improved cost effectiveness.

4. Therefore,

5. Better surgical techniques must go hand-in-hand with precise indications and better screening of potential surgical candidates.

AFTERWORD

Deciding to pursue a PhD is not easy. It is a long, challenging, solitary process—especially when concurrently pursuing one's normal professional occupation. At the beginning, one is excited, but as time flies, stress grows. Therefore, it is almost a necessity to take some time off now and then to regenerate enthusiasm and keep yourself sane. A frequently asked question was, "Why bother pursuing a PhD when it will not even increase your wages?" Everyone has his/her own motivation. I have been working for years at a university institution while having just a limited teaching workload. Moreover, in some countries, when it comes to teaching and transmitting knowledge, having a background as a researcher is as important as the content for instruction. "The cowl does not make the monk, but for sure, he can be recognized by his habit." I started a PhD because I believe that I will be helpful to my native country of Cameroon when I reach retirement. When the time will come to share my expertise, I want my surgical knowledge to be supported by research experience. A PhD title will not change my mind or substantially increase my neurosurgical skill. However, undoubtedly, my four years of PhD training have made me wiser, savvier, more focused, creative, perceptive, eloquent, and probably more professionally effective. I dreaded having my manuscripts repeatedly rejected, and yet, I had no choice but to keep improving in the publication game.

Another private reason for my commitment to PhD training was to show my children that it is never too late to be what you want to be. Franklin, my eldest son, is completing his residency in neurosurgery in five months from now. This gives me an opportunity to congratulate him and encourage

him to continue to look forward. I have similar wishes for Joël-Christian, my younger son, who works as a financial advisor. The financial field is so complex that it could continue to challenge a person for his lifetime. I encourage him to never stop improving his knowledge, but to continue learning. For my daughter Anne-Dominique, I read somewhere that computer algorithms are likely to play a factor in 90% of court cases in the coming decades. So, as a young lawyer, she is encouraged to keep learning and testing her intellectual limits. Finally, by keeping working hard, we will be examples to Cassandre, my just new born little granddaughter, to let her realize early in her life that "all growth depends upon activity. There is no development physically or intellectually without effort, and effort means work" [218].

REFERENCES

1. Deyo RA, Mirza SK, Martin BI. Back pain prevalence and visit rates: estimates from U.S. national surveys, 2002. *Spine.* Nov 01 2006;31(23):2724-2727.

2. Hoy D, Bain C, Williams G, et al. A systematic review of the global prevalence of low back pain. *Arthritis Rheum.* Jun 2012;64(6):2028-2037.

3. Lawrence RC, Helmick CG, Arnett FC, et al. Estimates of the prevalence of arthritis and selected musculoskeletal disorders in the United States. *Arthritis Rheum.* May 1998;41(5):778-799.

4. Manchikanti L, Boswell MV, Singh V, et al. Comprehensive review of neurophysiologic basis and diagnostic interventions in managing chronic spinal pain. *Pain Physician.* Jul-Aug 2009;12(4):E71-120.

5. Manchikanti L, Singh V, Falco FJ, Benyamin RM, Hirsch JA. Epidemiology of low back pain in adults. *Neuromodulation.* Oct 2014;17 Suppl 2:3-10.

6. Andersson GB. Epidemiological features of chronic low-back pain. *Lancet.* Aug 14 1999;354(9178):581-585.

7. van Tulder M, Becker A, Bekkering T, et al. Chapter 3. European guidelines for the management of acute nonspecific low back pain in primary care. *Eur Spine J.* Mar 2006;15 Suppl 2:S169-191.

8. Chou R, Qaseem A, Snow V, et al. Diagnosis and treatment of low back pain: a joint clinical practice guideline from the American College of Physicians and the American Pain Society. *Ann Intern Med.* Oct 2 2007;147(7):478-491.

9. Hoy D, March L, Brooks P, et al. The global burden of low back pain: estimates from the Global Burden of Disease 2010 study. *Ann Rheum Dis.* Jun 2014;73(6):968-974.

10. Frymoyer JW. Back pain and sciatica. *The New England journal of medicine.* Feb 4 1988;318(5):291-300.

11. Rosemont I. The Burden of Musculoskeletal Diseases in the United States (BMUS). Third Edition ed: United States Bone and Joint Initiative; 2014.

12. Zigler J, Delamarter R, Spivak JM, et al. Results of the prospective, randomized, multicenter Food and Drug Administration investigational device exemption study of the ProDisc-L total disc replacement versus circumferential fusion for the treatment of 1-level

degenerative disc disease. *Spine.* May 15 2007;32(11):1155-1162; discussion 1163.

13. Leeuw M, Goossens ME, Linton SJ, Crombez G, Boersma K, Vlaeyen JW. The fear-avoidance model of musculoskeletal pain: current state of scientific evidence. *Journal of behavioral medicine.* Feb 2007;30(1):77-94.

14. Cuesta-Vargas AI, Garcia-Romero JC, Arroyo-Morales M, Diego-Acosta AM, Daly DJ. Exercise, manual therapy, and education with or without high-intensity deep-water running for nonspecific chronic low back pain: a pragmatic randomized controlled trial. *Am J Phys Med Rehabil.* Jul 2011;90(7):526-534; quiz 535-528.

15. Van Wambeke P, Desomer A, Ailliet L, et al. Low Back Pain and radicular pain: assessment and management – Summary. Good Clinical Practice (GCP) Brussels. *Belgian Health Care Knowledge Centre (KCE).* 2017;KCE Reports 287Cs. (D/2017/10.273/35).

16. National Guideline C. National Institute for Health and Care Excellence: Clinical Guidelines. *Low Back Pain and Sciatica in Over 16s: Assessment and Management*. London: National Institute for Health and Care Excellence (UK)
Copyright (c) NICE, 2016.; 2016.

17. Reese C, Mittag O. Psychological interventions in the rehabilitation of patients with chronic low back pain: evidence and recommendations from systematic reviews and guidelines. *International journal of rehabilitation research. Internationale Zeitschrift fur Rehabilitationsforschung. Revue internationale de recherches de readaptation.* Mar 2013;36(1):6-12.

18. Turk DC, Wilson HD, Cahana A. Treatment of chronic non-cancer pain. *Lancet.* Jun 25 2011;377(9784):2226-2235.

19. Henschke N, Ostelo RW, van Tulder MW, et al. Behavioural treatment for chronic low-back pain. *The Cochrane database of systematic reviews.* Jul 7 2010(7):Cd002014.

20. van Tulder MW, Malmivaara A, Esmail R, Koes BW. Exercise therapy for low back pain. *The Cochrane database of systematic reviews.* 2000(2):Cd000335.

21. Gibson JN, Waddell G. Surgical interventions for lumbar disc prolapse: updated Cochrane Review. *Spine.* Jul 15 2007;32(16):1735-1747.

22. Gibson JN, Waddell G. Surgery for degenerative lumbar spondylosis: updated Cochrane Review. *Spine.* Oct 15 2005;30(20):2312-2320.

23. Smith ZA, Fessler RG. Paradigm changes in spine surgery: evolution of minimally invasive techniques. *Nature reviews. Neurology.* Aug 2012;8(8):443-450.
24. Froholdt A, Reikeraas O, Holm I, Keller A, Brox JI. No difference in 9-year outcome in CLBP patients randomized to lumbar fusion versus cognitive intervention and exercises. *Eur Spine J.* Dec 2012;21(12):2531-2538.
25. Phillips FM, Slosar PJ, Youssef JA, Andersson G, Papatheofanis F. Lumbar spine fusion for chronic low back pain due to degenerative disc disease: a systematic review. *Spine.* Apr 1 2013;38(7):E409-422.
26. Brox JI, Sørensen R, Friis A, et al. Randomized clinical trial of lumbar instrumented fusion and cognitive intervention and exercises in patients with chronic low back pain and disc degeneration. *Spine.* 2003;28(17):1913-1921.
27. Fairbank J, Frost H, Wilson-MacDonald J, et al. Randomised controlled trial to compare surgical stabilisation of the lumbar spine with an intensive rehabilitation programme for patients with chronic low back pain: the MRC spine stabilisation trial. *BMJ.* 2005;330(7502):1233.
28. Fritzell P, Hagg O, Wessberg P, Nordwall A. 2001 Volvo Award Winner in Clinical Studies: Lumbar fusion versus nonsurgical treatment for chronic low back pain: a multicenter randomized controlled trial from the Swedish Lumbar Spine Study Group. *Spine.* Dec 1 2001;26(23):2521-2532; discussion 2532-2524.
29. Tosteson ANA, Tosteson TD, Lurie JD, et al. Comparative effectiveness evidence from the spine patient outcomes research trial: surgical versus nonoperative care for spinal stenosis, degenerative spondylolisthesis, and intervertebral disc herniation. *Spine.* 2011;36(24):2061-2068.
30. Ibrahim T, Tleyjeh IM, Gabbar O. Surgical versus non-surgical treatment of chronic low back pain: a meta-analysis of randomised trials. *Int Orthop.* 2008;32(1):107-113.
31. Mirza SK, Deyo RA. Systematic review of randomized trials comparing lumbar fusion surgery to nonoperative care for treatment of chronic back pain. *Spine.* Apr 1 2007;32(7):816-823.
32. Harrington PR, Tullos HS. Reduction of severe spondylolisthesis in children. *Southern medical journal.* Jan 1969;62(1):1-7.
33. Du JP, Fan Y, Wu QN, Wang DH, Zhang J, Hao DJ. Accuracy of Pedicle Screw Insertion Among 3 Image-Guided Navigation Systems:

Systematic Review and Meta-Analysis. *World Neurosurg.* 2018;109:24-30.

34. Tian NF, Huang QS, Zhou P, et al. Pedicle screw insertion accuracy with different assisted methods: a systematic review and meta-analysis of comparative studies. *Eur Spine J.* Jun 2011;20(6):846-859.

35. Amiot LP, Lang K, Putzier M, Zippel H, Labelle H. Comparative results between conventional and computer-assisted pedicle screw installation in the thoracic, lumbar, and sacral spine. *Spine.* Mar 01 2000;25(5):606-614.

36. Assaker R, Reyns N, Vinchon M, Demondion X, Louis E. Transpedicular screw placement: image-guided versus lateral-view fluoroscopy: in vitro simulation. *Spine.* Oct 01 2001;26(19):2160-2164.

37. Kosmopoulos V, Schizas C. Pedicle screw placement accuracy: a meta-analysis. *Spine.* Feb 01 2007;32(3):E111-120.

38. Laine T, Lund T, Ylikoski M, Lohikoski J, Schlenzka D. Accuracy of pedicle screw insertion with and without computer assistance: a randomised controlled clinical study in 100 consecutive patients. *Eur Spine J.* Jun 2000;9(3):235-240.

39. Merloz P, Tonetti J, Pittet L, et al. Computer-assisted spine surgery. *Comput Aided Surg.* 1998;3(6):297-305.

40. Meyer RA, Jr., Gruber HE, Howard BA, et al. Safety of recombinant human bone morphogenetic protein-2 after spinal laminectomy in the dog. *Spine.* Apr 15 1999;24(8):747-754.

41. Papadopoulos EC, Girardi FP, Sama A, Sandhu HS, Cammisa FP, Jr. Accuracy of single-time, multilevel registration in image-guided spinal surgery. *Spine J.* May-Jun 2005;5(3):263-267; discussion 268.

42. Richter M, Mattes T, Cakir B. Computer-assisted posterior instrumentation of the cervical and cervico-thoracic spine. *Eur Spine J.* Feb 2004;13(1):50-59.

43. Laine T, Schlenzka D, Makitalo K, Tallroth K, Nolte LP, Visarius H. Improved accuracy of pedicle screw insertion with computer-assisted surgery. A prospective clinical trial of 30 patients. *Spine.* Jun 01 1997;22(11):1254-1258.

44. Liu H, Chen W, Liu T, Meng B, Yang H. Accuracy of pedicle screw placement based on preoperative computed tomography versus intraoperative data set acquisition for spinal navigation system. *Journal of orthopaedic surgery (Hong Kong).* May-Aug 2017;25(2):2309499017718901.

45. Merloz P, Troccaz J, Vouaillat H, et al. Fluoroscopy-based navigation system in spine surgery. *Proceedings of the Institution of Mechanical Engineers. Part H, Journal of Engineering in Medicine.* 2007-10 2007;221(7):813-820.

46. Gruetzner Paul Alfred WH, Vock Bernd , Axel Hebecker ALex, Nolte Lutz-Peter, Wentzensen Andreas. Navigation Using Fluoro-CT Technology Concept and Clinical Experience in a New Method for Intraoperative Navigation. *European Journal of Trauma.* 2004;30(3):161-170.

47. Bourgeois AC, Faulkner AR, Bradley YC, et al. Improved Accuracy of Minimally Invasive Transpedicular Screw Placement in the Lumbar Spine With 3-Dimensional Stereotactic Image Guidance: A Comparative Meta-Analysis. *J Spinal Disord Tech.* Nov 2015;28(9):324-329.

48. Costa F, Dorelli G, Ortolina A, et al. Computed tomography-based image-guided system in spinal surgery: state of the art through 10 years of experience. *Neurosurgery.* Mar 2015;11 Suppl 2:59-67; discussion 67-58.

49. Kraus M, Weiskopf J, Dreyhaupt J, Krischak G, Gebhard F. Computer-aided surgery does not increase the accuracy of dorsal pedicle screw placement in the thoracic and lumbar spine: a retrospective analysis of 2,003 pedicle screws in a level I trauma center. *Global spine journal.* Apr 2015;5(2):93-101.

50. Ling JM, Dinesh SK, Pang BC, et al. Routine spinal navigation for thoraco-lumbar pedicle screw insertion using the O-arm three-dimensional imaging system improves placement accuracy. *J Clin Neurosci.* Mar 2014;21(3):493-498.

51. Mason A, Paulsen R, Babuska JM, et al. The accuracy of pedicle screw placement using intraoperative image guidance systems. *J Neurosurg Spine.* Feb 2014;20(2):196-203.

52. Mendelsohn D, Strelzow J, Dea N, et al. Patient and surgeon radiation exposure during spinal instrumentation using intraoperative computed tomography-based navigation. *Spine J.* Mar 2016;16(3):343-354.

53. Nimjee SM, Karikari IO, Carolyn AHAB, et al. Safe and accurate placement of thoracic and thoracolumbar percutaneous pedicle screws without image-navigation. *Asian journal of neurosurgery.* Oct-Dec 2015;10(4):272-275.

54. Rivkin MA, Yocom SS. Thoracolumbar instrumentation with CT-guided navigation (O-arm) in 270 consecutive patients: accuracy rates and lessons learned. *Neurosurg Focus.* Mar 2014;36(3):E7.

55. Ruatti S, Dubois C, Chipon E, et al. Interest of intra-operative 3D imaging in spine surgery: a prospective randomized study. *Eur Spine J.* Jun 2016;25(6):1738-1744.
56. Santos ER, Sembrano JN, Yson SC, Polly DW, Jr. Comparison of open and percutaneous lumbar pedicle screw revision rate using 3-D image guidance and intraoperative CT. *Orthopedics.* Feb 2015;38(2):e129-134.
57. Shin BJ, James AR, Njoku IU, Hartl R. Pedicle screw navigation: a systematic review and meta-analysis of perforation risk for computer-navigated versus freehand insertion. *J Neurosurg Spine.* Aug 2012;17(2):113-122.
58. Tian W, Zeng C, An Y, Wang C, Liu Y, Li J. Accuracy and postoperative assessment of pedicle screw placement during scoliosis surgery with computer-assisted navigation: a meta-analysis. *Int J Med Robot.* Mar 2017;13(1).
59. Van de Kelft E, Costa F, Van der Planken D, Schils F. A prospective multicenter registry on the accuracy of pedicle screw placement in the thoracic, lumbar, and sacral levels with the use of the O-arm imaging system and StealthStation Navigation. *Spine.* Dec 01 2012;37(25):E1580-1587.
60. Waschke A, Walter J, Duenisch P, Reichart R, Kalff R, Ewald C. CT-navigation versus fluoroscopy-guided placement of pedicle screws at the thoracolumbar spine: single center experience of 4,500 screws. *Eur Spine J.* 2013;22(3):654-660.
61. Wood MJ, McMillen J. The surgical learning curve and accuracy of minimally invasive lumbar pedicle screw placement using CT based computer-assisted navigation plus continuous electromyography monitoring - a retrospective review of 627 screws in 150 patients. *Int J Spine Surg.* 2014;8.
62. Yang BP, Wahl MM, Idler CS. Percutaneous lumbar pedicle screw placement aided by computer-assisted fluoroscopy-based navigation: perioperative results of a prospective, comparative, multicenter study. *Spine.* Nov 15 2012;37(24):2055-2060.
63. Tian NF, Wu YS, Zhang XL, Xu HZ, Chi YL, Mao FM. Minimally invasive versus open transforaminal lumbar interbody fusion: a meta-analysis based on the current evidence. *Eur Spine J.* Aug 2013;22(8):1741-1749.
64. Burkus JK, Gornet MF, Dickman CA, Zdeblick TA. Anterior lumbar interbody fusion using rhBMP-2 with tapered interbody cages. *J Spinal Disord Tech.* Oct 2002;15(5):337-349.

65. Burkus JK, Transfeldt EE, Kitchel SH, Watkins RG, Balderston RA. Clinical and radiographic outcomes of anterior lumbar interbody fusion using recombinant human bone morphogenetic protein-2. *Spine.* Nov 1 2002;27(21):2396-2408.

66. Tannoury CA, An HS. Complications with the use of bone morphogenetic protein 2 (BMP-2) in spine surgery. *Spine J.* Mar 1 2014;14(3):552-559.

67. Thawani JP, Wang AC, Than KD, Lin CY, La Marca F, Park P. Bone morphogenetic proteins and cancer: review of the literature. *Neurosurgery.* Feb 2010;66(2):233-246; discussion 246.

68. Furlan JC, Perrin RG, Govender PV, et al. Use of osteogenic protein-1 in patients at high risk for spinal pseudarthrosis: a prospective cohort study assessing safety, health-related quality of life, and radiographic fusion. Invited submission from the Joint Section on Disorders of the Spine and Peripheral Nerves, March 2007. *J Neurosurg Spine.* Nov 2007;7(5):486-495.

69. Vaidya R, Weir R, Sethi A, Meisterling S, Hakeos W, Wybo CD. Interbody fusion with allograft and rhBMP-2 leads to consistent fusion but early subsidence. *J Bone Joint Surg Br.* Mar 2007;89(3):342-345.

70. Riederman BD, Butler BA, Lawton CD, Rosenthal BD, Balderama ES, Bernstein AJ. Recombinant human bone morphogenetic protein-2 versus iliac crest bone graft in anterior cervical discectomy and fusion: Dysphagia and dysphonia rates in the early postoperative period with review of the literature. *J Clin Neurosci.* Oct 2017;44:180-183.

71. Myeroff C, Archdeacon M. Autogenous bone graft: donor sites and techniques. *J Bone Joint Surg Am.* Dec 7 2011;93(23):2227-2236.

72. Sen MK, Miclau T. Autologous iliac crest bone graft: should it still be the gold standard for treating nonunions? *Injury.* Mar 2007;38 Suppl 1:S75-80.

73. Ahlmann E, Patzakis M, Roidis N, Shepherd L, Holtom P. Comparison of anterior and posterior iliac crest bone grafts in terms of harvest-site morbidity and functional outcomes. *J Bone Joint Surg Am.* May 2002;84-A(5):716-720.

74. Steffen T, Downer P, Steiner B, Hehli M, Aebi M. Minimally invasive bone harvesting tools. *Eur Spine J.* Feb 2000;9 Suppl 1:S114-118.

75. Hsu WK, Wang JC. The use of bone morphogenetic protein in spine fusion. *Spine J.* May-Jun 2008;8(3):419-425.

76. Arrington ED, Smith WJ, Chambers HG, Bucknell AL, Davino NA. Complications of iliac crest bone graft harvesting. *Clin Orthop Relat Res.* Aug 1996(329):300-309.
77. Banwart JC, Asher MA, Hassanein RS. Iliac crest bone graft harvest donor site morbidity. A statistical evaluation. *Spine.* May 01 1995;20(9):1055-1060.
78. Canady JW, Zeitler DP, Thompson SA, Nicholas CD. Suitability of the iliac crest as a site for harvest of autogenous bone grafts. *Cleft Palate Craniofac J.* Nov 1993;30(6):579-581.
79. Sawin PD, Traynelis VC, Menezes AH. A comparative analysis of fusion rates and donor-site morbidity for autogeneic rib and iliac crest bone grafts in posterior cervical fusions. *J Neurosurg.* Feb 1998;88(2):255-265.
80. Summers BN, Eisenstein SM. Donor site pain from the ilium. A complication of lumbar spine fusion. *J Bone Joint Surg Br.* Aug 1989;71(4):677-680.
81. Younger EM, Chapman MW. Morbidity at bone graft donor sites. *J Orthop Trauma.* 1989;3(3):192-195.
82. Hsu WK, Wang JC, Liu NQ, et al. Stem cells from human fat as cellular delivery vehicles in an athymic rat posterolateral spine fusion model. *J Bone Joint Surg Am.* May 2008;90(5):1043-1052.
83. Lu ZF, Doulabi BZ, Wuisman PI, Bank RA, Helder MN. Influence of collagen type II and nucleus pulposus cells on aggregation and differentiation of adipose tissue-derived stem cells. *Journal of cellular and molecular medicine.* Dec 2008;12(6B):2812-2822.
84. Mesimaki K, Lindroos B, Tornwall J, et al. Novel maxillary reconstruction with ectopic bone formation by GMP adipose stem cells. *Int J Oral Maxillofac Surg.* Mar 2009;38(3):201-209.
85. Niemeyer P, Fechner K, Milz S, et al. Comparison of mesenchymal stem cells from bone marrow and adipose tissue for bone regeneration in a critical size defect of the sheep tibia and the influence of platelet-rich plasma. *Biomaterials.* May 2010;31(13):3572-3579.
86. Niemeyer P, Szalay K, Luginbuhl R, Sudkamp NP, Kasten P. Transplantation of human mesenchymal stem cells in a non-autogenous setting for bone regeneration in a rabbit critical-size defect model. *Acta Biomater.* Mar 2010;6(3):900-908.
87. Schubert T, Lafont S, Beaurin G, et al. Critical size bone defect reconstruction by an autologous 3D osteogenic-like tissue derived from differentiated adipose MSCs. *Biomaterials.* Jun 2013;34(18):4428-4438.

88. Schubert T, Poilvache H, Galli C, Gianello P, Dufrane D. Galactosyl-knock-out engineered pig as a xenogenic donor source of adipose MSCs for bone regeneration. *Biomaterials.* Apr 2013;34(13):3279-3289.
89. Schubert T, Xhema D, Veriter S, et al. The enhanced performance of bone allografts using osteogenic-differentiated adipose-derived mesenchymal stem cells. *Biomaterials.* Dec 2011;32(34):8880-8891.
90. Formica M, Divano S, Cavagnaro L, et al. Lumbar total disc arthroplasty: outdated surgery or here to stay procedure? A systematic review of current literature. *J Orthop Traumatol.* Sep 2017;18(3):197-215.
91. Resnick DK, Watters WC. Lumbar disc arthroplasty: a critical review. *Clin Neurosurg.* 2007;54:83-87.
92. North RB, Campbell JN, James CS, et al. Failed back surgery syndrome: 5-year follow-up in 102 patients undergoing repeated operation. *Neurosurgery.* May 1991;28(5):685-690; discussion 690-681.
93. Simpson EL, Duenas A, Holmes MW, Papaioannou D, Chilcott J. Spinal cord stimulation for chronic pain of neuropathic or ischaemic origin: systematic review and economic evaluation. *Health technology assessment (Winchester, England).* Mar 2009;13(17):iii, ix-x, 1-154.
94. Raftopoulos C, Waterkeyn F, Fomekong E, Duprez T. Percutaneous pedicle screw implantation for refractory low back pain: from manual 2D to fully robotic intraoperative 2D/3D fluoroscopy. *Adv Tech Stand Neurosurg.* 2012;38:75-93.
95. Wang MY, Kim KA, Liu CY, Kim P, Apuzzo ML. Reliability of three-dimensional fluoroscopy for detecting pedicle screw violations in the thoracic and lumbar spine. *Neurosurgery.* May 2004;54(5):1138-1142; discussion 1142-1133.
96. Marios T, Theologos T, Dimitrios Z, Nikolaos S, Slavisa M, Christos T. Pedicle screw placement accuracy impact and comparison between grading systems. *Surg Neurol Int.* 2017;8:131.
97. Costa F, Villa T, Anasetti F, et al. Primary stability of pedicle screws depends on the screw positioning and alignment. *Spine J.* Dec 2013;13(12):1934-1939.
98. Bronsard N, Boli T, Challali M, et al. Comparison between percutaneous and traditional fixation of lumbar spine fracture: intraoperative radiation exposure levels and outcomes. *Orthopaedics*

& traumatology, surgery & research : OTSR. Apr 2013;99(2):162-168.

99. Fransen P. Fluoroscopic exposure in modern spinal surgery. *Acta orthopaedica Belgica.* Jun 2011;77(3):386-389.

100. Mariscalco MW, Yamashita T, Steinmetz MP, Krishnaney AA, Lieberman IH, Mroz TE. Radiation exposure to the surgeon during open lumbar microdiscectomy and minimally invasive microdiscectomy: a prospective, controlled trial. *Spine.* Feb 1 2011;36(3):255-260.

101. Wang J, Zhou Y, Zhang ZF, Li CQ, Zheng WJ, Liu J. Comparison of one-level minimally invasive and open transforaminal lumbar interbody fusion in degenerative and isthmic spondylolisthesis grades 1 and 2. *Eur Spine J.* Oct 2010;19(10):1780-1784.

102. Yu E, Khan SN. Does less invasive spine surgery result in increased radiation exposure? A systematic review. *Clin Orthop Relat Res.* Jun 2014;472(6):1738-1748.

103. Fischetti M. Exposed. Medical imaging delivers big doses of radiation. *Scientific American.* May 2011;304(5):96.

104. McCollough CH, Schueler BA. Calculation of effective dose. *Medical physics.* May 2000;27(5):828-837.

105. Giordano BD, Grauer JN, Miller CP, Morgan TL, Rechtine GR, 2nd. Radiation exposure issues in orthopaedics. *J Bone Joint Surg Am.* Jun 15 2011;93(12):e69(61-10).

106. von Jako R, Finn MA, Yonemura KS, et al. Minimally invasive percutaneous transpedicular screw fixation: increased accuracy and reduced radiation exposure by means of a novel electromagnetic navigation system. *Acta Neurochir (Wien).* Mar 2011;153(3):589-596.

107. Gelalis ID, Paschos NK, Pakos EE, et al. Accuracy of pedicle screw placement: a systematic review of prospective in vivo studies comparing free hand, fluoroscopy guidance and navigation techniques. *Eur Spine J.* Feb 2012;21(2):247-255.

108. Tian NF, Xu HZ. Image-guided pedicle screw insertion accuracy: a meta-analysis. *Int Orthop.* Aug 2009;33(4):895-903.

109. Foley KT, Simon DA, Rampersaud YR. Virtual fluoroscopy: computer-assisted fluoroscopic navigation. *Spine.* Feb 15 2001;26(4):347-351.

110. Kalfas IH. Image-guided spinal navigation. *Clin Neurosurg.* 2000;46:70-88.

111. Schlenzka D, Laine T, Lund T. Computer-assisted spine surgery. *Eur Spine J.* Feb 2000;9 Suppl 1:S57-64.
112. Innocenzi G, Bistazzoni S, D'Ercole M, Cardarelli G, Ricciardi F. Does Navigation Improve Pedicle Screw Placement Accuracy? Comparison Between Navigated and Non-navigated Percutaneous and Open Fixations. *Acta Neurochir Suppl.* 2017;124:289-295.
113. Gebhard F, Weidner A, Liener UC, Stockle U, Arand M. Navigation at the spine. *Injury.* Jun 2004;35 Suppl 1:S-A35-45.
114. Nelson EM, Monazzam SM, Kim KD, Seibert JA, Klineberg EO. Intraoperative fluoroscopy, portable X-ray, and CT: patient and operating room personnel radiation exposure in spinal surgery. *Spine J.* Dec 01 2014;14(12):2985-2991.
115. Fomekong E, Dufrane D, Berg BV, et al. Application of a three-dimensional graft of autologous osteodifferentiated adipose stem cells in patients undergoing minimally invasive transforaminal lumbar interbody fusion: clinical proof of concept. *Acta Neurochir (Wien).* Mar 2017;159(3):527-536.
116. Dewey P, Incoll I. Evaluation of thyroid shields for reduction of radiation exposure to orthopaedic surgeons. *Aust N Z J Surg.* Sep 1998;68(9):635-636.
117. Mroz TE, Abdullah KG, Steinmetz MP, Klineberg EO, Lieberman IH. Radiation exposure to the surgeon during percutaneous pedicle screw placement. *J Spinal Disord Tech.* Jun 2011;24(4):264-267.
118. Ul Haque M, Shufflebarger HL, O'Brien M, Macagno A. Radiation exposure during pedicle screw placement in adolescent idiopathic scoliosis: is fluoroscopy safe? *Spine.* Oct 01 2006;31(21):2516-2520.
119. Leschka SC, Babic D, El Shikh S, Wossmann C, Schumacher M, Taschner CA. C-arm cone beam computed tomography needle path overlay for image-guided procedures of the spine and pelvis. *Neuroradiology.* Mar 2012;54(3):215-223.
120. von Jako RA, Cselik Z. Percutaneous laser discectomy guided with stereotactic computer-assisted surgical navigation. *Lasers Surg Med.* Jan 2009;41(1):42-51.
121. Izadpanah K, Konrad G, Sudkamp NP, Oberst M. Computer navigation in balloon kyphoplasty reduces the intraoperative radiation exposure. *Spine.* May 20 2009;34(12):1325-1329.
122. Takahashi S, Saruhashi Y, Odate S, Matsusue Y, Morikawa S. Percutaneous aspiration of spinal terminal ventricle cysts using real-time magnetic resonance imaging and navigation. *Spine.* Mar 15 2009;34(6):629-634.

123. Hofstetter R, Slomczykowski M, Sati M, Nolte LP. Fluoroscopy as an imaging means for computer-assisted surgical navigation. *Comput Aided Surg.* 1999;4(2):65-76.
124. Holly LT, Foley KT. Three-dimensional fluoroscopy-guided percutaneous thoracolumbar pedicle screw placement. Technical note. *J Neurosurg.* Oct 2003;99(3 Suppl):324-329.
125. Kim CW, Lee YP, Taylor W, Oygar A, Kim WK. Use of navigation-assisted fluoroscopy to decrease radiation exposure during minimally invasive spine surgery. *Spine J.* Jul-Aug 2008;8(4):584-590.
126. Tjardes T, Shafizadeh S, Rixen D, et al. Image-guided spine surgery: state of the art and future directions. *Eur Spine J.* Jan 2010;19(1):25-45.
127. Navarro-Ramirez R, Lang G, Lian X, et al. Total Navigation in Spine Surgery; A Concise Guide to Eliminate Fluoroscopy Using a Portable Intraoperative Computed Tomography 3-Dimensional Navigation System. *World Neurosurg.* Apr 2017;100:325-335.
128. Villard J, Ryang YM, Demetriades AK, et al. Radiation exposure to the surgeon and the patient during posterior lumbar spinal instrumentation: a prospective randomized comparison of navigated versus non-navigated freehand techniques. *Spine.* Jun 01 2014;39(13):1004-1009.
129. Smith HE, Welsch MD, Sasso RC, Vaccaro AR. Comparison of radiation exposure in lumbar pedicle screw placement with fluoroscopy vs computer-assisted image guidance with intraoperative three-dimensional imaging. *J Spinal Cord Med.* 2008;31(5):532-537.
130. Nottmeier EW, Bowman C, Nelson KL. Surgeon radiation exposure in cone beam computed tomography-based, image-guided spinal surgery. *Int J Med Robot.* Jun 2012;8(2):196-200.
131. Verma SK, Singh PK, Agrawal D, et al. O-arm with navigation versus C-arm: a review of screw placement over 3 years at a major trauma center. *Br J Neurosurg.* Dec 2016;30(6):658-661.
132. Perisinakis K, Theocharopoulos N, Damilakis J, et al. Estimation of patient dose and associated radiogenic risks from fluoroscopically guided pedicle screw insertion. *Spine.* Jul 15 2004;29(14):1555-1560.
133. Davne SH, Myers DL. Complications of lumbar spinal fusion with transpedicular instrumentation. *Spine.* Jun 1992;17(6 Suppl):S184-189.
134. Esses SI, Sachs BL, Dreyzin V. Complications associated with the technique of pedicle screw fixation. A selected survey of ABS members. *Spine.* Nov 1993;18(15):2231-2238; discussion 2238-2239.

135. Vaccaro AR, Rizzolo SJ, Allardyce TJ, et al. Placement of pedicle screws in the thoracic spine. Part I: Morphometric analysis of the thoracic vertebrae. *J Bone Joint Surg Am.* Aug 1995;77(8):1193-1199.
136. Youkilis AS, Quint DJ, McGillicuddy JE, Papadopoulos SM. Stereotactic navigation for placement of pedicle screws in the thoracic spine. *Neurosurgery.* Apr 2001;48(4):771-778; discussion 778-779.
137. Kalfas IH, Kormos DW, Murphy MA, et al. Application of frameless stereotaxy to pedicle screw fixation of the spine. *J Neurosurg.* Oct 1995;83(4):641-647.
138. Lim MR, Girardi FP, Yoon SC, Huang RC, Cammisa FP, Jr. Accuracy of computerized frameless stereotactic image-guided pedicle screw placement into previously fused lumbar spines. *Spine.* Aug 01 2005;30(15):1793-1798.
139. Nottmeier EW, Seemer W, Young PM. Placement of thoracolumbar pedicle screws using three-dimensional image guidance: experience in a large patient cohort. *J Neurosurg Spine.* Jan 2009;10(1):33-39.
140. Austin MS, Vaccaro AR, Brislin B, Nachwalter R, Hilibrand AS, Albert TJ. Image-guided spine surgery: a cadaver study comparing conventional open laminoforaminotomy and two image-guided techniques for pedicle screw placement in posterolateral fusion and nonfusion models. *Spine.* Nov 15 2002;27(22):2503-2508.
141. Fraser J, Gebhard H, Irie D, Parikh K, Hartl R. Iso-C/3-dimensional neuronavigation versus conventional fluoroscopy for minimally invasive pedicle screw placement in lumbar fusion. *Minim Invasive Neurosurg.* Aug 2010;53(4):184-190.
142. Luther N, Tomasino A, Parikh K, Hartl R. Neuronavigation in the minimally invasive presacral approach for lumbosacral fusion. *Minim Invasive Neurosurg.* Aug 2009;52(4):196-200.
143. Mirza SK, Wiggins GC, Kuntz Ct, et al. Accuracy of thoracic vertebral body screw placement using standard fluoroscopy, fluoroscopic image guidance, and computed tomographic image guidance: a cadaver study. *Spine.* Feb 15 2003;28(4):402-413.
144. Sagi HC, Manos R, Benz R, Ordway NR, Connolly PJ. Electromagnetic field-based image-guided spine surgery part one: results of a cadaveric study evaluating lumbar pedicle screw placement. *Spine.* Sep 01 2003;28(17):2013-2018.
145. Sagi HC, Manos R, Park SC, Von Jako R, Ordway NR, Connolly PJ. Electromagnetic field-based image-guided spine surgery part two: results of a cadaveric study evaluating thoracic pedicle screw placement. *Spine.* Sep 01 2003;28(17):E351-354.

146. Villavicencio AT, Burneikiene S, Bulsara KR, Thramann JJ. Utility of computerized isocentric fluoroscopy for minimally invasive spinal surgical techniques. *J Spinal Disord Tech.* Aug 2005;18(4):369-375.
147. Roy-Camille R, Saillant G, Mazel C. Plating of thoracic, thoracolumbar, and lumbar injuries with pedicle screw plates. *Orthop Clin North Am.* Jan 1986;17(1):147-159.
148. Cinotti G, Gumina S, Ripani M, Postacchini F. Pedicle instrumentation in the thoracic spine. A morphometric and cadaveric study for placement of screws. *Spine.* Jan 15 1999;24(2):114-119.
149. Laine T, Makitalo K, Schlenzka D, Tallroth K, Poussa M, Alho A. Accuracy of pedicle screw insertion: a prospective CT study in 30 low back patients. *Eur Spine J.* 1997;6(6):402-405.
150. Quinones-Hinojosa A, Robert Kolen E, Jun P, Rosenberg WS, Weinstein PR. Accuracy over space and time of computer-assisted fluoroscopic navigation in the lumbar spine in vivo. *J Spinal Disord Tech.* Apr 2006;19(2):109-113.
151. Schwab FJ, Nazarian DG, Mahmud F, Michelsen CB. Effects of spinal instrumentation on fusion of the lumbosacral spine. *Spine.* Sep 15 1995;20(18):2023-2028.
152. Vaccaro AR, Rizzolo SJ, Balderston RA, et al. Placement of pedicle screws in the thoracic spine. Part II: An anatomical and radiographic assessment. *J Bone Joint Surg Am.* Aug 1995;77(8):1200-1206.
153. Weinstein JN, Spratt KF, Spengler D, Brick C, Reid S. Spinal pedicle fixation: reliability and validity of roentgenogram-based assessment and surgical factors on successful screw placement. *Spine.* Sep 1988;13(9):1012-1018.
154. Xu R, Ebraheim NA, Ou Y, Yeasting RA. Anatomic considerations of pedicle screw placement in the thoracic spine. Roy-Camille technique versus open-lamina technique. *Spine.* May 01 1998;23(9):1065-1068.
155. Kim KD, Patrick Johnson J, Bloch BO, Masciopinto JE. Computer-assisted thoracic pedicle screw placement: an in vitro feasibility study. *Spine.* Feb 15 2001;26(4):360-364.
156. Merloz P, Tonetti J, Pittet L, Coulomb M, Lavallee S, Sautot P. Pedicle screw placement using image guided techniques. *Clin Orthop Relat Res.* Sep 1998(354):39-48.
157. Nakagawa H, Kamimura M, Uchiyama S, Takahara K, Itsubo T, Miyasaka T. The accuracy and safety of image-guidance system using intraoperative fluoroscopic images: an in vitro feasibility study. *J Clin Neurosci.* Mar 2003;10(2):226-230.

158. Bledsoe JM, Fenton D, Fogelson JL, Nottmeier EW. Accuracy of upper thoracic pedicle screw placement using three-dimensional image guidance. *Spine J.* Oct 2009;9(10):817-821.
159. Hott JS, Deshmukh VR, Klopfenstein JD, et al. Intraoperative Iso-C C-arm navigation in craniospinal surgery: the first 60 cases. *Neurosurgery.* May 2004;54(5):1131-1136; discussion 1136-1137.
160. Ito Y, Sugimoto Y, Tomioka M, Hasegawa Y, Nakago K, Yagata Y. Clinical accuracy of 3D fluoroscopy-assisted cervical pedicle screw insertion. *J Neurosurg Spine.* Nov 2008;9(5):450-453.
161. Richter M, Cakir B, Schmidt R. Cervical pedicle screws: conventional versus computer-assisted placement of cannulated screws. *Spine.* Oct 15 2005;30(20):2280-2287.
162. Boon Tow BP, Yue WM, Srivastava A, et al. Does Navigation Improve Accuracy of Placement of Pedicle Screws in Single-level Lumbar Degenerative Spondylolisthesis?: A Comparison Between Free-hand and Three-dimensional O-Arm Navigation Techniques. *J Spinal Disord Tech.* Oct 2015;28(8):E472-477.
163. Bindal RK, Glaze S, Ognoskie M, Tunner V, Malone R, Ghosh S. Surgeon and patient radiation exposure in minimally invasive transforaminal lumbar interbody fusion. *J Neurosurg Spine.* Dec 2008;9(6):570-573.
164. Ntoukas V, Muller A. Minimally invasive approach versus traditional open approach for one level posterior lumbar interbody fusion. *Minim Invasive Neurosurg.* Feb 2010;53(1):21-24.
165. Slomczykowski M, Roberto M, Schneeberger P, Ozdoba C, Vock P. Radiation dose for pedicle screw insertion. Fluoroscopic method versus computer-assisted surgery. *Spine.* May 15 1999;24(10):975-982; discussion 983.
166. Wang J, Zhou Y, Feng Zhang Z, Qing Li C, Jie Zheng W, Liu J. Comparison of the clinical outcome in overweight or obese patients after minimally invasive versus open transforaminal lumbar interbody fusion. *J Spinal Disord Tech.* Jun 2014;27(4):202-206.
167. Khanna AR, Yanamadala V, Coumans JV. Effect of intraoperative navigation on operative time in 1-level lumbar fusion surgery. *J Clin Neurosci.* Oct 2016;32:72-76.
168. Khanna R, McDevitt JL, Abecassis ZA, et al. An Outcome and Cost Analysis Comparing Single-Level Minimally Invasive Transforaminal Lumbar Interbody Fusion Using Intraoperative Fluoroscopy versus Computed Tomography-Guided Navigation. *World Neurosurg.* 2016;94:255-260.

169. Weinstein JN, Lurie JD, Olson PR, Bronner KK, Fisher ES. United States' trends and regional variations in lumbar spine surgery: 1992-2003. *Spine.* Nov 1 2006;31(23):2707-2714.
170. Werner BC, Li X, Shen FH. Stem cells in preclinical spine studies. *Spine J.* Mar 1 2014;14(3):542-551.
171. Keller EE, Triplett WW. Iliac bone grafting: review of 160 consecutive cases. *Journal of oral and maxillofacial surgery : official journal of the American Association of Oral and Maxillofacial Surgeons.* Jan 1987;45(1):11-14.
172. Fischer CR, Cassilly R, Cantor W, Edusei E, Hammouri Q, Errico T. A systematic review of comparative studies on bone graft alternatives for common spine fusion procedures. *Eur Spine J.* Jun 2013;22(6):1423-1435.
173. Hsu WK, Nickoli MS, Wang JC, et al. Improving the clinical evidence of bone graft substitute technology in lumbar spine surgery. *Global spine journal.* Dec 2012;2(4):239-248.
174. Rihn JA, Kirkpatrick K, Albert TJ. Graft options in posterolateral and posterior interbody lumbar fusion. *Spine.* Aug 1 2010;35(17):1629-1639.
175. Boden SD, Schimandle JH, Hutton WC. An experimental lumbar intertransverse process spinal fusion model. Radiographic, histologic, and biomechanical healing characteristics. *Spine.* Feb 15 1995;20(4):412-420.
176. Glassman SD, Dimar JR, Carreon LY, Campbell MJ, Puno RM, Johnson JR. Initial fusion rates with recombinant human bone morphogenetic protein-2/compression resistant matrix and a hydroxyapatite and tricalcium phosphate/collagen carrier in posterolateral spinal fusion. *Spine.* Aug 1 2005;30(15):1694-1698.
177. Schimandle JH, Boden SD, Hutton WC. Experimental spinal fusion with recombinant human bone morphogenetic protein-2. *Spine.* Jun 15 1995;20(12):1326-1337.
178. Singh K, Ahmadinia K, Park DK, et al. Complications of spinal fusion with utilization of bone morphogenetic protein: a systematic review of the literature. *Spine.* Jan 1 2014;39(1):91-101.
179. Cahill KS, Chi JH, Day A, Claus EB. Prevalence, complications, and hospital charges associated with use of bone-morphogenetic proteins in spinal fusion procedures. *Jama.* Jul 1 2009;302(1):58-66.
180. Joseph V, Rampersaud YR. Heterotopic bone formation with the use of rhBMP2 in posterior minimal access interbody fusion: a CT analysis. *Spine.* Dec 1 2007;32(25):2885-2890.

181. Mindea SA, Shih P, Song JK. Recombinant human bone morphogenetic protein-2-induced radiculitis in elective minimally invasive transforaminal lumbar interbody fusions: a series review. *Spine.* Jun 15 2009;34(14):1480-1484; discussion 1485.
182. Pittenger MF, Mackay AM, Beck SC, et al. Multilineage potential of adult human mesenchymal stem cells. *Science.* Apr 2 1999;284(5411):143-147.
183. Wyles CC, Houdek MT, Crespo-Diaz RJ, et al. Adipose-derived Mesenchymal Stem Cells Are Phenotypically Superior for Regeneration in the Setting of Osteonecrosis of the Femoral Head. *Clin Orthop Relat Res.* Oct 2015;473(10):3080-3090.
184. Yang XF, He X, He J, et al. High efficient isolation and systematic identification of human adipose-derived mesenchymal stem cells. *Journal of biomedical science.* 2011;18:59.
185. Zhu Y, Liu T, Song K, Fan X, Ma X, Cui Z. Adipose-derived stem cell: a better stem cell than BMSC. *Cell biochemistry and function.* Aug 2008;26(6):664-675.
186. Dufrane D, Docquier PL, Delloye C, Poirel HA, Andre W, Aouassar N. Scaffold-free Three-dimensional Graft From Autologous Adipose-derived Stem Cells for Large Bone Defect Reconstruction: Clinical Proof of Concept. *Medicine.* Dec 2015;94(50):e2220.
187. Veriter S, Andre W, Aouassar N, et al. Human Adipose-Derived Mesenchymal Stem Cells in Cell Therapy: Safety and Feasibility in Different "Hospital Exemption" Clinical Applications. *PloS one.* 2015;10(10):e0139566.
188. Khashan M, Inoue S, Berven SH. Cell based therapies as compared to autologous bone grafts for spinal arthrodesis. *Spine.* Oct 1 2013;38(21):1885-1891.
189. Shunwu F, Xing Z, Fengdong Z, Xiangqian F. Minimally invasive transforaminal lumbar interbody fusion for the treatment of degenerative lumbar diseases. *Spine.* Aug 1 2010;35(17):1615-1620.
190. Zdeblick TA. A prospective, randomized study of lumbar fusion. Preliminary results. *Spine.* Jun 15 1993;18(8):983-991.
191. Epstein NE. Complications due to the use of BMP/INFUSE in spine surgery: The evidence continues to mount. *Surg Neurol Int.* 2013;4(Suppl 5):S343-352.
192. Schultz DG. Medical-device safety and the FDA. *The New England journal of medicine.* Jul 3 2008;359(1):88-89; author reply 89.
193. Thalgott JS, Giuffre JM, Fritts K, Timlin M, Klezl Z. Instrumented posterolateral lumbar fusion using coralline hydroxyapatite with or

without demineralized bone matrix, as an adjunct to autologous bone. *Spine J.* Mar-Apr 2001;1(2):131-137.

194. Epstein NE, Epstein JA. SF-36 outcomes and fusion rates after multilevel laminectomies and 1 and 2-level instrumented posterolateral fusions using lamina autograft and demineralized bone matrix. *J Spinal Disord Tech.* Apr 2007;20(2):139-145.

195. Kang J, An H, Hilibrand A, Yoon ST, Kavanagh E, Boden S. Grafton and local bone have comparable outcomes to iliac crest bone in instrumented single-level lumbar fusions. *Spine.* May 20 2012;37(12):1083-1091.

196. Duhoux FP, Ameye G, Lambot V, et al. Refinement of 1p36 alterations not involving PRDM16 in myeloid and lymphoid malignancies. *PloS one.* 2011;6(10):e26311.

197. Mannion RJ, Nowitzke AM, Wood MJ. Promoting fusion in minimally invasive lumbar interbody stabilization with low-dose bone morphogenic protein-2--but what is the cost? *Spine J.* Jun 2011;11(6):527-533.

198. Fischgrund JS, Mackay M, Herkowitz HN, Brower R, Montgomery DM, Kurz LT. 1997 Volvo Award winner in clinical studies. Degenerative lumbar spondylolisthesis with spinal stenosis: a prospective, randomized study comparing decompressive laminectomy and arthrodesis with and without spinal instrumentation. *Spine.* Dec 15 1997;22(24):2807-2812.

199. Vaccaro AR, Lawrence JP, Patel T, et al. The safety and efficacy of OP-1 (rhBMP-7) as a replacement for iliac crest autograft in posterolateral lumbar arthrodesis: a long-term (>4 years) pivotal study. *Spine.* Dec 15 2008;33(26):2850-2862.

200. Dimar JR, 2nd, Glassman SD, Burkus JK, Pryor PW, Hardacker JW, Carreon LY. Two-year fusion and clinical outcomes in 224 patients treated with a single-level instrumented posterolateral fusion with iliac crest bone graft. *Spine J.* Nov 2009;9(11):880-885.

201. Dimar JR, Glassman SD, Burkus KJ, Carreon LY. Clinical outcomes and fusion success at 2 years of single-level instrumented posterolateral fusions with recombinant human bone morphogenetic protein-2/compression resistant matrix versus iliac crest bone graft. *Spine.* Oct 15 2006;31(22):2534-2539; discussion 2540.

202. Luo X, Chen J, Song WX, et al. Osteogenic BMPs promote tumor growth of human osteosarcomas that harbor differentiation defects. *Laboratory investigation; a journal of technical methods and pathology.* Dec 2008;88(12):1264-1277.

203. Wang L, Park P, Zhang H, et al. BMP-2 inhibits the tumorigenicity of cancer stem cells in human osteosarcoma OS99-1 cell line. *Cancer biology & therapy.* Mar 1 2011;11(5):457-463.
204. Rubio R, Abarrategi A, Garcia-Castro J, et al. Bone environment is essential for osteosarcoma development from transformed mesenchymal stem cells. *Stem cells.* May 2014;32(5):1136-1148.
205. Perrot P, Rousseau J, Bouffaut AL, et al. Safety concern between autologous fat graft, mesenchymal stem cell and osteosarcoma recurrence. *PloS one.* 2010;5(6):e10999.
206. Bernardo ME, Zaffaroni N, Novara F, et al. Human bone marrow derived mesenchymal stem cells do not undergo transformation after long-term in vitro culture and do not exhibit telomere maintenance mechanisms. *Cancer research.* Oct 1 2007;67(19):9142-9149.
207. Meza-Zepeda LA, Noer A, Dahl JA, Micci F, Myklebost O, Collas P. High-resolution analysis of genetic stability of human adipose tissue stem cells cultured to senescence. *Journal of cellular and molecular medicine.* Apr 2008;12(2):553-563.
208. Roemeling-van Rhijn M, de Klein A, Douben H, et al. Culture expansion induces non-tumorigenic aneuploidy in adipose tissue-derived mesenchymal stromal cells. *Cytotherapy.* Nov 2013;15(11):1352-1361.
209. Ohtori S, Suzuki M, Koshi T, et al. Single-level instrumented posterolateral fusion of the lumbar spine with a local bone graft versus an iliac crest bone graft: a prospective, randomized study with a 2-year follow-up. *European spine journal : official publication of the European Spine Society, the European Spinal Deformity Society, and the European Section of the Cervical Spine Research Society.* Apr 2011;20(4):635-639.
210. Sengupta DK, Truumees E, Patel CK, et al. Outcome of local bone versus autogenous iliac crest bone graft in the instrumented posterolateral fusion of the lumbar spine. *Spine.* Apr 20 2006;31(9):985-991.
211. Schizas C, Triantafyllopoulos D, Kosmopoulos V, Stafylas K. Impact of iliac crest bone graft harvesting on fusion rates and postoperative pain during instrumented posterolateral lumbar fusion. *Int Orthop.* Feb 2009;33(1):187-189.
212. Lee SC, Chen JF, Wu CT, Lee ST. In situ local autograft for instrumented lower lumbar or lumbosacral posterolateral fusion. *J Clin Neurosci.* Jan 2009;16(1):37-43.

213. Ryang YM, Villard J, Obermuller T, et al. Learning curve of 3D fluoroscopy image-guided pedicle screw placement in the thoracolumbar spine. *Spine J.* Mar 1 2015;15(3):467-476.
214. Foley KT, Lefkowitz MA. Advances in minimally invasive spine surgery. *Clin Neurosurg.* 2002;49:499-517.
215. Kawaguchi Y, Matsui H, Tsuji H. Back muscle injury after posterior lumbar spine surgery. A histologic and enzymatic analysis. *Spine.* Apr 15 1996;21(8):941-944.
216. Kawaguchi Y, Yabuki S, Styf J, et al. Back muscle injury after posterior lumbar spine surgery. Topographic evaluation of intramuscular pressure and blood flow in the porcine back muscle during surgery. *Spine.* Nov 15 1996;21(22):2683-2688.
217. Raftopoulos C. Spine neurosurgery in Belgium. *World Neurosurg.* Oct-Nov 2010;74(4-5):430-431.
218. Coolidge C. Biography of 30th US president. 1872-1933.

This page intentionally left blank